Seismicity Potential Risk of Istanbul and Possible Scenario of a 7.6 Magnitude Earthquake

Ahmet Turan Erturk

MSc in Geographic Information Science
Technological University Dublin

Supervisor: Eugen Niculae

October, 2024

ABSTRACT

This study focuses on an earthquake risk assessment and scenario development for the city of Istanbul. Considering the city's seismicity and its resilience to seismic events, geological data, historical earthquake records, as well as structural and demographic data will be employed to elucidate the earthquake potential using the multi-criteria decision-making method known as the Analytic Hierarchy Process (AHP). The research aims to develop two distinct earthquake scenarios. The first scenario will involve a 7.6 magnitude earthquake simulated through ArcGIS Pro, calculating the potential damage across the city and predicting casualties and building damage levels on a district basis. The second scenario will be constructed using the ELER programme.

Ultimately, this research aims to conduct a situational assessment of Istanbul's seismic hazards and to estimate losses and damages for the potential 7.6 magnitude earthquake scenario. The findings are anticipated to contribute to the implementation of measures addressing earthquake risks in Istanbul.

Keywords: Istanbul, AHP, earthquake risk assessment, earthquake scenario

DECLARATION

I certify that this dissertation which I now submit for examination for the award of MSc Geographic Information Science, is entirely my own work and has not been taken from the work of others save and to the extent that such work has been cited and acknowledged within the text of my work.

This dissertation was prepared according to the regulations for postgraduate study by research of the Technological University Dublin City Campus and has not been submitted in whole or in part for an award in any other Institute or University.

The work reported on in this dissertation conforms to the principles and requirements of the universities' guidelines for ethics in research.

The University has permission to keep, to lend or to copy this dissertation in whole or in part, on condition that any such use of the material of the dissertation is duly acknowledged.

Signature: Ahmet Turan Erturk **Date**: 29.10.2024

ACKNOWLEDGEMENTS

I would like to express my deepest gratitude to the esteemed faculty members of the Master of Science in Geographical Information Science programme at Technological University Dublin: Alain Chenaux, Andrea Curley, Audrey Martin, Dermot Hore, Eimar McNearny, Niamh O'Reilly, Paula Kelly, Santos Fernandez Noguerol, Sojan Mathew, and my supervisor Eugen Niculae, for their unwavering support and guidance, which greatly contributed to my personal and academic development and made this an exceptional experience.

I am also profoundly grateful to Prof. Dr. Murat Ercanoğlu from Hacettepe University, whose introduction to the field of Geographic Information Science inspired me to pursue my master's degree.

My heartfelt thanks also go to my dear friends in both Ankara and Dublin, who provided me with constant motivation throughout this journey. I would especially like to thank my friend and geologist, Bengisu Dinç, for her invaluable assistance in helping me contact institutions to obtain some of the data used in this thesis.

Finally, I wish to express my deepest appreciation to my beloved mother, father, and sister for their unwavering emotional and financial support throughout this journey. Their presence by my side has been a pillar of strength**.**

TO MY MOTHER.

ABBREVIATIONS LIST

AHP - Analytic Hierarchy Process

AD - Anno Domini

AFAD - Disaster and Emergency Management Authority (Türkiye)

CR - Consistency Ratio

DEM - Digital Elevation Model

ELER - Earthquake Loss Estimation Routine

ESRI - Environmental Systems Research Institute

GIS - Geographic Information System

HGM - General Directorate of Maps (Türkiye)

IMM - Istanbul Metropolitan Municipality

MCMD - Multi-Criteria Decision Making

MTA - General Directorate of Mineral Research and Exploration (Türkiye)

NAFZ - North Anatolian Fault Zone

PGA - Peak Ground Acceleration

TUIK - Turkish Statistical Institute

USGS - United States Geological Survey

TABLE OF CONTENTS

LIST OF FIGURES

LIST OF TABLES

1.INTRODUCTION

Since the formation of the Earth, tectonic movements triggered by convective motions within the mantle have ultimately resulted in earthquakes, which are the most significant natural disasters. In many countries around the world, earthquakes have created a seismic zone due to the tectonic movements that lead to large, destructive disasters. Despite substantial losses have occurred, throughout history, major cities and metropolises have been established along these seismic zones. Following these earthquakes and the other natural disasters and events they trigger, significant loss of life and property has been experienced in these regions, and the effects of these earthquakes have persisted for an extended period. (Uzun & Balyamez, 2020)

When examining the Republic of Türkiye, historical records and the history of seismic activity have focused on the city of Istanbul, which has continuously existed throughout various periods and has a population that is consistently larger compared to other regions. Due to the high population density and the fact that the region has been documented and under observation throughout history, access to the seismicity of Istanbul and its surroundings is possible, even though historical records are limited. According to data from Disaster and Emergency Management Presidency (AFAD) and conducted statistics, it has been determined that severe seismic movements have been observed at 50-year intervals and very severe movements in 250-year intervals around Istanbul. This natural disaster, which has continuity and recurs at specific intervals, is a matter that requires attention, contemplation, and necessary precautions to be taken in Türkiye. (Cansiz, 2022)

This study will assess earthquake risk and potential damage areas for Istanbul using GIS, and a simulation of a major earthquake that occurs every 250 years and is anticipated will be conducted to examine the potential damages and losses that may occur post-earthquake for Istanbul.

1.1. Study Area

Istanbul, one of the most significant cities in world history, has always played a vital role by bridging Asia and Europe and has remained an important city for humanity. Additionally, this city has been the centre of empires, kingdoms, and many civilizations, reaching the present day as a cultural and historical heritage. (IMM, 2024)

Throughout history, Istanbul has been known by many names, with Augusta, Constantinople, and Islambol being the most well-known. It is widely accepted that the name Istanbul is derived

from the Greek phrase *'eis tin polin'* meaning 'in the city' or 'into the city.' (Avcı and Gezerler, 2024)

Istanbul is the only city in the world that spans two continents, with a sea running through it, connecting the Black Sea and the Sea of Marmara while separating the continents of Asia and Europe. To the north of the city lies the Black Sea, to the east the Kocaeli Mountains, to the south the Sea of Marmara, and to the west the Ergene Basin. Its highest point, Aydos Hill, stands at approximately 536 meters. (Güler, 2016)

According to the latest address-based population registration system published by the Turkish Statistical Institute, Istanbul is home to 15,655,924 people, of whom 7,806,787 are male and 7,849,137 are female. With these figures, Istanbul holds the title of the most populous city in Türkiye, accounting for approximately 18.34% of the country's total population. (TUIK, 2024)

Istanbul consists of a total of 39 districts, 25 of which are located on the European side, while 14 are situated on the Asian side, known as the Anatolian Side. The total number of buildings in all districts combined has been recorded as 1,159,543. Furthermore, the average household size in Istanbul has been calculated to be 3.

The study area defined within the scope of this research is limited to the borders of Istanbul. All results and outputs from the analyses and procedures conducted are drawn exclusively from within the boundaries of the province of Istanbul.

Figure 1. Location Map of the Study Area.

1.2. Research Aim and Scope

Istanbul, the only city located on two continents, has existed for centuries in human history and has been a target for various kingdoms and empires due to its geopolitical position. Established over an area of approximately 5,461 km², this city has been governed by different empires, including the Eastern Roman Empire, the Byzantine Empire, and the Ottoman Empire. After the establishment of the Republic of Türkiye in 1923, Istanbul became the largest metropolis in the country.

Throughout history, the earthquakes experienced in this city have presented significant challenges during various periods. The recurrent earthquakes, occurring at specific intervals, have left substantial impacts and damages on the various civilizations and societies that have inhabited Istanbul.

The last major earthquake to affect Istanbul occurred on August 18, 1999, reminding its residents and officials that preparedness for earthquakes is always necessary. Following this earthquake, the academic community and scientists began to focus on the Northeast Anatolian Fault Zone (NAFZ) and the seismicity of the region, conducting various studies to uncover its dynamics.

With advancements in technology and academia, Geographic Information Systems have emerged, helping to minimize damages and risks by making assessments such as pre-emptive damage and risk predictions regarding natural disasters. Numerous studies have been conducted by creating scenarios based on past and historical earthquakes.

In this thesis, the seismicity of Istanbul has been highlighted, and the earthquake risk in the region has been assessed by establishing specific criteria, leading to the creation of earthquake risk maps for Istanbul. A simulation scenario for a 7.6 magnitude earthquake has been developed for these recurrent seismic events, calculating the potential building damages and loss of life.

This study utilises ArcGIS Pro, developed by ESRI (Environmental Systems Research Institute), and the ELER (Earthquake Loss Evaluation and Recovery) program developed by Kandilli Observatory for the scenario analysis.

2. LITERATURE REVIEW

2.1. The Structure and Mechanisms of Earthquakes

Billions of years ago, Earth was a fiery mass made up of molten rock and gases. Over time, the outer layers of the Earth cooled, forming a solid layer called the crust. This crust, Earth's outermost layer, varies in thickness from approximately 6 km to 90 km. Beneath the crust lies the mantle, about 2,900 km thick and denser than the crust. The mantle is hotter than the crust and consists of partially molten rock and solid materials. This structure can move due to convection currents. Below the mantle is the outer core, approximately 2,000 km thick. Although liquid like the mantle, the outer core is much denser. At the centre of the Earth lies the inner core, which is highly dense and solid. The inner core is about 1,200 km thick and has extremely high temperatures (de Klerk, 2024).

Although the Earth's internal structure is chemically composed of the core, mantle, and crust, mechanically it consists of the inner core, outer core, lower mantle, upper mantle, asthenosphere, and lithosphere. The lithosphere, made up of the uppermost part of the mantle and the crust, is also referred to as the plate. Despite being solid, these plates rest on the asthenosphere, which is more plastic in nature and capable of flow. (Martin et all., 2008)

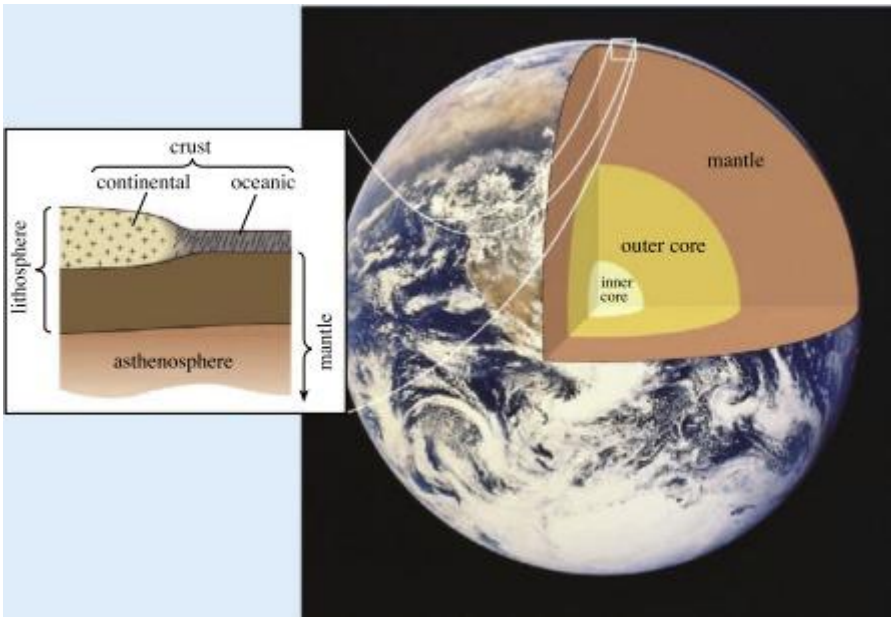

Figure 2. The Internal Structure of the Earth (de Klerk, 2024).

In 1912, Alfred Wegener proposed a theory suggesting that all continents were once part of a single landmass. However, since Wegener was a meteorologist, he did not receive sufficient recognition in the scientific community and had few supporters. In 1928, British geologist

Arthur Holmes proposed that continents could move by demonstrating that heat within the mantle creates convection currents that drag the continents. This mechanism became a foundational model for plate tectonics. In the 1960s, the view emerged that the movement of solid parts in the lithosphere is limited and occurs in different directions. Due to the rigid nature of the plates, they generally do not undergo deformation; however, areas at their boundaries may become deformed. In regions where plates collide and interact, mountain formations, volcanoes, and earthquakes often occur, while ocean basins arise in areas where they separate and move apart. The movements of the plates continuously alter the appearance of the continents. According to the research of scientists, particularly geologists, the movement of one plate will also affect others, filling the gaps created. These constantly moving and shifting plate movements are among the most significant factors triggering earthquakes. (Kusky, 2008)

In the theory of plate tectonics, small-scale studies of relatively moving plates have shown that in certain locations, these movements can be clearly and easily identified. These structures, which experience two different types of displacement, are referred to as faults. Fault lengths can vary and may extend for hundreds of kilometres. The fault mechanism can sometimes manifest itself on the surface. However, the existence of a fault does not necessarily mean that it will trigger an earthquake. Likewise, the absence of visible faulting does not imply that an earthquake will not occur. Not every fault rupture reaches the surface. (Kramer, 1996)

Faults can be classified based on their movement. Dip-slip faults are generally divided into normal faults, reverse faults, and thrust faults. Normal faults involve two plates moving away from each other, while reverse faults involve compressional forces that push the plates together. Thrust faults, on the other hand, have a gentler angle of inclination compared to reverse faults. Another type of fault, strike-slip faults, is known for horizontal movement either to the right or left along the fault line. Strike-slip faults may also exhibit vertical motion, causing significant impact. The San Andreas Fault in the United States is a right-lateral strike-slip fault. Studies have shown that during the 1906 earthquake, it displaced a road by 6 meters. (Kramer, 1996)

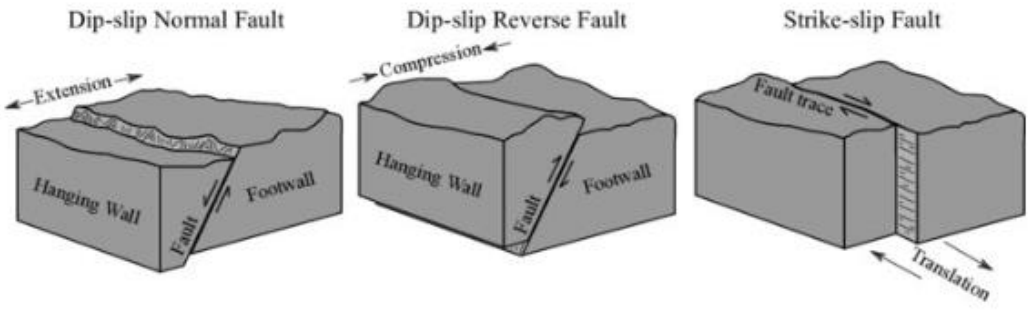

Figure 3. Representations of Normal Fault, Reverse Fault, and Strike-Slip Fault (Efthymiou and Makris, 2022)

When the energy accumulated by faulting is released and the fault breaks, waves propagate and radiate to create an earthquake. These seismic waves also dissipate as they reach the surface. These waves are known as P waves, S waves, and surface waves, and their speeds and durations in reaching the surface are analysed by seismographs to study the source and magnitude of the earthquake. P waves are the fastest seismic waves and can travel through solids, liquids, and gases, exhibiting push-pull motion. S waves, on the other hand, move more slowly than P waves and generate shear waves, creating shear stresses. Surface waves are divided into Rayleigh waves and Love waves. Rayleigh waves move in an up-and-down motion, resembling ocean waves. Love waves, however, create sliding motions that cause horizontal deformation. (Rao, 2015)

The first earthquake measuring device in history was invented by Chinese Zhang Heng in AD 132, and this instrument determined the direction of earthquakes. With advancing technology, by the late 19th century, a period known as the instrumental era began, and seismographs were developed. Seismometers were later integrated with recording equipment to obtain permanent records. Data from three different seismographs is used to determine the epicentre of an earthquake. (Rajasekaran, 2009)

When measuring an earthquake, two concepts are prominent: earthquake intensity and earthquake magnitude. Earthquake intensity is generally damage-focused and involves assessing physical effects observed at specific locations. Since this method cannot be directly measured with instruments or seismographs, historical records of earthquakes have typically been defined by intensity calculations, leading to variations based on proximity to the fault and

the type of ground. In 1902, Italian seismologist and volcanologist Giuseppe Mercalli developed the "Modified Mercalli Intensity Scale" (MMI), which consists of 12 degrees from I to XII, and this scale is still in use today (Table 1). This intensity scale assesses factors such as the extent to which earthquakes are felt by people and animals, the resistance of structures to earthquakes, and general changes in the environment. Earthquake magnitude, on the other hand, was defined in 1935 by Charles Richter, following the instrumental era. Richter introduced a scale (Table 2) based on the periods of seismic waves recorded by seismographs, calculating the magnitude by considering the amplitude of the waveforms and the distance from the actual earthquake location (Rajasekaran, 2009).

Table 1. Mercalli Earthquake Intensity Scale (Khilyuk et al., 2000)

Intensity Level	**Description**
I	Earthquakes that are not felt by people or are rarely noticed and can only be detected by instrumental devices.
II	Felt by people living in the upper floors of buildings or by sensitive individuals. Some hanging objects may sway.
III	Felt by most people indoors, even if not noticeable outdoors.
IV	Felt by people both indoors and outdoors. The vibrations can be compared to the shaking caused by a heavy truck passing by.
V	Felt by everyone indoors and by many people outdoors. Some glass or objects may break, and unsecured items may fall.
VI	Felt by everyone. Some buildings may experience light damage. Household objects may topple. People may panic and feel fear.
VII	It may become difficult for people to remain standing. People in moving vehicles can notice the earthquake. Significant cracks may appear in buildings.
VIII	It causes great panic and fear among people. Trees may shake violently and sometimes break. Even buildings constructed according to earthquake regulations may suffer minor damage, while non-compliant structures may collapse.

IX	Cracks form in the ground. Significant damage occurs in many buildings, and some collapse. It can cause extensive damage to infrastructure.
X	Cracks several meters wide may form, especially in loose soils. Landslides are triggered. Railway tracks may bend.
XI	Major damage occurs to structures like bridges and dams. Ground deformations, landslides, and tsunamis may occur.
XII	All structures can be damaged. Numerous cracks and fissures appear in the ground. Landslides and rockfalls are widely observed. The surface of the ground may exhibit wavelike features.

Table 2. Richter Magnitude Scale (Khilyuk et al., 2000)

Richter Magnitude	**Typical Effects**
2.0 and under	Earthquakes are not felt by individuals.
3.0	They may be felt by individuals in indoor settings without causing damage.
4.0	Most individuals can sense them; some objects may be displaced without causing structural damage.
5.0	Cracks may be observed in the walls and chimneys of buildings.
6.0	Weak structures may crack or topple, resulting in moderate damage.
7.0	The collapse of buildings that do not comply with regulations may occur, and cracks may develop in the walls of robust structures.
8.0 and over	Damage can be observed everywhere.

2.2. Impacts of Earthquake

When the energy accumulated in the Earth's crust is suddenly released, waves spread and cause shaking in the ground, which is called an earthquake. As a result of these tremors, secondary hazards such as landslides, fires, and tsunamis may also occur. The chain of events following the earthquake can lead to loss of life and economic damage in the affected region. (Şimşek and Gündüz, 2021)

Seismographs established around the world measure approximately 500,000 earthquakes annually. About one-fifth of these measured earthquakes, or 100,000, are large enough to be noticed by people. Research has determined that nearly 100 earthquakes each year are powerful enough to cause building damage and result in loss of life. The United States Geological Survey (USGS) has reported that from 2000 to 2019, a total of 3,071 earthquakes with a magnitude of 6 or higher occurred globally. During the same period, the number of significant earthquakes in Türkiye was recorded as 9, with 886 fatalities reported. (Emre et al., 2020)

Earthquakes have been one of the most significant natural events affecting human lives since the dawn of humanity. Approximately 1,350 earthquakes recorded since the 1900s have resulted in the deaths of 857,246 individuals, with millions more injured and a direct impact on economic life (Demir and Altaş, 2024).

2.3. Earthquakes and Geographic Information Sciences (GIS)

Earthquake hazard refers to the probability of ground motion causing potential loss of life and property damage within a specific area and timeframe due to an earthquake. Earthquake risk, on the other hand, is defined as the numerical probability of loss of life and property as a result of an earthquake. Seismic hazard studies generally aim to determine the potential magnitude of an earthquake for a particular settlement. By creating earthquake scenarios, the goal is to estimate the extent and level of impact that such an event would have on the area. (Işık et al., 2019)

Earthquakes have continuously made themselves known throughout history, negatively impacting human life, and causing significant damage. Considering that these damages will persist into the future, every precaution taken holds crucial importance. Geographic Information Systems (GIS) play a significant role in preventing or mitigating these adverse effects (Yalçın and Sabah, 2017). In the parameters established for seismic hazard assessment, fault length, distance to active faults, number of seismic source focal points, and size of the alluvial area are considered (Yalçın and Sabah, 2017).

In a study conducted by Deligiannakis in 2018, four distinct methodologies stand out. Firstly, the focus lies on the identification of seismic sources, determination of fault lengths and characteristics, and organization of these data. Secondly, attention is directed towards determining fault lengths, earthquake magnitudes, and seismic slip relationships. Thirdly, emphasis is placed on identifying the detrimental effects of major earthquakes, particularly on areas causing damage to well-constructed buildings, as per the Mercalli Intensity Scale. Lastly,

the comparison of seismic shaking on bedrock with sediment filled areas in the region constitutes the fourth methodology. (Eris et al., 2023)

2.4. Geology of Istanbul

Within the city of Istanbul, subsystems from the Palaeozoic, Mesozoic, and Cenozoic periods are observed. The oldest and lowest formations in Istanbul are Palaeozoic units, composed of sedimentary rocks such as siltstone, sandstone, shale, and greywacke. Additionally, Palaeozoic-aged deposits are occasionally intersected by magmatic rocks like granite, diorite, diabase, andesite, and basalt. (Demirelli, 2001)

Within Istanbul, there are two major sequences: one metamorphic and the other non-metamorphic. The metamorphic sequence is known as the Istranca Unit, while the non-metamorphic sequence is referred to as the 'Istanbul Unit.' The Istranca Unit is primarily composed of Palaeozoic and Mesozoic-aged magmatic and sedimentary rocks, which occupy a significant portion of this unit's stratigraphy. The Istanbul Unit, on the other hand, consists of Palaeozoic deposits representing the Ordovician-Carboniferous period, as well as older rock units from the Permian-Triassic transition. (Özgül, 2011)

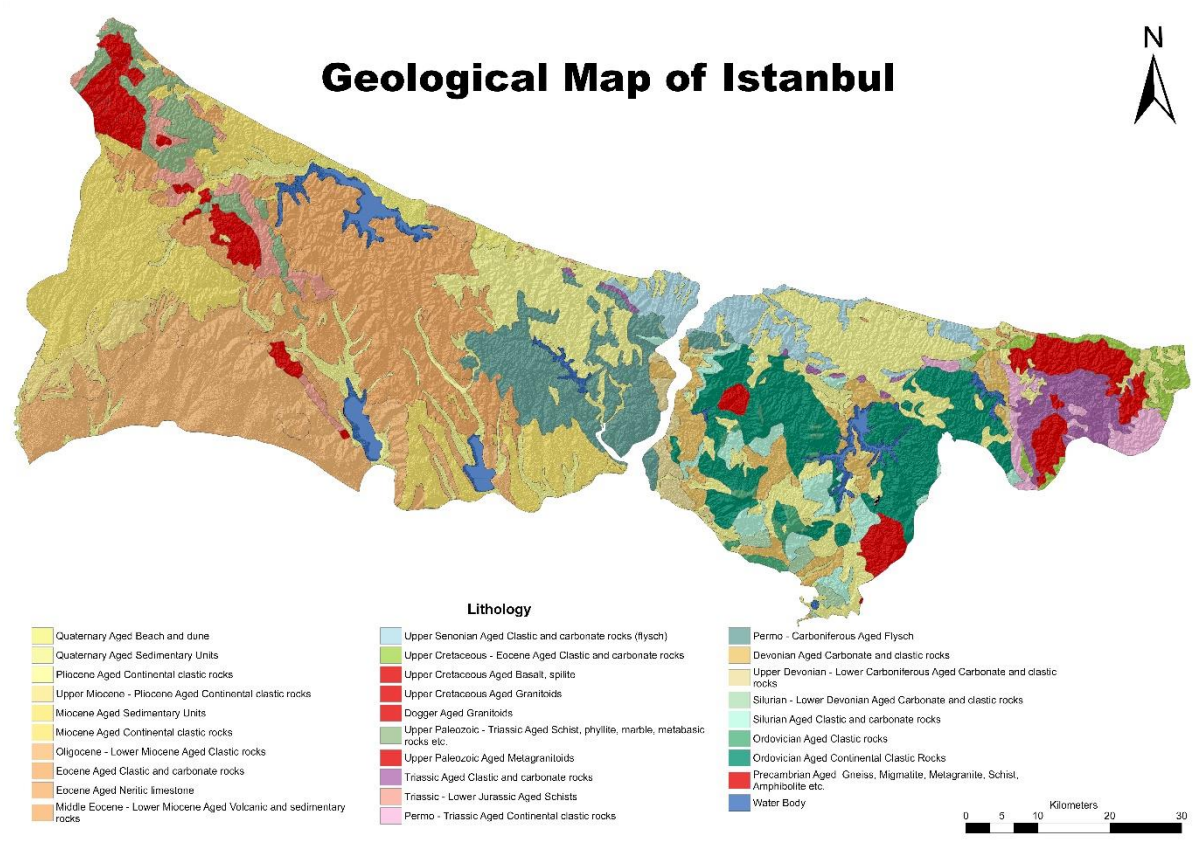

Figure 4. Geological Map of Istanbul (Created using data from MTA)

2.4.1. Palaeozoic Era

Recent studies on the Paleozoic stratigraphy of Istanbul have revealed that there are nine formations associated with this region. These are: the Kocatöngel Formation, which is of Lower Ordovician age; the Kurtköy Formation, also of Lower Ordovician age; the Kınalıada Formation, of Middle-Upper Ordovician age; the Aydos Formation, of Middle-Upper Ordovician age; the Yayalar Formation, of Upper Ordovician-Lower Silurian age; the Pelitli Formation, of Upper Silurian-Lower Devonian age; the Pendik Formation, of Middle-Upper Devonian age; the Denizli Formation, of Upper Devonian-Lower Carboniferous age; and the Trakya Formation, of Lower Carboniferous age. (Lom et al., 2016)

The lowest unit is the Kocatöngel Formation, which is known to consist of clastic covering a foundation that has not surfaced within the borders of Istanbul. This formation is composed of gray-green laminated schist and siltstones, and it has been observed to form in marine or lacustrine environments. No fossils are found within this formation. The formation is characterized by its type locality at the Yeniçiftlik Stream, located south of the Mahmutşevketpaşa village. Based on the surface exposure in the valley, a thickness of approximately 1500-2000 meters is estimated. (Lom et al., 2016)

The Kurtköy Formation continues with purple and green-coloured schist, sandstone, siltstone, and conglomerates at higher levels. The sediment deposition of this formation began with turbidity currents, followed by a rapid transition from a marine to a terrestrial environment, ending with clastic deposits. In Istanbul, a clear section of the formation has been exposed in road cuts at the Küçükyalı-Gülsayı intersections. The thickness of the formation is estimated to exceed 1000 meters. No fossils have been found within this formation. (Özgül, 2011)

The Kınalıada Formation is composed of feldspathic sandstones and quartz, along with siltstone, micaceous clay, and silica-cemented sandstones in the upper sections. This formation is generally exposed in the Adalar region, with the observed thickness of approximately 250 meters. No fossils were found in this formation either. (Özgül, 2011)

The Aydos Formation is mainly composed of quartzites, forming the high and mountainous areas of the city. The highest point of the city, Aydos Mountain, constitutes a large part of this formation. The thickness of the formation varies across different regions, but the most significant exposure is at Aydos Mountain, where the thickness is accepted as 100 meters. Trace fossils have been found on this formation. (Özgül, 2011)

The Yayalar Formation is largely composed of micaceous sandstones. The type locality of the formation, named after the neighbourhood, located north of Tuzla, has been proposed to be the Kınalı Dere Valley, located to the northeast of the neighbourhood. The observed thickness here is estimated to be between 280-300 meters. Numerous macrofossils, such as brachiopods and crinoids, have been observed in this formation. (Özgül, 2011)

The Pelitli Formation is predominantly composed of limestones. The formation starts with shallow marine limestones and ends with nodular limestones in the upper sections. It is exposed in the Kartal and Ümraniye areas of Istanbul, where its thickness has been measured at 320-360 meters. Numerous macrofossils, such as gastropods, brachiopods, and large crinoids, have been found in this formation. (Özgül, 2011)

The Pendik Formation primarily consists of clay-rich, mica-silty fine-grained rocks, with limestone present at certain levels. The southern regions of Kartal district and Şile have been identified as the type locality for this formation. Observations in these areas suggest that the formation's thickness may range from 400 to 600 meters. Moreover, this formation contains a diverse array of macrofossils, including trilobites, gastropods, corals, and crinoids. (Özgül, 2011)

The Denizli Köyü Formation comprises clayey, nodular limestones and flintstones. This formation is exposed in the Şile district, where examinations have revealed a thickness of 25 to 75 meters. Fossils of conodonts and trilobites have been observed within this formation. (Özgül, 2011)

The Trakya Formation is composed of alternating clastic rocks such as sandstone, shale, siltstone, and occasionally conglomerates. It generally contains limestone and lenses of varying thicknesses in its lower sections. The areas covered by this formation extend from the Bosphorus on the European side to the Küçükçekmece and Büyükçekmece lakes, while on the Anatolian side, it is observed between Üsküdar and Kadıköy. The estimated thickness of the Thrace Formation is around 1500 meters. Although the formation is largely fossil-free, macrofossils are occasionally found. (Özgül, 2011)

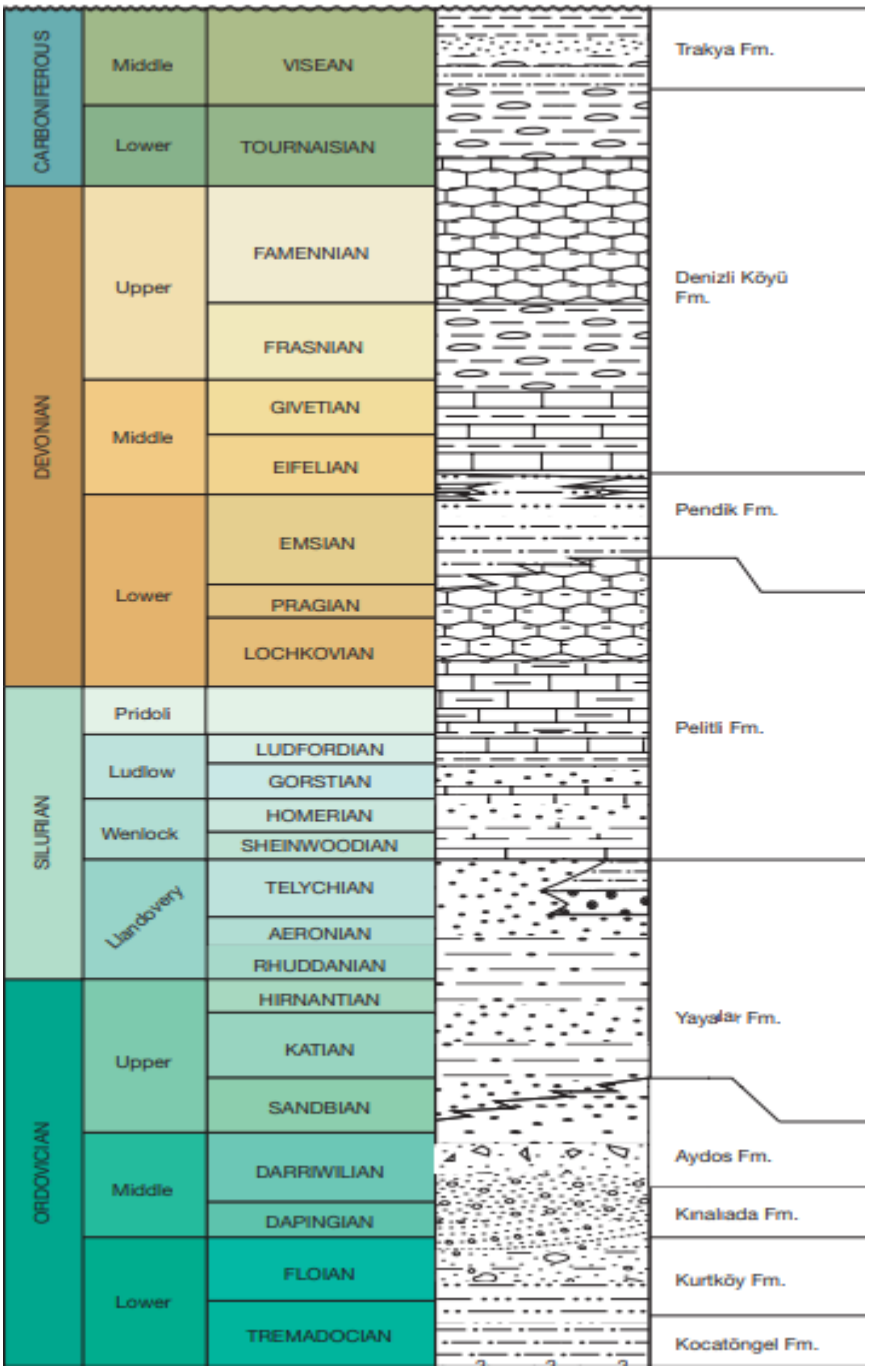

Figure 5.Stratigraphic Section of the Palaeozoic Era for Istanbul. (Lom et al., 2016)

2.4.2. Mesozoic Era

The Kocatarla Formation consists of basaltic lava flows. The Triassic-aged units, exposed in the northwest of Istanbul, unconformably overlie Carboniferous-aged units (Cebeci, 2017).

The Çiftalan Formation generally consists of thickly bedded white-coloured massive units, along with sublitharenite and quartzite (Cebeci, 2017).

The Köseler Formation is known to be covered with limestone. (Cebeci, 2017)

The Bakırlıkıran Formation contains limestone, sandstone, and shales. (Ülgen et al., 2018)

The Sarıyer Group is an Upper Cretaceous assemblage of clastic and volcanic rocks that is distributed across both the Asian and European sides of Istanbul, primarily outcropping in areas close to the Black Sea coast. This group contains two formations: the Bozhane Formation and the Garipçe Formation. The Bozhane Formation consists of gravelly coarse sandstones, marls, volcanic fragmental sandstones, and calcareous shales. It is estimated that the thickness of this formation is approximately 500 meters. The other formation associated with the Sarıyer Group, the Garipçe Formation, features thickly layered sandstones, limestones, basaltic andesitic lava varieties, greenish basalt, and volcaniclastic units. The thickness of the Garipçe Formation is estimated to be around 550 meters. (Özgül, 2011)

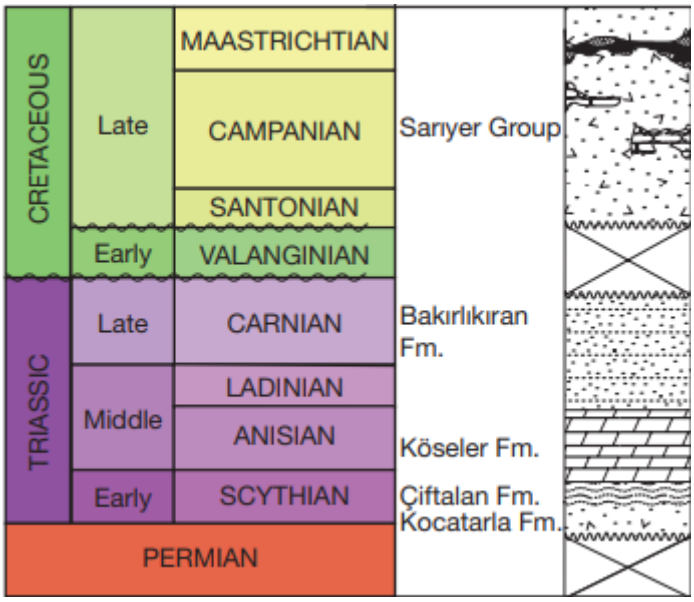

Figure 6.Stratigraphic Section of the Mesozoic Era for Istanbul. (Lom et al., 2016)

2.4.3. Cenozoic Era

The Akveren Formation consists of limestone and calcarenite, which cover a large area. The lower levels contain varying proportions of clayey limestones, clay stones, and marly intercalations. This formation, which covers a wide area in the eastern part of Istanbul, particularly around Şile, shows a thickness of 125 meters. Macro-fossils such as echinoids, ammonites, and belemnites have been identified within the formation. (Özgül, 2011)

The Şile Formation includes sandstone, claystone, and marl units containing debris flows. It is outcropped in the Şile district, which gives the formation its name. The estimated thickness of

this formation ranges between 50 and 100 meters. It contains fossils such as gastropods and small-sized Nummulites. (Özgül, 2011)

The Yunuslubayır Formation consists of yellowish sandstones, limestones, and conglomerates. This formation, which appears approximately 5 kilometres east of the Şile district, shows a thickness of about 40 to 50 meters. Fossils such as Nummulites are noticeable within the sandstones of the formation. (Özgül, 2011)

The Koyunbaba Formation contains clastics formed by the marine sediments of the Cenozoic era, located in the northern part of Thrace, known as the Ergene Basin. The formation comprises conglomerates, sandstones, and marls. Koyunbaba village, after which the formation is named, is the location where this formation outcrops. Studies conducted here have recorded the thickness of the formation as 100 meters. Although rare, fossils such as nummulite, Plesiopod, and Gastropod have been observed. (Özgül, 2011)

The Soğucak Formation is dominated by limestones and has been observed scattered across the Thrace basin. Composed of light cream, dirty white, and greyish limestones, this formation has been measured up to 400 meters in thickness. It encompasses communities of echinoids, bryozoans, benthic macro, and microfossils. (Özgül, 2011)

The Ceylan Formation consists of clay stones, limestones, and particularly marl intercalations, with alternating limestones and sandstones observed. The thickness of this formation, observed around Büyükçekmece, varies between 40-50 meters and 150-200 meters. Traces of transported macrofossils and Nummulites have been identified within the formation. (Özgül, 2011)

The Pınarhisar Formation is characterized by intercalations of gravel stones, limestones, and gravelly sandstones. This formation is observed in the Çatalca region. Although the thickness of the formation varies in places, it has been measured between 70 and 80 meters. Gastropod and fish fossils have been observed in the Pınarhisar Formation. (Özgül, 2011)

The Danişmen Formation consists primarily of sandstones, siltstones, mudstones, shales, and gravelstones. This formation has been exposed in the North Thrace basin, with a calculated thickness of 30-40 meters. (Özgül, 2011)

The Çamurluhan Formation consists of calcareous shales, gravel, quartz conglomerate, sandstones, and limestones. The formation is located south of Küçükköy and Cebeciköy. The thickness of the formation reaches approximately 700 meters. (Ozer, 2020)

Known as the Çekmece Group, this group includes the Çukurçeşme, Güngören, and Bakırköy formations. It is predominantly exposed in the districts known as Büyükçekmece and Küçükçekmece. If ordered from bottom to top, this group encompasses three different levels dominated by sandstone-gravel stone, claystone, siltstone, and marl-limestone, with a maximum thickness of approximately 150 to 200 meters. Representing lake, lagoon, and river environments, this group provides numerous fossil examples. (Özgül, 2011)

The Pliocene-aged Belgrad Formation consists of sand, silt, gravel, and coarse clastic materials. This formation is observed in the northeastern part of the Beykoz district. (Demirelli, 2021)

In the area of Istanbul, alluvial deposits have developed at the bottoms of river valleys flowing into the Black Sea, the Sea of Marmara, and the Bosphorus, typically consisting of fine gravel deposits that are less than about 10 cm in size. These deposits are generally composed of low to medium-sized, semi-rounded clasts and typically consist of sandstone, limestone, and volcanic derivatives. Although their thickness varies in places, it has been observed that this unit exceeds 40 m. (Özgül, 2011)

In some rivers flowing into the Sea of Marmara, beach deposits have formed. These deposits, which extend 5-6 meters below sea level, have generally developed with coastal currents leading into the sea and have persisted in coves protected by waves. Similarly, beach deposits that have emerged along the Black Sea coast have formed coarse sand deposits in locations where rivers opening into the sea narrow. (Demirelli, 2021) (Özgül, 2011)

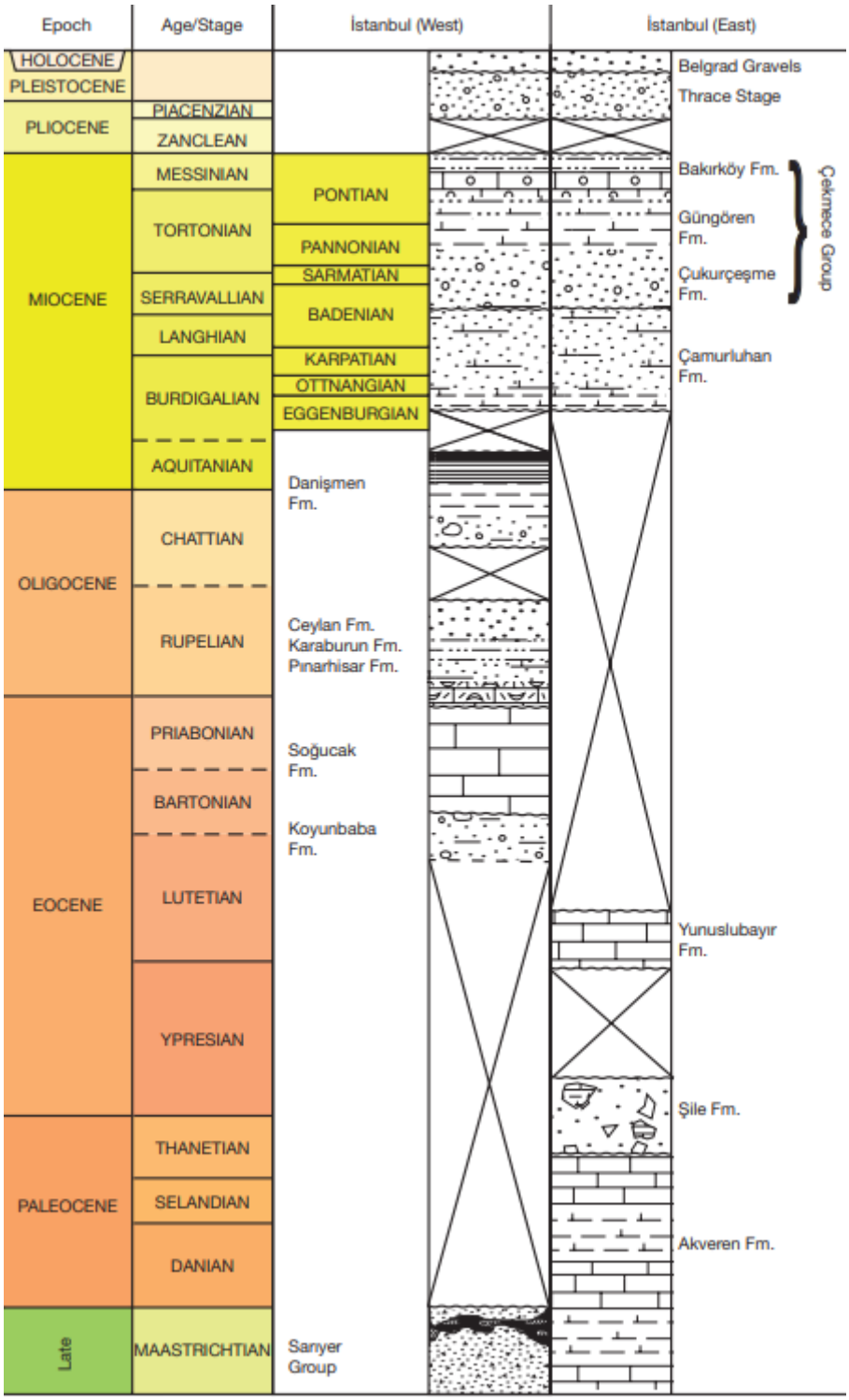

Figure 7. Stratigraphic Section of the Cenozoic Era for Istanbul. (Lom et al., 2016)

2.5. Seismicity of Istanbul and The North Anatolian Fault Zone

Türkiye is located in a major active fault zone, with the East Anatolian Fault in the east, the North Anatolian Fault in the north, and graben systems in the Aegean region. Despite nearly 90% of the country being at risk of earthquakes, it has been caught unprepared for these seismic

events. As a result of the earthquakes that occurred on August 17 and then on November 12, 1999, approximately 20,000 people lost their lives, and tens of thousands were injured or permanently disabled. Additionally, around 400,000 homes and businesses suffered severe damage. (Şimşek and Gündüz, 2021)

2.5.1. North Anatolian Fault Zone (NAFZ)

The North Anatolian Fault Zone (NAFZ), located at the boundary between the Anatolian Plate and the Eurasian Plate, is characterized by high seismic activity and is often likened to a fishbone geometry. With an approximate length of 1,500 km, this fault has been studied in three main segments: eastern, central, and western (Emre et al., 2020). This fault, which is an important structure determining the country's seismic activity, begins in the east at Karlıova. Additionally, it is suggested that this fault is situated within the soft fill created by the Palaeotethys and Neotethys oceans (Şengör and Zabcı, 2019).

Figure 8.The North Anatolian Fault Zone (NAFZ) and Certain Historical Earthquakes.

2.5.2. Historical Earthquakes

Istanbul, which has experienced numerous earthquakes throughout its history and feels the effects of the North Anatolian Fault Line passing through the Marmara region during each seismic event, is documented by Ambraseys as having endured 26 destructive earthquakes during the Byzantine era out of a total of 72. According to records from the Ottoman period, severe earthquakes resulted in the deaths of thousands of people and caused significant structural damage in the city. These include the earthquakes of 1509, 1719, 1766, 1894, and 1912. (Şimşek and Gündüz, 2021)

The earthquake that occurred in AD 32 was felt in Bithynia and destroyed many homes. The intensity of the tremors was noted to have been felt as far away as Athens. (Demirelli, 2021)

In 69, another earthquake struck Bithynia, resulting in numerous casualties. The Roman Imperial treasury assisted in rebuilding efforts following this earthquake, compensating for losses and providing financial support to those who survived. (Demirelli, 2021)

In 155, a significant earthquake occurred in Hellespontus, severely distorting the landscape. The tremor affected the region and caused widespread panic as far as İzmir (Smyrna) and Ephesus. It was reconstructed with the support of Rome. (Demirelli, 2021)

The earthquake of August 24, 358, referred to as a great disaster, resulted in substantial losses. Prominent city figures, including governors and bishops, lost their lives in this earthquake, while subsequent landslides, fires, and ground deformations affected the area. (Demirelli, 2021)

After the earthquake in 396 that struck the European regions of Constantinople, the populace preferred to remain in the streets due to the aftershocks. (Demirelli, 2021)

The earthquake on April 1, 407, which occurred in Hebdomon, now Bakırköy, resulted in the destruction of most homes and caused significant damage in Constantinople. Many ships became unserviceable due to the waves generated by the earthquake. (Demirelli, 2021)

In the earthquake of November 6, 447, a large portion of the city walls of Istanbul collapsed, creating fissures and pits in the ground. Flooding following the tremors and aftershocks persisted for months. (Demirelli, 2021)

The earthquake on December 14, 557, affected the southern part of Istanbul, destroying houses and public buildings of that era, and resulted in numerous fatalities. The damaging aftershocks forced the populace to seek shelter outdoors. (Demirelli, 2021)

The earthquake of October 26, 740, caused significant loss of life and property. Houses, public buildings, churches, and monasteries were destroyed. The retreat of seawater altered the coastal shorelines in some areas. This earthquake demolished more than half of the walls of Constantinople. Aftershocks persisted for a year, instilling fear in the populace. The imperial government imposed additional taxes for the city's reconstruction and recovery. (Demirelli, 2021)

On January 9, 869, an earthquake in Constantinople resulted in casualties and damage to structures, causing the destruction of part of the St. Sophia Cathedral and the Church of the Apostles. The Nika monument, the Hippodrome, and the Church of Anna were also left damaged, necessitating repairs. Aftershocks persisted for over a month. (Demirelli, 2021)

In the earthquake of September 23, 1063, the region between Constantinople and the Dardanelles suffered severe damage, leading to the destruction of most structures. Aftershocks continued for two years following this earthquake. (Demirelli, 2021)

The earthquake that occurred on October 18, 1343, resulted in the destruction of the city walls in Constantinople, damaging and collapsing some defensive fortifications. Aftershocks persisted for one year. (Demirelli, 2021)

On January 16, 1489, an earthquake occurred during the Ottoman Empire, destroying the minarets of several mosques in Istanbul. (Demirelli, 2021)

The major earthquake that occurred on September 14, 1509, referred to in literature as the "little apocalypse," directly demolished over a thousand homes. While varying estimates exist, it is believed that approximately 10,000-13,000 lives were lost in this event. Additionally, historical sources indicate that this earthquake triggered a tsunami and that some individuals fell into fissures and pits formed by the quake. (Şimşek and Gündüz, 2021)

The earthquake of May 22, 1766, is one of the largest to have directly affected Istanbul and continued to exert its influence with aftershocks. Estimated to have a magnitude of 7.2, this earthquake caused destruction in surrounding provinces as well. It has been recorded that more than 5,000 individuals lost their lives as a result. (Şimşek and Gündüz, 2021)

The earthquake on August 17, 1999, had a magnitude of 7.4 and was rated IX on the Mercalli intensity scale, affecting a region inhabited by approximately 15 million people. This disaster resulted in the deaths of 18,373 individuals and injured 48,901 others severely or moderately. Around 100,000 homes were rendered uninhabitable. (Şimşek and Gündüz, 2021)

On the 26th of September 2019, a 5.8 magnitude earthquake occurred along the Kumburgaz segment of the North Anatolian Fault within the Sea of Marmara. Although this earthquake did not cause destructive damage, it served as a stark reminder to the region of the ever-present earthquake risk. It is the most significant earthquake to have affected the region since the August 17th earthquake. The tremor was also felt in neighbouring provinces outside of Istanbul. (Zülfikar et al., 2020)

2.6. Analytic Hierarchy Process

AHP (Analytic Hierarchy Process), identified as an alternative for complex decision-making problems, is a method developed by Saaty in 1977 and 1980. This method is notable for its ease of application and comprehension, as it does not require extensive mathematical computations

and is applicable to a large number of criteria. Suitable for both quantitative and qualitative data, it has been widely used as an essential tool for pairwise comparisons and consistency calculations. Another feature of this method is its ability to be employed in multi-criteria decision-making processes to calculate and determine weights in decision-making problems. (Dişkaya and Emir, 2021)

Determining the weights of the accepted criteria within the AHP analysis is highly significant, as they directly impact the outcome. Once the criteria are selected and defined, each criterion is compared with the others to identify the priorities between pairs of criteria. (Yalçın and Sabah, 2018)

Following the pairwise comparison, a matrix is created, and the consistency ratio (CR) is calculated. If the CR is less than 0.10, the method is considered acceptable. However, if a value greater than 0.10 is obtained, the pairwise comparisons must be carefully reviewed and redone. (Demir and Altaş, 2024)

To determine and calculate the ranks and consistency ratios of AHP weights, Goepel developed a web-based application called AHP-OS in 2018. This online tool facilitates pairwise comparisons and automatically computes the CR value. (Demir and Altaş, 2024)

2.7. ELER (Earthquake Loss Estimation Routine)

In 2009, the ELER software, developed by Boğaziçi University's Kandilli Observatory and Earthquake Research Institute to estimate earthquake tremors and potential loss analyses, incorporates five distinct modules. These modules are known as Hazard, Level 0, Level 1, Level 2, and the Pipeline Damage Module. (ELER, 2024)

The primary purpose of the ELER program is to identify the settlement areas affected by earthquakes and produce maps and data on the estimated number of damaged buildings, fatalities, and injuries that may result from seismic activity in these regions. (Sabah and Bayraktar, 2020)

The data required for this program include earthquake information, demographic data, and fault data. For the analysis, maps of earthquake intensity distribution are generated using attenuation relationships and source parameters from the Hazard Analysis module. In Levels 0, 1, and 2, estimated building damages, fatalities, injuries, and economic losses resulting from a potential earthquake are calculated using the data produced by Hazard Analysis. (Zülfikar et al., 2012)

The ELER program follows the methodology outlined below:

- For the input data of earthquake magnitude and epicenter information, ground motion distributions in the selected area are interpreted using location-specific motion equations and wave velocity distributions.
- If available, real ground motion data is used instead of theoretical information.
- Estimating potential building damages and human casualties.
- Estimating the potential economic losses resulting from building damages after the earthquake.
- Estimating potential pipeline damage following the earthquake. (ELER, 2024)

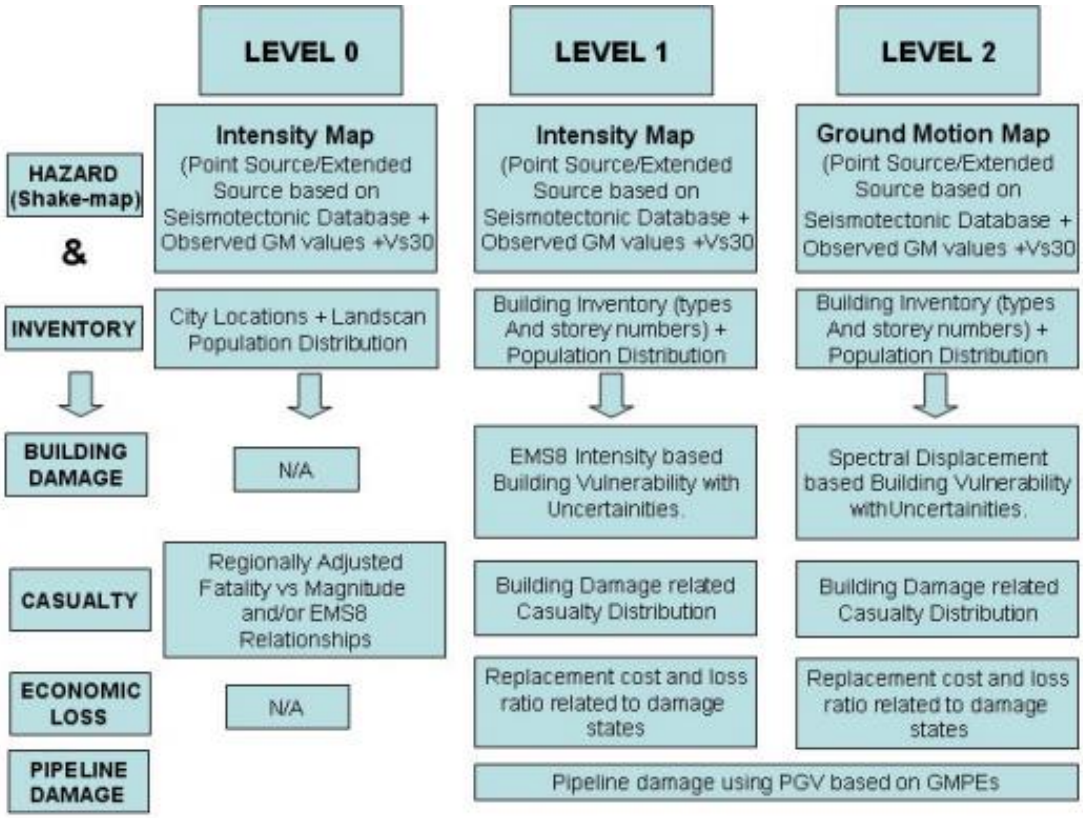

Figure 9. Methodology of ELER (ELER, 2024)

2.8. Previous Studies

Natural disasters and hazards such as floods, fires, and earthquakes significantly impact the societies and geographies they affect. Although these natural events are often brief in duration, their effects on infrastructure damage and other material losses can persist. The proposed risk models are reshaping the perspectives and approaches of scientists, experts, and regional administrators towards natural disaster management. By utilising data derived from hazard,

risk, and damage assessment models, they can seek early solutions for their respective regions. (Karimzadeh et al., 2014)

In terms of disaster planning and management, scenario creation studies, particularly in response to natural disasters such as earthquakes, landslides, and tsunamis, which can directly impact human life, have gained significant attention in recent years. These scenarios have helped identify risks and hazards both before and after disasters, assisting scientists and governments in pre-determining disaster management strategies and emergency response actions. Such scenario studies have increasingly been implemented in developing countries. The Marmara Region has become the primary focus of these efforts due to its historical records of seismic activity and the significant potential for damage and loss. (Erıs et al., 2023)

Risk and damage assessment models are typically constructed using various parameters and mathematical formulations. These models are divided into two main groups as global or local models. Developing a new model for seismic hazard analysis and global assessment of hazard risk using GIS technologies can be highly beneficial for research and development. (Jena et al, 2020)

Creating earthquake scenarios in urban areas is typically divided into a framework or grid format. Earthquake hazard can be interpreted using probabilistic approaches. Probabilities may not occur simultaneously in all created grids or frameworks. Therefore, all losses or damages do not occur to the same extent. Earthquake scenarios contribute significantly by presenting the distribution with probabilities. Taking the example of Istanbul, important components of a scenario earthquake occurring on the North Anatolian Fault include the appropriate analysis and mapping of topographic, geological, and geotechnical data, along with the determination of suitable models. (BU ARC, 2003)

Despite advances in modern technology, it is still impossible to accurately predict the location, depth, and timing of earthquakes. However, tracking fault lines, developing statistical models, creating earthquake risk and potential maps, and analysing historical earthquakes can provide some insights into future seismic events. The energy accumulating along the North Anatolian Fault beneath the Marmara Sea, south of Istanbul, suggests a high probability of rupture in the near future. This impending earthquake is expected to impact Istanbul and nearby provinces, leading to both loss of life and economic damage. (Emre et al., 2020)

Risk identification, planning, and studies can be conducted at national, regional, and local levels. However, the most complex among these are the studies at the city level. It is essential

to consider the multifaceted risks within the city, systematically define the economic and social characteristics of the city and assess its physical conditions. In addition to municipalities and other administrations, social communities and organizations within the city should also support such initiatives. Prior to the occurrence of disasters, it is crucial to collaborate with these communities and raise their awareness. (Erdem, 2013)

Understanding the destructive forces of disasters, particularly earthquakes, has made Geographic Information Systems (GIS) a critical tool for implementing pre- and post-event preventive measures. It is crucial to identify necessary precautions against potential structural damage and casualties in the event of future earthquakes. The ability to guide search and rescue operations during post-earthquake building collapses based on loss estimates further highlights the significance of these applications. Numerous countries and organizations have initiated research in this area, developing various software solutions for loss and damage assessment, resulting in predictive tools for estimating potential impacts and losses. (Nemutlu et al., 2023)

Some of these include the OpenQuake program, developed in Italy, which is an open-source application capable of performing earthquake risk analyses. The SELENA program, developed in Norway, detects seismic waves, determines their location, and analyses them to reveal associated risks. The EQRM (Earthquake Risk Model), developed in Australia, was created by scientists at Geoscience Australia, the country's national geological agency. This program identifies earthquake risks, runs simulations based on parameters, and aids in reducing the risks of seismic activity, contributing to proactive planning for potential hazards. The InaSafe software, developed in Indonesia, evaluates the potential impact of natural disasters resulting from seismic events in the region. This model also has the capability to predict potential damage and casualties. (Hosseinpour et al., 2021)

Another software used in creating earthquake scenarios is ELER (Earthquake Loss Estimation Routine), developed by the Kandilli Observatory as part of a European Union project. This software aims to present the potential physical, social, and economic impacts of earthquakes on society. It starts by analysing earthquake parameters, then focuses on ground motions and soil effects, generating earthquake distribution maps and estimating potential damage and casualties based on these ground movements. (Hancılar et al., 2019)

3. RESEARCH METHODOLOGY

In this thesis, the potential earthquake risk that could affect Istanbul was determined based on criteria found in the literature. To assess the maximum magnitude an earthquake could reach, as well as the damage and impact it might cause in the region, an earthquake scenario was developed. These scenarios were designed within a Geographic Information System (GIS), and the necessary analyses were conducted accordingly. The criteria and literature used to assess the potential earthquake risk are presented in Table 3. The earthquake scenario was created using ArcGIS Pro, a software developed by Esri, and the associated damage and casualties were calculated using this tool. Furthermore, additional damage and casualty analyses were carried out using the ELER software, developed by Kandilli Observatory, where location and magnitude inputs remained consistent with other parameters.

Table 3. The Criteria Found in the Literature and Their Sources

Literature ---------- **Criteria**	**Malakar and Rai, 2023**	**Demir and Altaş, 2024**	**Wen et al., 2016**	**Shrestha and Poudel, 2018**	**Ahmed et al., 2023**	**Jena et al., 2020**	**Atik and Safi, 2024**	**Karimzadeh et al., 2014**	**Hassanzadeh, 2013**	**Aydin et al., 2024**	**Özkazanç et al., 2020**
Building age		☑									
Building density	☑					☑	☑	☑	☑		
Earthquake events	☑			☑	☑	☑	☑				
Elevation (DEM)	☑			☑	☑				☑	☑	☑
Lithology	☑	☑		☑	☑	☑		☑	☑	☑	☑
Distance to Fault	☑	☑			☑	☑	☑	☑			☑
Land use									☑	☑	☑

PGA	☑	☑	☑							☑	
Population	☑					☑	☑	☑	☑	☑	
Slope		☑	☑	☑	☑		☑				☑
Distance to road	☑		☑				☑	☑	☑		

3.1. Data Collection

For the purposes of this thesis, geological data provided by the General Directorate of Mineral Research and Exploration (MTA) at a 1:500,000 scale was used. The lithological and chronological information contained in this data set was utilised in calculating the earthquake potential.

Fault data, Peak Ground Acceleration (PGA) data, and the primary, secondary, and all highway data within Istanbul were obtained from the Istanbul Metropolitan Municipality (IMM). These data sets are of great significance in the calculation of potential earthquake risks.

District-based population and building data for Istanbul were also acquired from the Istanbul Metropolitan Municipality (IMM). Building data were categorized into three time periods: pre-1980, 1980-2000, and post-2000, and were utilised both in the earthquake potential risk map and in damage estimation stages within the scenario.

With the Digital Elevation Model obtained from the United States Geological Survey (USGS), the highest and lowest points of Istanbul were determined. Slope data derived from the Digital Elevation Model were used in the earthquake potential risk map.

Historical earthquake data were obtained from both Disaster and Emergency Management Authority (AFAD) and USGS, utilising two different datasets. AFAD's historical and instrumental earthquake data contributed to the potential risk map.

Land use data, produced and adjusted by the Esri team, were used to show changes between 2017 and 2023.

The data for provincial and district boundaries have been obtained from the General Directorate of Maps (HGM).

Table 4. The Data Used in the Study, Data Sources, and Formats

Criteria	Data Source	Data Type (Format)
Geological data	MTA	Shapefile (.shp)
Population and Building	IMM	XLSX files (.xslx)
PGA, Fault and Road	IMM	Shapefile (.shp)
DEM	USGS	Raster (.tiff)
Historical Earthquake	AFAD	CSV files (.csv)
Land Use	ESRI	Shapefile (.shp)
Boundaries	HGM	Shapefile (.shp)

The coordinate system selected for this study is WGS 1984 UTM Zone 35N.

3.2. Seismic Potential Assessment and Risk Mapping

In the creation of the earthquake potential risk map, geological data, fault data, Digital Elevation Model (DEM), slope, population, building count, building age, Peak Ground Acceleration (PGA), road data, land use, and historical earthquake data have been utilised. These datasets have initially been formatted appropriately before being displayed on the map.

The aim of this study is to identify earthquake risk zones in Istanbul using the Analytical Hierarchy Process (AHP) within a Multi-Criteria Decision-Making (MCMD) framework. The weightings of the criteria used in the research were determined through pairwise comparisons in AHP, based on data reviewed in the literature. These weightings were applied to analyse the criteria, leading to the identification and mapping of regions with earthquake potential and associated risks.

A classification from 1 to 10 has been established for the criteria intended for use in the calculation of potential risk values. In this context, a value of 10 has been designated as the location with the highest earthquake risk. The classification of the criteria is presented in Table 5. When combined with the weights obtained through AHP, these classified criteria constitute the earthquake potential risk.

3.2.1. Criteria

Building Ages: The building data obtained by the Istanbul Metropolitan Municipality (IMM) for the city of Istanbul has been categorised into three distinct classifications based on district: pre-1980, 1980-2000, and post-2000. Upon aggregation of the data pertaining to these districts, it has been determined that there are 516,538 buildings constructed prior to 1980, 1,096,052 buildings erected between 1980 and 2000, and 719,282 buildings constructed after 2000 in Istanbul. It is feasible to anticipate potential damages and economic losses associated with buildings constructed prior to 2000, which do not conform to the regulations amended following the earthquake on 17 August 1999. This criterion has been proposed by Sarvar (2011) and further supported by Demir and Altaş (2024).

Buildings: Buildings plays a crucial role in potential risk assessments, being one of the key factors that increases the likelihood of damage and collapse in the event of seismic activity. For a densely populated city like Istanbul, this criterion has been suggested in the literature by Atik and Safi (2024).

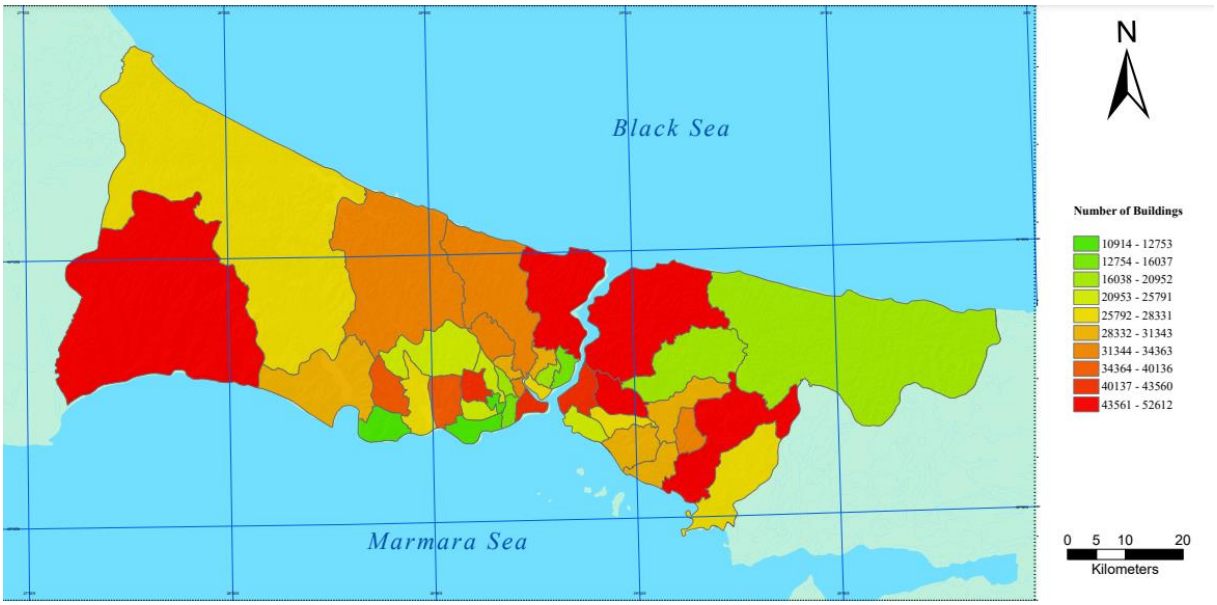

Figure 10. Number of Buildings by District

Earthquake events: Earthquakes follow recurrence intervals, and once these periods elapse, the likelihood of an earthquake reoccurring and impacting the region becomes significant. Areas with a history of frequent seismic activity, especially those in close proximity, are at higher risk of direct impact.

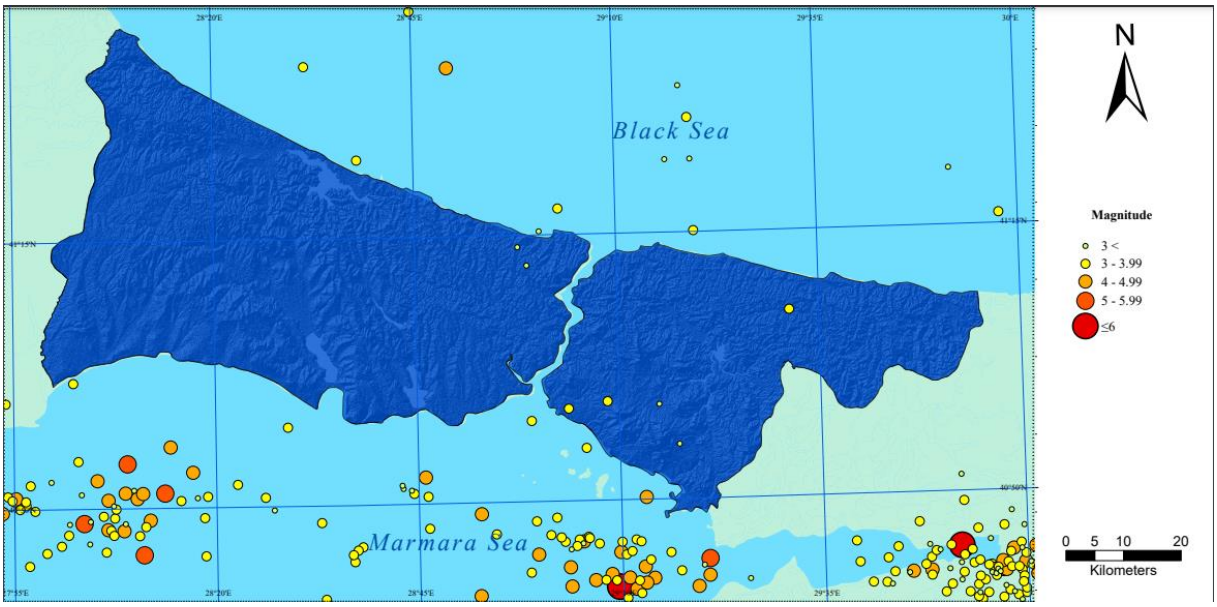

Figure 11. Earthquake Activity Map (Created using data from AFAD)

Digital Elevation Model (DEM): Elevated areas are affected more than flat and gentle regions due to their tectonic and structural forms. This criterion, encountered in the literature and proposed by many researchers, has been articulated by Malakar and Rai (2023) as well as Shrestha and Poudel (2016).

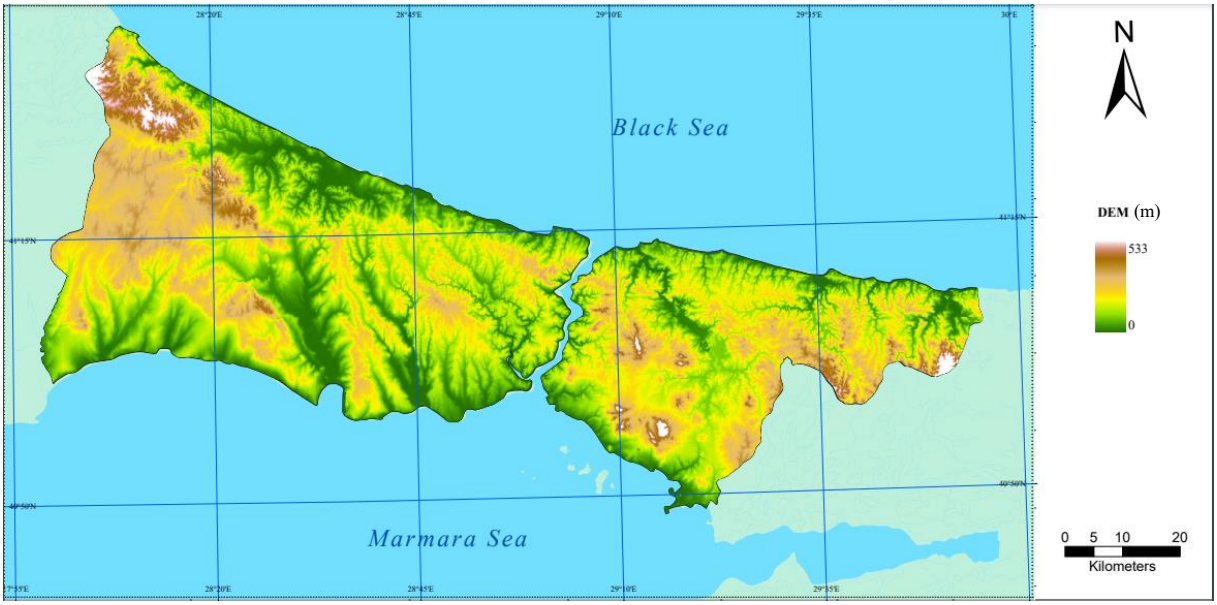

Figure 12. Digital Elevation Model (DEM) Map of Istanbul

Lithology: Upon review of the literature, it is evident that lithology is one of the essential criteria to be included in studies concerning earthquake damage and risk potential. Many studies have reached a consensus on this criterion, as the type of rock present in the soil has a direct

influence on its properties and significantly affects earthquake resistance. Soft, unconsolidated materials such as sandstone and shale may lead to higher levels of damage during seismic events. The amplification factor of seismic waves through rocks plays a crucial role in determining earthquake risk. (Jena and Pradhan, 2020)

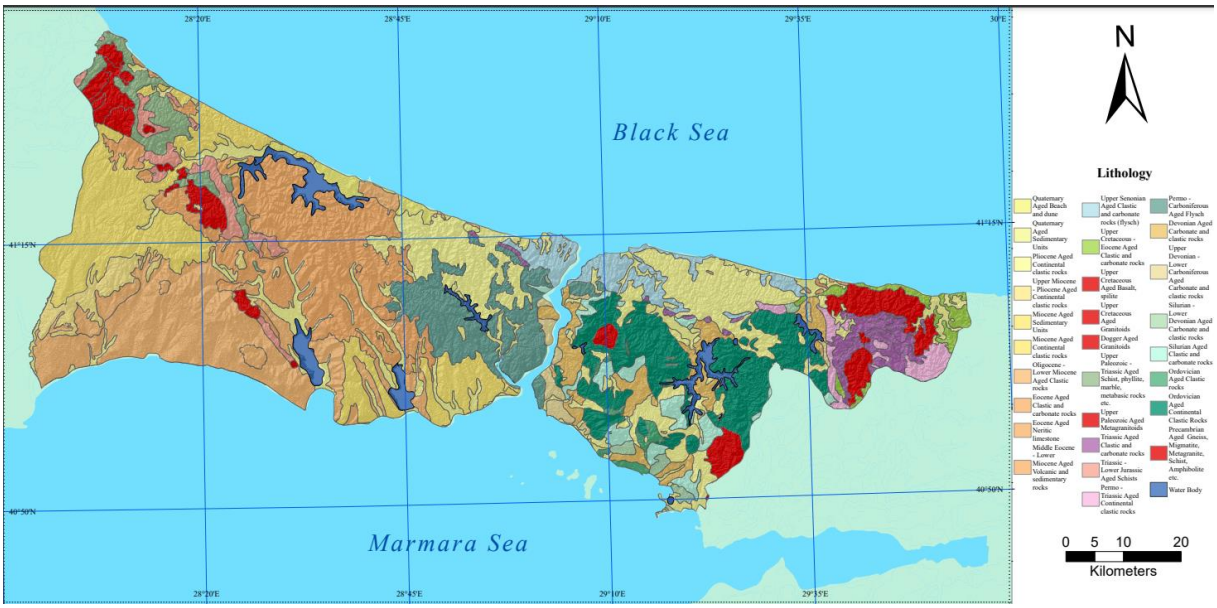

Figure 13. Map of the Lithological Units within Istanbul

Distance to Fault: One of the most significant criteria in understanding earthquake damage risk is the proximity to fault lines. Generally, if the ground and structures near active faults are weak, the risk is further exacerbated. Therefore, constructing buildings and other structures at a safe distance from fault lines contributes to risk reduction. In this study, fault distances were determined based on a review of the relevant literature.

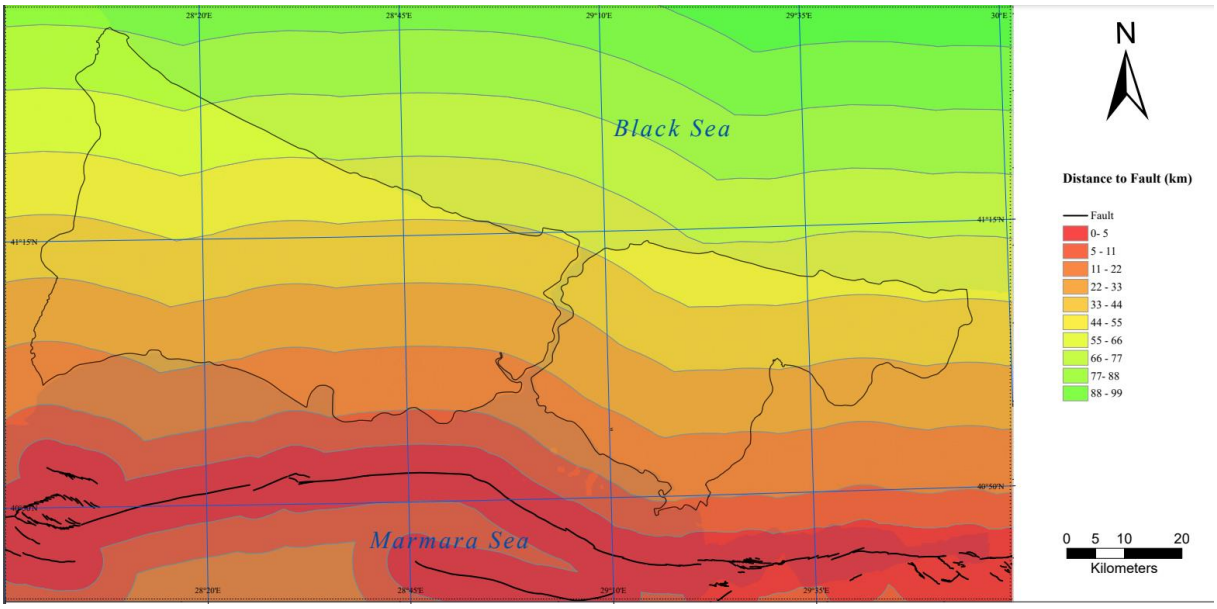

Figure 14. Fault and Distance to Fault Map

Land use: Understanding land uses and purposes during an earthquake is one of the criteria employed to assess risk potential. In the literature review, this criterion has been proposed by Özkazanç et al. (2020), Aydin et al. (2024), and Hassanzadeh et al. (2013).

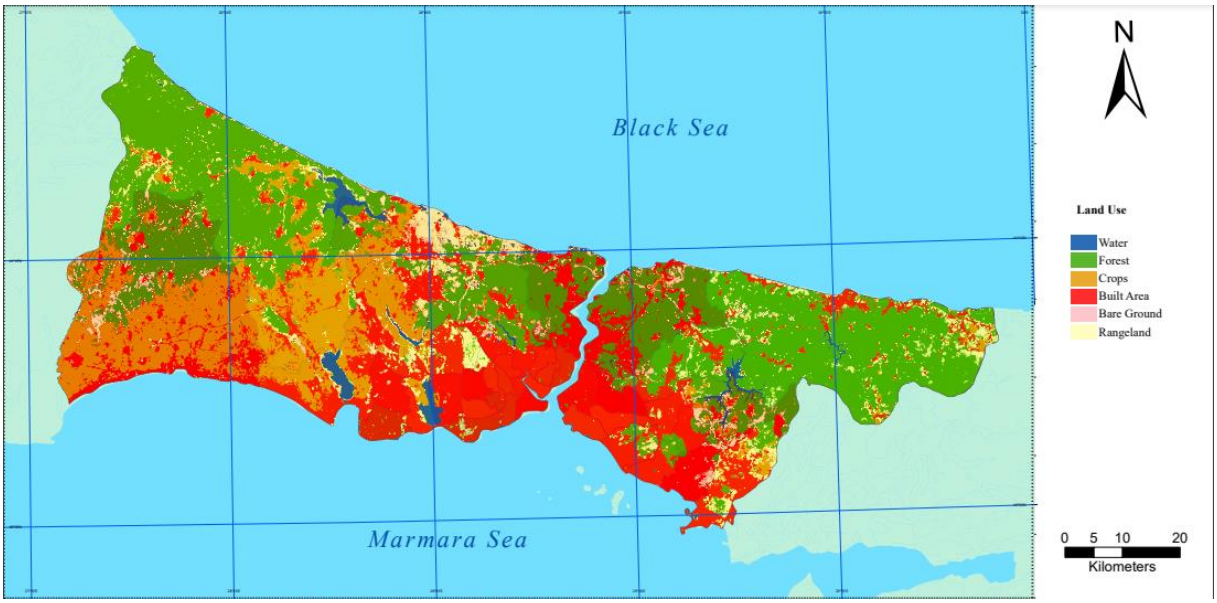

Figure 15. Land Use Map for the City of Istanbul

PGA: Once an earthquake occurs at a specific location, varying levels of ground shaking propagate from the epicentre to different areas. Peak Ground Acceleration (PGA), which measures these horizontal ground motions, is the most critical criterion in calculating

earthquake risk potential. Literature reviews have identified PGA as the factor most significantly influencing earthquake impact.

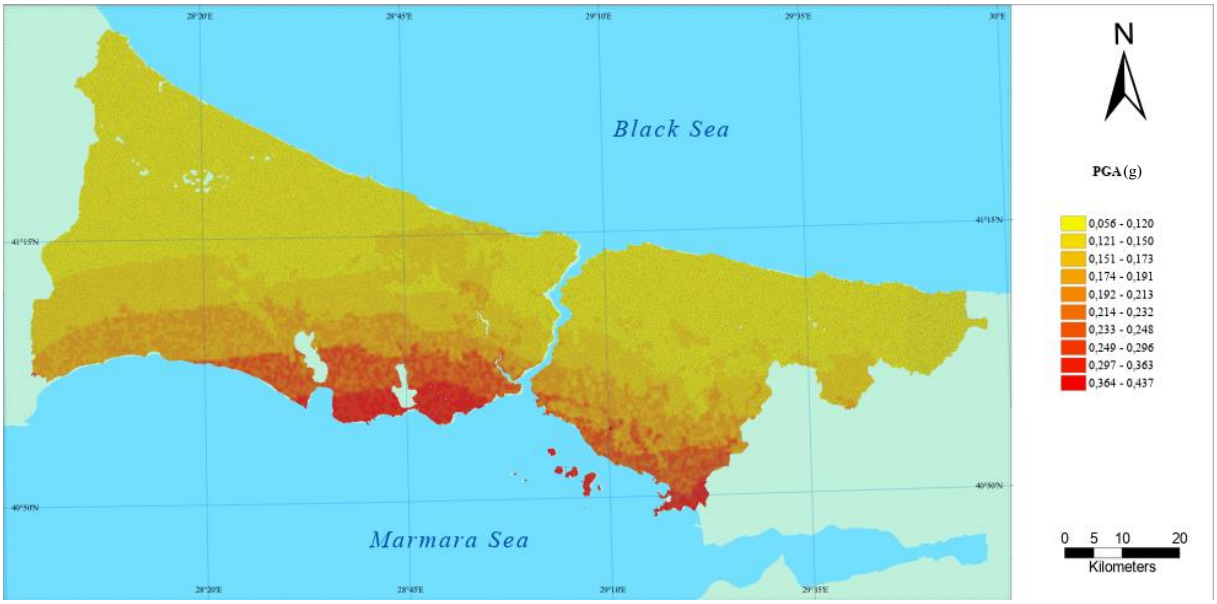

Figure 16. Peak Ground Acceleration (PGA) Map of Istanbul

Population: The literature frequently highlights the population of cities and individuals who experience and face the impacts of earthquakes. In regions located closer to seismic activities, higher population density generally reduces the overall resilience of the area.

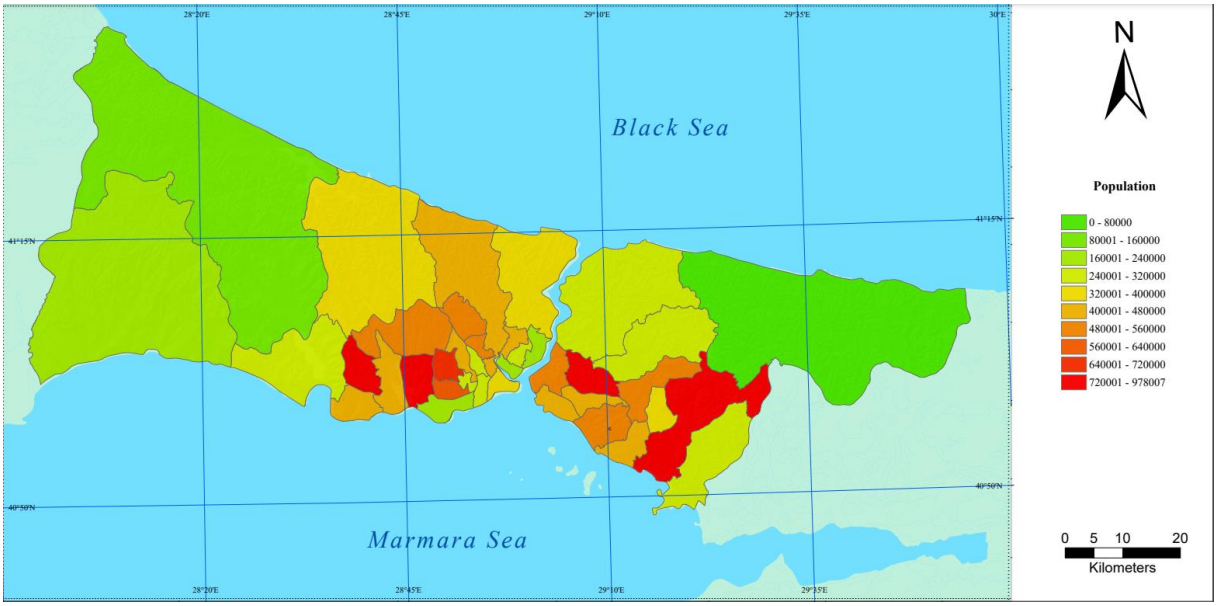

Figure 17. Population Distribution Map by Districts of Istanbul

Slope: Another criterion frequently selected in literature reviews is slope, where areas with steep gradients exhibit a higher potential for damage, often leading to instability in certain

structures during an earthquake. Additionally, regions with significant slopes are at risk of potential landslides or mass movements triggered by seismic activity, posing further hazards (Demir and Altaş, 2024).

Figure 18. Istanbul Slope Map

Distance to Road: Another crucial criterion for both pre- and post-earthquake scenarios is the road infrastructure that facilitates transportation. The continuity of safe access via primary and secondary roads, as well as highways, has been proposed in the literature by Yang et al. (2021).

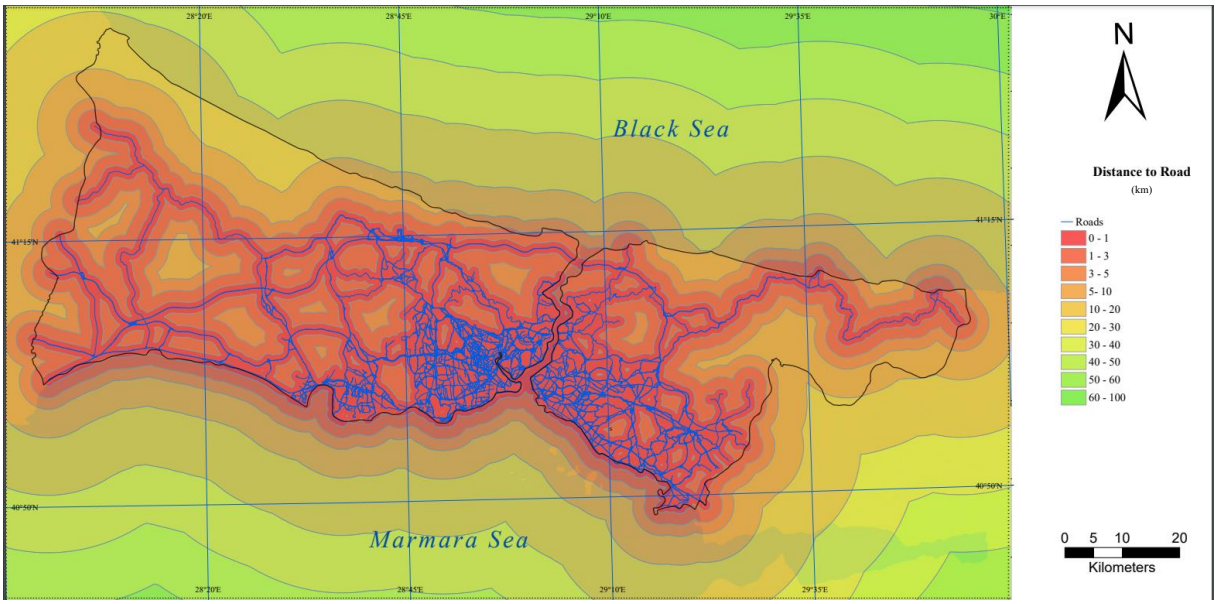

Figure 19. Distance Map Representation of Primary, Secondary, and Highway Networks Used in Istanbul

Table 5. Reclassification of the Data into 10 classes.

Criteria	Value		Reclassified	
PGA	0.056 - 0.120	0.214 – 0.232	1	6
	0.121 - 0.150	0.233 – 0.248	2	7
	0.151 - 0.173	0.249 – 0.296	3	8
	0.174 – 0.191	0.297 – 0.363	4	9
	0.192 – 0.213	0.363 – 0.437	5	10
Distance to fault (km)	88 - 99	44 – 33	1	6
	77 - 88	33 – 22	2	7
	77 – 66	22 – 11	3	8
	66 – 55	11 - 5	4	9
	55 – 44	5 – 0	5	10
Lithology	-	Volcanic Rocks	1	6
	-	Cenozoic Rocks	2	7
	Palaeozoic Rocks	Sedimentary Rocks	3	8
	Mesozoic Rocks	-	4	9
	-	-	5	10
Earthquake events (km)	88 - 99	44 – 33	1	6
	77 - 88	33 – 22	2	7

	77 – 66	22 – 11	3	8
	66 – 55	11 - 5	4	9
	55 – 44	5 – 0	5	10
Buildings	10914 – 12753	28332- 31343	1	6
	12754 – 16037	31344 – 34363	2	7
	16038 – 20952	34364 - 40136	3	8
	20953 – 25791	40137 - 43560	4	9
	25792 – 28331	43561 - 52612	5	10
Buildings ages	-	1980 – 2000	1	6
(year)	-	-	2	7
	Post 2000	-	3	8
	-	Pre – 1980	4	9
	-	-	5	10
Population	0 – 80000	400001 - 480000	1	6
	80001 – 160000	480001 - 560000	2	7
	160001 – 240000	560001 – 640000	3	8
	240001 – 320000	640001 – 720000	4	9
	320001 – 400000	720000 – 1000000	5	10
Land use	-	Crops	1	6
	Water	-	2	7
	Bare ground	Built Area	3	8
	Forest	-	4	9
	Rangeland	-	5	10
DEM	0 – 35.5	171.40 – 204.83	1	6
(m)	35.6 – 75. 24	204.84 – 244.55	2	7
	75.25 – 108.69	244.56 – 294.71	3	8
	108.70 – 140.04	294.72 – 361.60	4	9
	140.05 – 171.39	361.61 - 533	5	10
Slope	0 – 2	9.26- 11.26	1	6
(degrees) (°)	2.1 – 3.70	11.27 – 13.72	2	7
	3.71- 5.55	13.73 – 16.65	3	8
	5.56 – 7.40	16.66 – 20. 66	4	9
	7.41 – 9.25	20.67 – 39.34	5	10

Distance to road (km)	100	20	1	6
	60	10	2	7
	50	5	3	8
	40	3	4	9
	30	1	5	10

3.2.2. Analysis

The Analytic Hierarchy Process (AHP), one of the recommended techniques for conducting Multi-Criteria Decision Making (MCDM), was developed by Saaty (1980) and has become a widely used decision-making mechanism. AHP seeks to solve problems by scoring each criterion in order of importance or by assigning weights based on priority. The first step in AHP involves selecting criteria and categorising them into sub-criteria or classifications. Each criterion is compared pairwise, establishing a relative importance order and creating a pairwise comparison matrix. The pairwise comparison scale ranges from 1 to 9, as illustrated in Table 6. Following the preparation of the pairwise comparison matrix, the consistency ratio (CR) calculated should be less than 0.10. Otherwise, it is anticipated that the decisions are inconsistent, necessitating a re-evaluation of the pairwise comparisons.

Table 6. The Pairwise Comparison Scale

Scores	Definition
1	Equal importance
3	Moderate importance
5	Strong importance
7	Very strong importance
9	Extreme importances
2,4,6,8	Intermediate values

A pairwise comparison-based AHP decision survey has been prepared for the criteria identified in the literature to assess earthquake risk potential. For the study area, decisions were made using AHP-OS, which is available online as an open-source web-based tool. A total of 55 pairwise comparisons were conducted to create a matrix based on the 11 selected criteria.

Table 7. The AHP Matrix and Resulting Weights Generated

	1	**2**	**3**	**4**	**5**	**6**	**7**	**8**	**9**	**10**	**11**	**Weight (%)**
1	1	3	5	7	9	9	7	9	9	9	9	33.3
2	0.33	1	3	5	7	7	7	5	9	9	9	21.8
3	0.2	0.33	1	3	5	5	7	5	7	7	9	14.5
4	0.14	0.2	0.33	1	5	5	7	5	7	7	9	11.4
5	0.11	0.14	0.2	0.2	1	0.33	1	0.33	0.33	0.33	5	2.4
6	0.11	0.14	0.2	0.2	3	1	1	0.33	1	1	1	2.6
7	0.11	0.14	0.14	0.14	1	1	1	0.33	1	1	1	2.1
8	0.14	0.2	0.2	0.2	3	3	3	1	3	3	5	5.2
9	0.11	0.11	0.14	0.14	3	1	1	0.33	1	1	1	2.4
10	0.11	0.11	0.14	0.14	3	1	1	0.33	1	1	1	2.4
11	0.11	0.11	0.11	0.11	0.2	1	1	0.2	1	1	1	1.8

(1- PGA, 2- Distance to fault, 3- Lithology, 4- Earthquake Events, 5- Buildings,

6- Buildings ages, 7- Population, 8- Land use, 9- DEM, 10- Slope, 11- Distance to road)

As a result of the calculations performed on the obtained matrix, the consistency ratio was computed to be 0.089, thus satisfying the criterion of CR < 0.1.

At this stage of the study, the data were assigned weight values based on the AHP criteria. The raster data produced using ArcGIS Pro and reclassified for each criterion, together with the weights derived from the matrix results, constitute the earthquake damage-risk potential map for Istanbul.

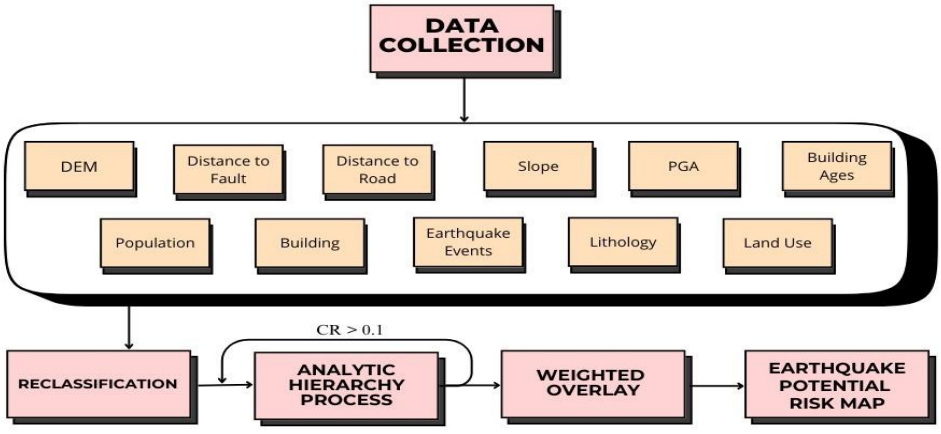

Figure 20. Potential Risk Research Model.

3.3. Creating an Earthquake Scenario

To create an earthquake scenario, it is essential to first ascertain the location and magnitude of the earthquake. Following the identification of the location on a fault that triggers the earthquake, magnitude calculations were conducted using the formula developed by Wells and Coppersmith (1994) found in the literature. In the formula, M represents the magnitude of the earthquake, and L denotes the length of the fault.

$$M = 5.16 + 1.22 * \log(L)$$

As part of the scenario development, an earthquake calculation has been made assuming the simultaneous rupture of the Kumburgaz, Adalar, and Çınarcık segments of the North Anatolian Fault, which is known to produce a significant earthquake approximately every 250 years. The total length of these segments is 152 km. When this value is entered into the above formula, the magnitude (M) is calculated as 7.6.

Using the obtained magnitude of 7.6, two different scenarios have been applied employing the coefficients from the August 17, 1999, earthquake and the ELER software. The designated location for this 7.6 magnitude earthquake is at the coordinates 28.86° E, 40.88° N.

3.3.1. Scenario 1

To predict the potential impact of the identified fault in the creation of earthquake scenarios, intensity maps are being developed. The intensity calculation for a possible Istanbul earthquake will be conducted using the attenuation relationship derived by Erdik and Eren (1983) for the North Anatolian Fault. In this formula, I represent the intensity value, M denotes the earthquake magnitude, and R is defined as the distance to the fault.

$$I = 0.34 + 1.54\ M - 1.24\ \mathrm{Ln}(R)$$

The relationship between the intensity and fault distance obtained for the identified earthquake of magnitude 7.6 has been calculated based on the formula and is presented in Table 8.

Table 8. The Relationship Between Intensity and Distance to Fault for an Earthquake of Magnitude 7.6

Intensity (I)	R (km)
I	7354.71
II	3285.02
III	1466.93
IV	654.75
V	292.35
VI	130.57
VII	58.32
VIII	26.06
IX	11.64
X	5.20
XI	2.32
XII	1.04

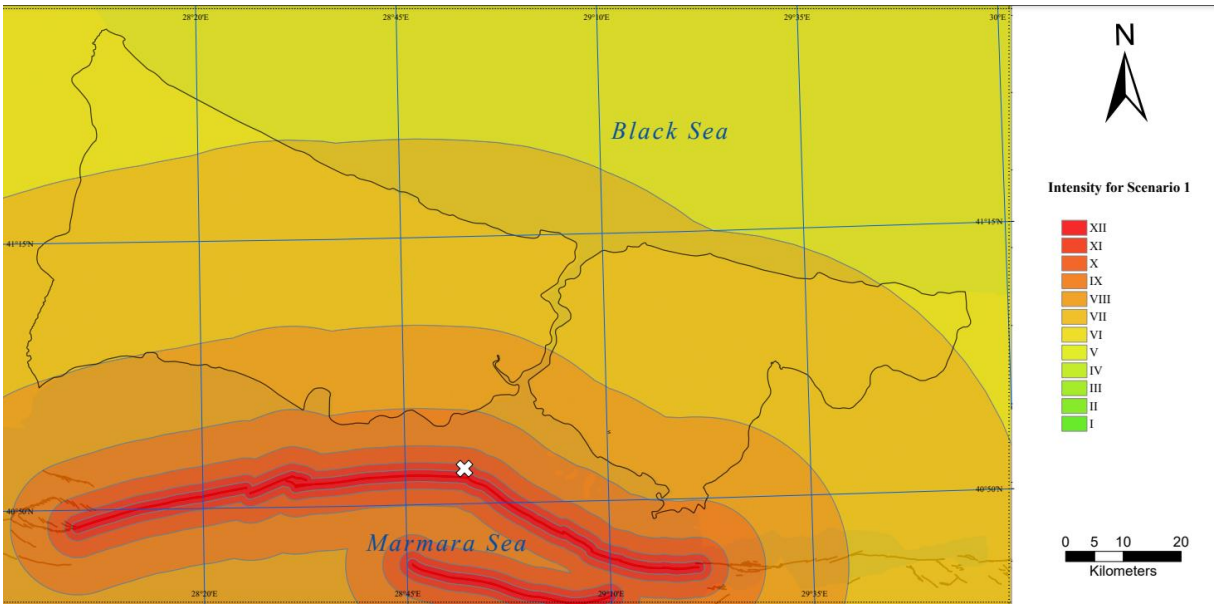

Figure 21.Distance to Fault and Intensity Distribution Map

The percentages of buildings that sustained severe damage or collapsed, as well as those that experienced moderate and slight damage, according to varying intensity levels in the 17 August

1999 earthquake, have been obtained by Bayraktar and Hossın (2021). The percentages are provided for intensities VI, VII, VIII, IX, and X.

Table 9. The Relationship Between the Intensity and Distribution of Building Damage Resulting from the Earthquake of 17th August 1999.

Intensity	Severe damage or collapsed (%)	Moderate Damage (%)	Slight Damage (%)
VI	0,04	0.22	0.24
VII	0.91	2.67	2.59
VIII	2.82	4.41	5.31
IX	15.70	18.16	22.75
X	33.06	15.29	19.04

Using data obtained from the 17 August 1999 earthquake, calculations and equations related to the number of housing units, the number of severely damaged buildings, the number of moderately damaged buildings, the number of slightly damaged buildings, the number of fatalities, the number of injuries, the number of people left homeless, and the need for tents after the earthquake have been derived by Sabah and Bayraktar (2020). These equations are presented below.

$$Number\ of\ Fatalities = Number\ of\ Severely\ Damaged\ Buildings * 0.26$$

$$Number\ of\ Injuries = Number\ of\ Fatalities * 2.515$$

$$Number\ of\ People\ Left\ Homeless = (Total\ Number\ of\ Severely\ and\ Moderately\ Damaged\ Buildings) * Number\ of\ Households.$$

$$Number\ of\ Tents\ Required = Number\ of\ People\ Left\ Homeless / Number\ of\ Households.$$

The equations for the needs that may arise after an earthquake, including toilets, showers, bandages, field hospitals, daily drinking water, canned food, bread, and blankets, have been determined by Hassanzadeh et al. (2023). These equations are as follows.

$$Total\ Damaged\ Population\ (TDP) = Total\ population - Casualties$$

$$Emergency\ Toilet = TDP / 20$$

$$Emergency\ Bath = TDP / 20$$

*Bandage = (Hospitalized injuries + Injured and not hospitalized) * 10*

Field Hospital = Hospitalized injuries / 100

*Drinking Water (bottle per day) = 3 * TDP*

*Canned Food (per day) = 4 * TDP*

*Bread (Loaves per day) = 2 * TDP*

*Blanket = 1 * TDP*

Using the equations, data has been obtained for the assessment of potential damage and loss resulting from a possible 7.6 earthquake in Istanbul, including the number of heavily, moderately, and lightly damaged buildings; the number of deceased and injured individuals; the number of people who will be left homeless; the number of tents; and the necessary facilities required after the earthquake, such as toilets, baths, field hospitals, bandages, water, food, bread, and blankets.

3.3.2. Scenario 2

In Scenario-2, created using the ELER program, the same location and earthquake magnitude were used once again. For this application, a grid was generated for Istanbul, and population and building data were processed using data from the Istanbul Metropolitan Municipality (IMM). The ELER software consists of four sections: Hazard Analysis, Level 0, Level 1, and Level 2.

In the Hazard Analysis section, parameters such as the selected location, earthquake magnitude, fault geometry, fault type, and other factors are used to automatically calculate PGA, PGV, intensity, and ground motion periods (for 0.2 and 1 seconds), and these are provided as output. In Level 0, intensity maps are produced for large regions and areas, and based on the population, estimated casualties are analysed, with a map output generated. In Level 1, using 0.05° x 0.05° grids for the region, building damage and casualties are estimated based on the building and population data, and isoseismic maps and damage assessments for buildings and casualties are created based on the grid data. In Level 2, using 0.2 and 1-second ground motion data and the PGA data generated, isoseismic and ground motion maps are produced, incorporating building inventory and population data for the grids. Furthermore, the program uses different literature formulas to create separate maps for building damage, casualties, and economic losses.

For Scenario-2, using 300 different grids and a 7.6 magnitude earthquake at the location of 28.66° E, 40.88° N, the Boore and Atkinson (2008) ground motion model was selected in the program, and since the NAFZ is a strike-slip fault, fault type 2 was chosen. To generate the intensity map, the parameters from Atkinson and Kaka (2007) were used, and the program was run. With the obtained intensity map, in the Level 0 section, three different casualty estimates for Istanbul were completed, listed, and mapped. In Level 1, the intensity data and grid data created for Istanbul were processed, and building damage estimations were made according to five different damage levels defined by ELER. Additionally, three different casualty estimates were calculated based on Coburn, Risk UE, and KOERI (2002). In Level 2, the program was run using the grid data and ground motion data at 0.2 and 1 seconds, and building damage, casualties, and economic losses were calculated.

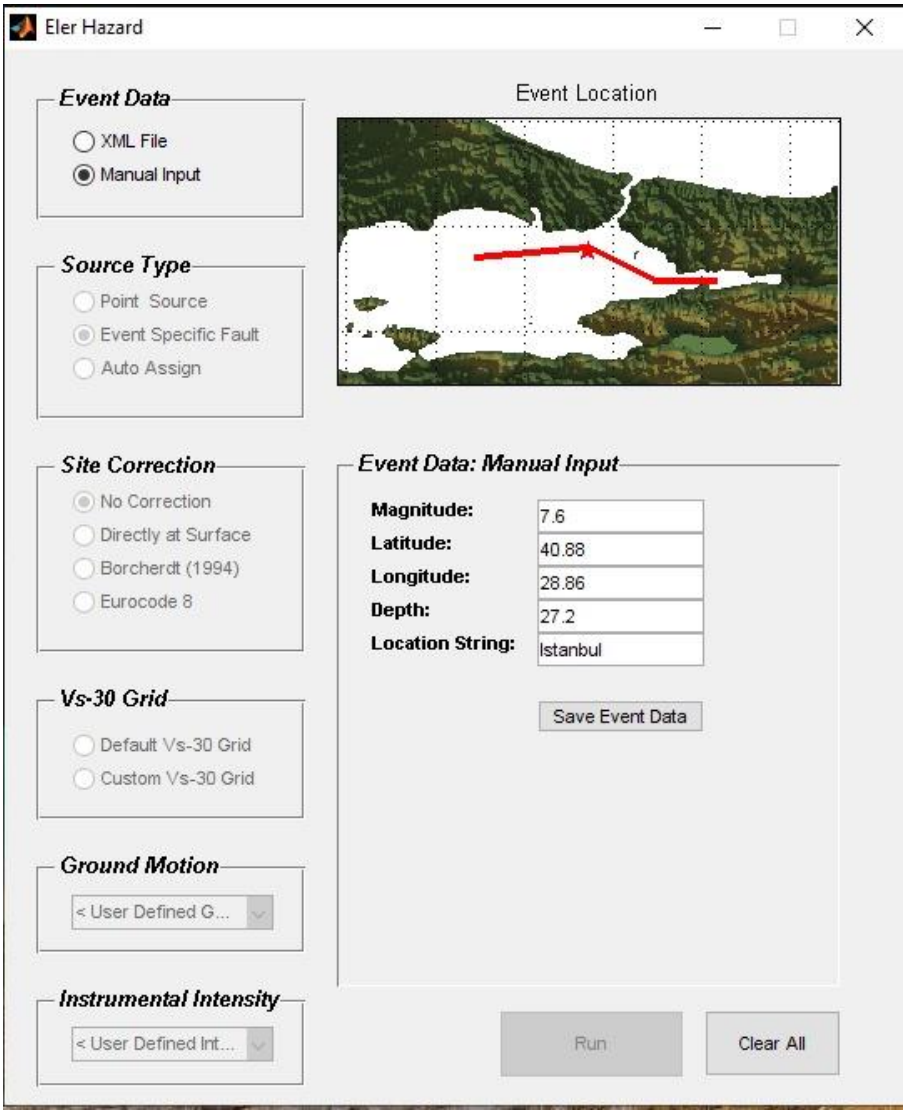

Figure 22. Entering Earthquake Data in the Hazard Analysis Section of the ELER programme

4. RESEARCH FINDINGS

The raster data for each criterion was reclassified on a scale from 1 (low risk) to 10 (high risk), and the earthquake potential risk values for Istanbul were calculated by multiplying these values by the weights derived from the AHP. Following these calculations, the maximum value was determined to be 8.65, and the minimum value was 2.60. The risk levels were classified as follows: 2.60-4.14 for "low," 4.15-5.30 for "moderate," 5.31-6.44 for "high," and 6.46-8.65 for "very high," and these were mapped accordingly.

Using the output of these values, a table showing the maximum, minimum, and mean values for each district was generated through the Zonal Statistics tool in ArcGIS Pro. Based on the results, Bahçelievler, Beylikdüzü, and Küçükçekmece emerged as the highest-risk districts in Istanbul, while Çatalca, Şile, and Beykoz were identified as having lower risk levels.

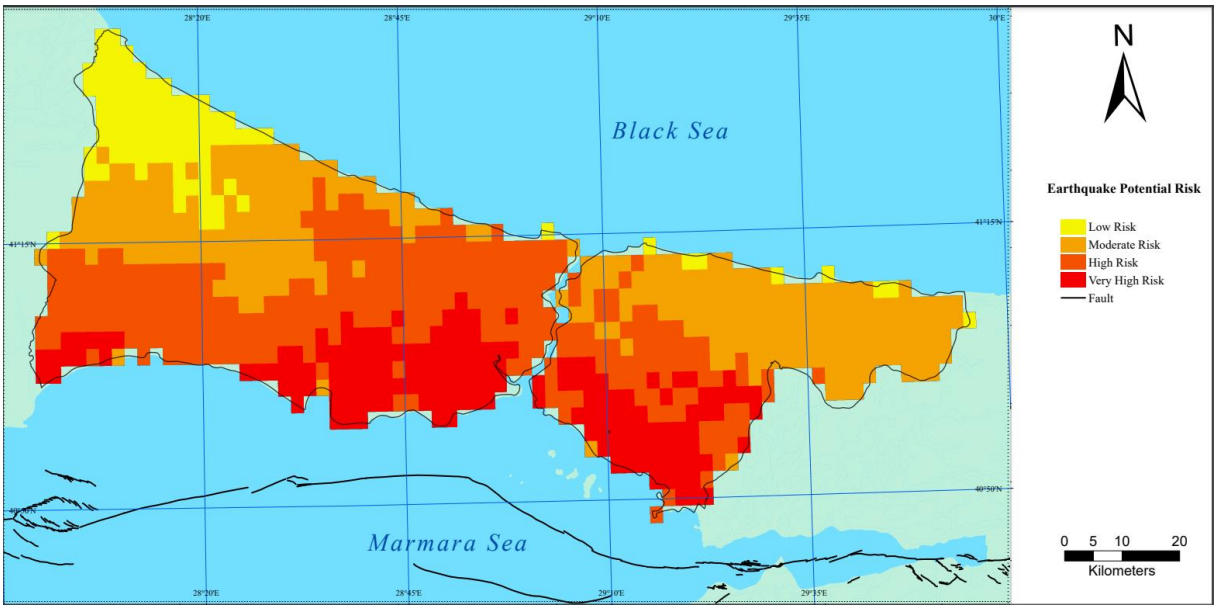

Figure 23. Istanbul Earthquake Potential Risk Map

For Scenario-1, district-based calculations have been conducted separately, yielding the following results. In total, 47,663 buildings in Istanbul are estimated to have sustained severe damage or collapsed, 66,191 buildings experienced moderate damage, and 79,928 buildings were able to withstand the earthquake with minor damage.

In the district-based calculations, the municipalities in Istanbul experiencing the maximum intensity of shaking have been identified as Adalar (X), Avcılar (IX), Bakırköy (IX), Beylikdüzü (IX), Küçükçekmece (IX), and Tuzla (IX). Conversely, the districts expected to experience the lowest intensity are Beykoz (VII), Çekmeköy (VII), Sarıyer (VII), and Şile (VII).

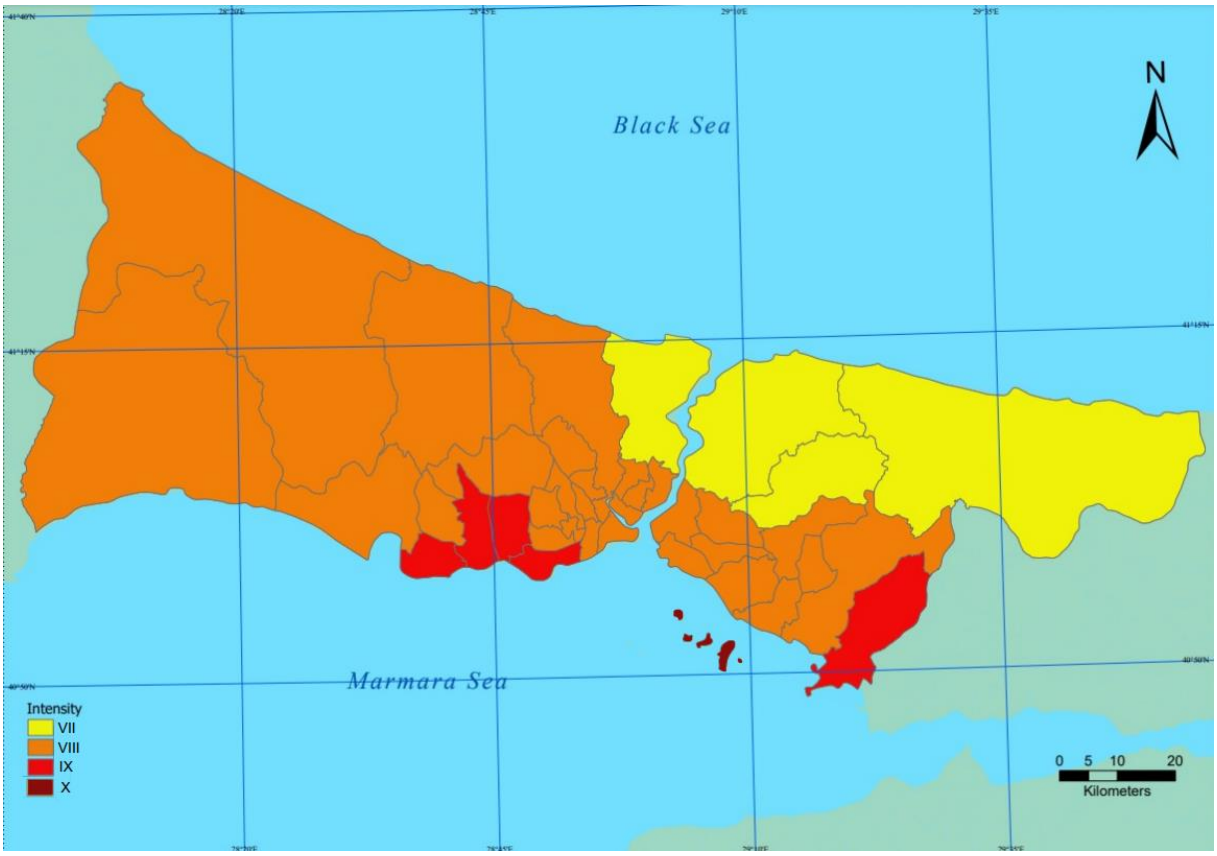

Figure 24. Intensity Map of Istanbul

Table 10. District-Based Building Damage Conditions for Istanbul (Scenario 1).

DISTRICT NAME	INTENSITY	BUILDINGS	SEVERE DAMAGE	MODERATE DAMAGE	SLIGHT DAMAGE
ADALAR	10	6720	2222	1027	1286
ARNAVUTKÖY	8	31941	901	1409	1696
ATAŞEHİR	8	27583	778	1216	1465
AVCILAR	9	26762	4201	4860	6088
BAĞCILAR	8	42439	1197	1872	2254
BAHÇELİEVLER	8	23276	656	1026	1236
BAKIRKÖY	9	11950	1876	2173	2719
BAŞAKŞEHİR	8	25791	727	1137	1370
BAYRAMPAŞA	8	20952	591	924	1113
BEŞİKTAŞ	8	16037	452	707	852
BEYKOZ	7	51201	466	1367	1326

BEYLİKDÜZÜ	9	12753	2002	2316	2901
BEYOĞLU	8	27335	771	1205	1451
BÜYÜKÇEKMECE	8	31343	884	1382	1664
ÇATALCA	8	27293	770	1204	1449
ÇEKMEKÖY	7	20787	189	555	538
ESENLER	8	23661	667	1043	1256
ESENYURT	8	38685	1091	1706	2054
EYÜP	8	34363	969	1515	1825
FATİH	8	43560	1228	1921	2313
GAZİ OSMANPAŞA	8	29283	826	1291	1555
GÜNGÖREN	8	10914	308	481	580
KADIKÖY	8	25210	711	1112	1339
KAĞITHANE	8	29103	821	1283	1545
KARTAL	8	29962	845	1321	1591
KÜÇÜKÇEKMECE	9	40136	6301	7289	9130
MALTEPE	8	28742	811	1268	1526
PENDİK	8	51491	1452	2271	2734
SANCAKTEPE	8	30293	854	1336	1609
SARIYER	7	49360	449	1317	1278
SİLİVRİ	8	50014	1410	2206	2656
SULTANBEYLİ	8	33911	956	1495	1801
SULTANGAZİ	8	33947	957	1497	1803
ŞİLE	7	20102	182	536	521
ŞİŞLİ	8	20689	583	912	1099
TUZLA	9	28331	4447	5145	6445
ÜMRANİYE	8	52612	1484	2320	2794
ÜSKÜDAR	8	41731	1177	1840	2216
ZEYTİNBURNU	8	16000	451	706	850
(TOTAL)		**1166263**	**47663**	**66191**	**79928**

When examining the districts in terms of severe damage and destruction, Küçükçekmece emerges as the most affected district, with 6,301 buildings sustaining damage. It is followed by Tuzla, with 4,447 damaged buildings, and Avcılar, with 4,201 buildings affected.

It is projected that this earthquake will result in the loss of 12,394 lives and that the number of injured individuals will reach 31,167. Additionally, the total number of people expected to be left homeless is estimated to be 355,582.

Table 11. District-Based Numbers of Deceased, Injured, and Displaced Individuals for Istanbul (Scenario 1).

DISTRICT NAME	INTENSITY	POPULATION	CASUALTIES	INJURED	DISPLACED
ADALAR	10	15623	578	1453	7635
ARNAVUTKÖY	8	336062	234	589	8801
ATAŞEHİR	8	416529	202	508	5902
AVCILAR	9	437221	1092	2746	29448
BAĞCILAR	8	719071	311	782	11386
BAHÇELİEVLER	8	567848	171	430	5483
BAKIRKÖY	9	220476	488	1227	11216
BAŞAKŞEHİR	8	509915	189	475	6785
BAYRAMPAŞA	8	268850	154	387	4848
BEŞİKTAŞ	8	169022	118	297	2700
BEYKOZ	7	245647	121	304	5719
BEYLİKDÜZÜ	9	409347	521	1310	13990
BEYOĞLU	8	218589	200	503	5711
BÜYÜKÇEKMECE	8	276572	230	578	7093
ÇATALCA	8	80007	200	503	5310
ÇEKMEKÖY	7	299806	49	123	2396
ESENLER	8	427901	173	435	6122
ESENYURT	8	978007	284	714	9594
EYÜP	8	420194	252	634	8470
FATİH	8	356025	319	802	8943
GAZİ OSMANPAŞA	8	483830	215	541	7113

GÜNGÖREN	8	269944	80	201	2564
KADIKÖY	8	467919	185	465	4229
KAĞITHANE	8	445672	213	536	6375
KARTAL	8	475042	220	553	6433
KÜÇÜKÇEKMECE	9	743774	1638	4120	44439
MALTEPE	8	523137	211	531	5863
PENDİK	8	743774	378	951	12025
SANCAKTEPE	8	492804	222	558	7709
SARIYER	7	344250	117	294	5121
SİLİVRİ	8	221723	367	923	9040
SULTANBEYLİ	8	360702	249	626	7206
SULTANGAZİ	8	532802	249	626	6061
ŞİLE	7	48537	47	118	2822
ŞİŞLİ	8	264736	152	382	5771
TUZLA	9	293604	1156	2907	30215
ÜMRANİYE	8	723760	386	971	12173
ÜSKÜDAR	8	517348	306	770	8810
ZEYTİNBURNU	8	280896	117	294	4061
(TOTAL)		**15606966**	**12394**	**31167**	**355582**

The estimated total number of tents needed following the earthquake is 113,854.

The field hospitals established post-earthquake play a crucial role. In this scenario, the total number of field hospitals anticipated to be set up is projected to be 3,867.

Literature calculations have identified the daily requirements for materials needed after the earthquake, including water, canned food, and bread. Based on the calculations made for this scenario, the daily requirement for bottled water is estimated to be 1,160,247. Furthermore, the daily need for canned food is projected to be 1,546,996. The daily bread requirement has been established at 773,498.

Another critical aspect of health is maintaining cleanliness, which necessitates the establishment of portable toilets and baths for public use. The anticipated numbers to meet this need are 19,337 toilets and 19,337 baths.

Table 12. Potential Needs Following an Earthquake.

DISTRICT NAME	TDP	TOILET	BATH	WATER	BREAD	CANNED	BANDAGE	FIELD HOSPITAL
ADALAR	9088	454,4	454,4	27264	18176	36352	90880	90,88
ARNAVUTKÖY	9390	469,5	469,5	28170	18780	37560	93900	93,9
ATAŞEHİR	6410	320,5	320,5	19230	12820	25640	64100	64,1
AVCILAR	32194	1609,7	1609,7	96582	64388	128776	321940	321,94
BAĞCILAR	12168	608,4	608,4	36504	24336	48672	121680	121,68
BAHÇELİEVLER	5913	295,65	295,65	17739	11826	23652	59130	59,13
BAKIRKÖY	12443	622,15	622,15	37329	24886	49772	124430	124,43
BAŞAKŞEHİR	7260	363	363	21780	14520	29040	72600	72,6
BAYRAMPAŞA	5235	261,75	261,75	15705	10470	20940	52350	52,35
BEŞİKTAŞ	2997	149,85	149,85	8991	5994	11988	29970	29,97
BEYKOZ	6023	301,15	301,15	18069	12046	24092	60230	60,23
BEYLİKDÜZÜ	15300	765	765	45900	30600	61200	153000	153
BEYOĞLU	6214	310,7	310,7	18642	12428	24856	62140	62,14
BÜYÜKÇEKMECE	7671	383,55	383,55	23013	15342	30684	76710	76,71
ÇATALCA	5813	290,65	290,65	17439	11626	23252	58130	58,13
ÇEKMEKÖY	2519	125,95	125,95	7557	5038	10076	25190	25,19
ESENLER	6557	327,85	327,85	19671	13114	26228	65570	65,57
ESENYURT	10308	515,4	515,4	30924	20616	41232	103080	103,08
EYÜP	9104	455,2	455,2	27312	18208	36416	91040	91,04
FATİH	9745	487,25	487,25	29235	19490	38980	97450	97,45
GAZİ OSMANPAŞA	7654	382,7	382,7	22962	15308	30616	76540	76,54
GÜNGÖREN	2765	138,25	138,25	8295	5530	11060	27650	27,65
KADIKÖY	4694	234,7	234,7	14082	9388	18776	46940	46,94
KAĞITHANE	6911	345,55	345,55	20733	13822	27644	69110	69,11
KARTAL	6986	349,3	349,3	20958	13972	27944	69860	69,86
KÜÇÜKÇEKMECE	48559	2427,95	2427,95	145677	97118	194236	485590	485,59
MALTEPE	6394	319,7	319,7	19182	12788	25576	63940	63,94

PENDİK	12976	648,8	648,8	38928	25952	51904	129760	129,76
SANCAKTEPE	8267	413,35	413,35	24801	16534	33068	82670	82,67
SARIYER	5415	270,75	270,75	16245	10830	21660	54150	54,15
SİLİVRİ	9963	498,15	498,15	29889	19926	39852	99630	99,63
SULTANBEYLİ	7832	391,6	391,6	23496	15664	31328	78320	78,32
SULTANGAZİ	6687	334,35	334,35	20061	13374	26748	66870	66,87
ŞİLE	2940	147	147	8820	5880	11760	29400	29,4
ŞİŞLİ	6153	307,65	307,65	18459	12306	24612	61530	61,53
TUZLA	33122	1656,1	1656,1	99366	66244	132488	331220	331,22
ÜMRANİYE	13144	657,2	657,2	39432	26288	52576	131440	131,44
ÜSKÜDAR	9580	479	479	28740	19160	38320	95800	95,8
ZEYTİNBURNU	4355	217,75	217,75	13065	8710	17420	43550	43,55
(TOTAL)	**386749**	**19337**	**19337**	**1160247**	**773498**	**1546996**	**3867490**	**3867**

In the ELER programme, based on the earthquake location and magnitude data input, a seismic intensity map was generated using the Boore and Atkinson (2008) ground motion model and the Atkinson and Kaka (2007) Intensity model. This data was then used for loss estimation within the ELER software. According to the loss estimation created in the Level 0 section, three models were applied for Istanbul: Model 1 by Samardkieva and Badal (2002), Model 2 by RGELFE (1992), and Model 3 by Vacaream (2004). Model 1 predicted a total of 16,672 fatalities, Model 2 estimated 6,920, and Model 3 forecasted 5,359 deaths.

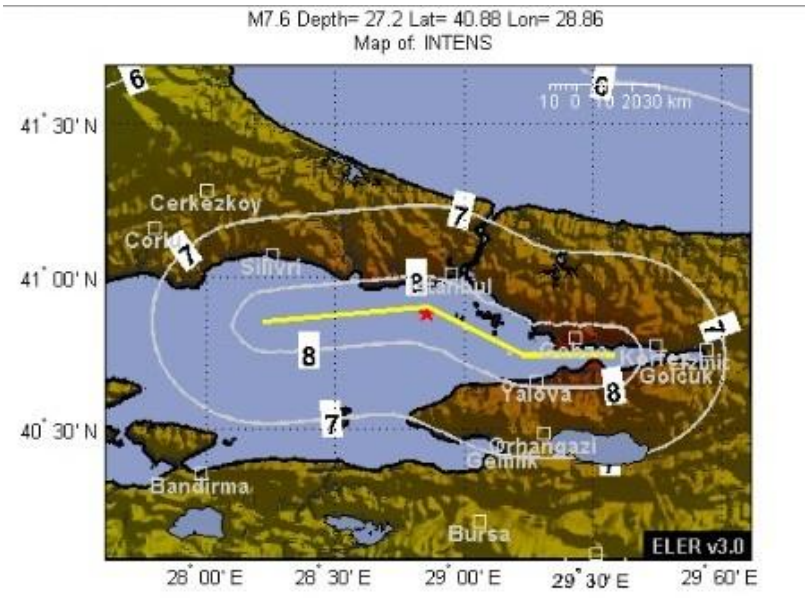

Figure 25. Intensity Map Generated Using the ELER programme.

The intensity data generated was combined with population and building data to prepare a damage estimate in the Level 1 section. After inputting these parameters, the potential fatality count was calculated based on Coburn and Spence (1992), Risk EU, and KOERI (2002) models.

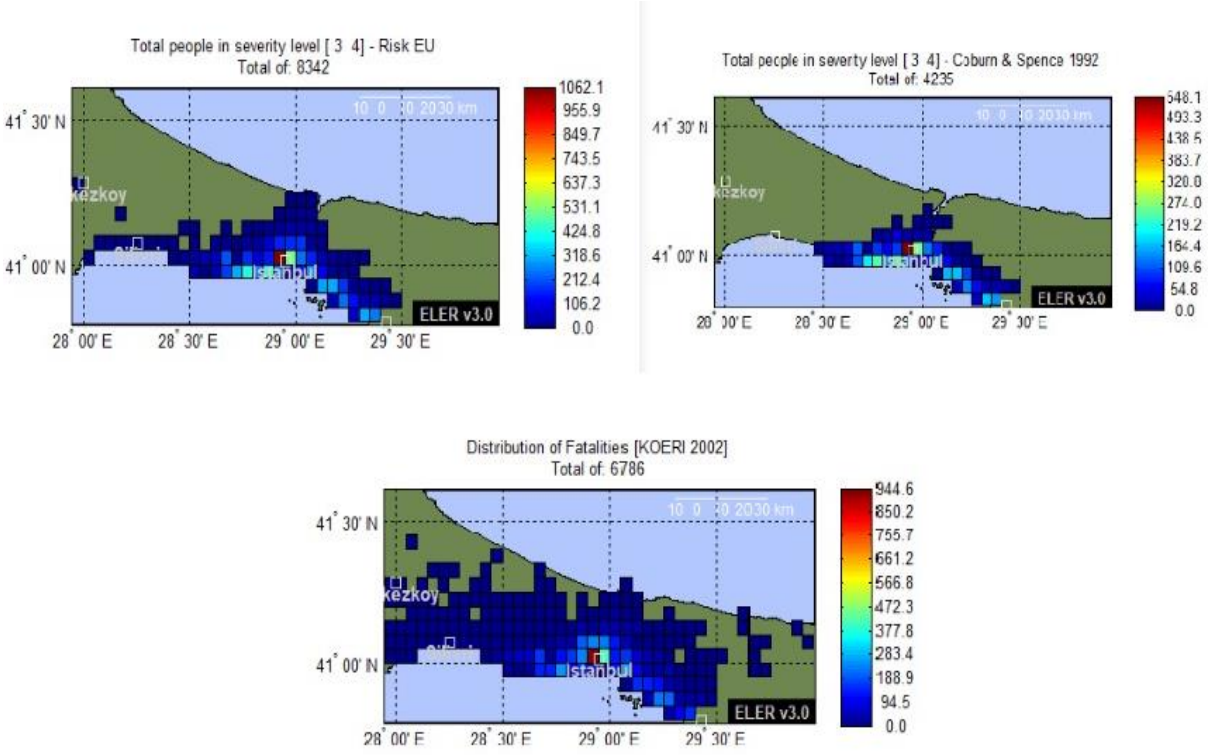

Figure 26. Casualties Map Generated in the ELER Programme According to Risk EU, Coburn and Space (1992), and KOERI (2002)

According to Coburn and Spence (1992), the number of fatalities was 4,235; Risk EU parameters estimated 8,342 deaths, while KOERI (2002) projected 6,786 deaths and 27,144 injuries. The total number of severely damaged buildings calculated in Level 1 was 60,897.

For Level 2, the earthquake parameters along with ground motion periods (for 0.2 and 1.0 seconds) were input into the programme. The total number of severely damaged and collapsed buildings was estimated at 45,476, with a projected 6,603 fatalities.

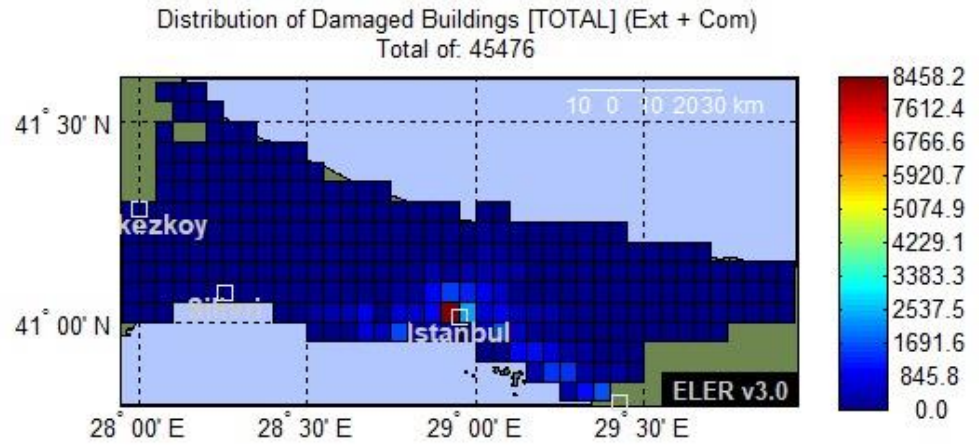

Figure 27. Building Damage Estimate (ELER - Level 2)

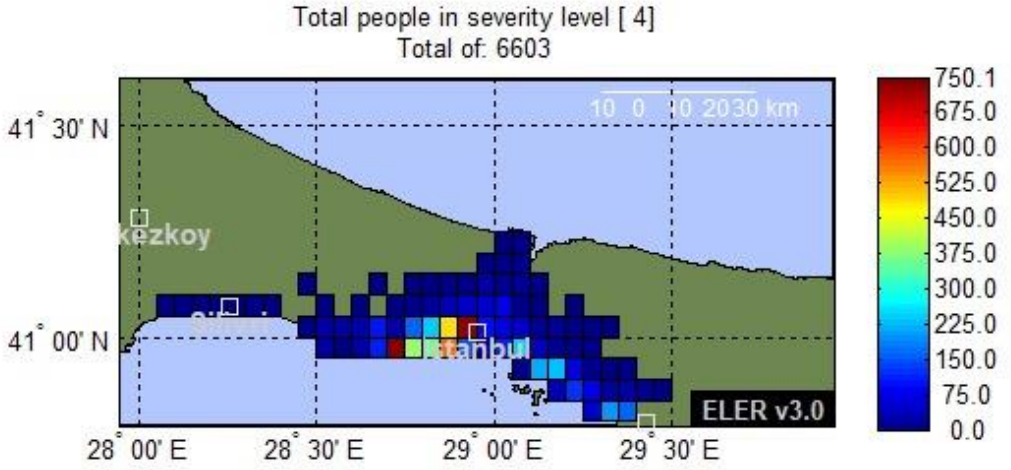

Figure 28. Casualties Estimate (ELER - Level 2)

5. CONCLUSIONS AND RECOMMENDATIONS

Efforts to mitigate damage before natural risks escalate into disasters hold critical importance. While it is impossible to completely prevent natural disasters, it is feasible to reduce their impacts, thereby minimizing damage and losses. Türkiye's geographical location places it on significant seismic zones, directly affecting major cities like Istanbul, where historical earthquakes pose considerable risks. This study aims to identify the earthquake potential for the city of Istanbul, which is home to approximately 20% of Türkiye's population, based on the collected data. Furthermore, the research seeks to formulate potential earthquake scenarios to forecast possible damages and losses.

The close proximity of the coastal strip in the southern regions of the city to fault lines presents a significant risk. This risk is notably high in 24 out of the 39 districts, indicating that these areas may incur more severe damages compared to others in the event of an earthquake. Consequently, the earthquake potential in Istanbul should be continuously monitored and examined through various methodologies and criteria.

Possible earthquake scenarios predicting a magnitude of 7.6 on the North Anatolian Fault suggest that certain regions in Istanbul could experience significant destruction and damage. In the initial scenario, buffer zones were created to identify intensity areas, determining the districts contained within these intensity values. By calculating the population and number of buildings in these regions, estimates were made for structures likely to sustain damage during an earthquake, alongside projections for fatalities, injuries, and the number of individuals who would be rendered homeless. Furthermore, assessments were conducted to evaluate the quantities of essential supplies required post-earthquake, including canned food, water, bread, and blankets. The results of the first scenario indicated that the area of highest density in Istanbul is the Adalar district, classified at intensity level X. It has been observed that in areas where the earthquake's intensity is markedly felt, the number of casualties and injuries tends to rise. According to data from the August 17, 1999, earthquake, the total casualties were identified as 12,394. Literature specifies that the expected mortality rate in earthquakes in Türkiye is one in every 1,000 individuals. This study demonstrates a 20% reduction in this ratio. A simulated earthquake scenario of equivalent magnitude and location was executed in the ELER (Earthquake Loss Estimation and Risk) program, revealing variations in expected fatalities based on differing parameters. The ELER program simulation indicated a maximum expected death toll of 18,147, while the minimum was calculated at 4,235. These prospective scenarios

exclude illegal and unlicensed constructions and do not account for individuals residing in Istanbul without official registration.

Different loss and damage estimates have been determined in the earthquake scenarios due to the use of different models. The estimated data calculated in Scenario 1 and Scenario 2 arise from the distinct parameters emphasised by the two models. While Scenario 1 considers only earthquake magnitude and intensity, Scenario 2 incorporates additional parameters such as magnitude, intensity, PGA, and ground motion periods. Moreover, the variations in the parameters and sources utilised within the ELER program in Scenario 2 have led to differing damage and loss estimates in this scenario.

Research has shown that in earthquakes occurring in Turkey, at most, one in every 1,000 individuals loses their life. In Scenario 1, the estimated number of casualties is 12,394. Assuming a population of 15,606,966, this ratio aligns with the losses observed in previous earthquakes.

Earthquakes trigger various natural disasters, such as tsunamis and landslides, and the potential damages and losses arising from other disaster scenarios that may occur following an earthquake are beyond the scope of this study.

The proximity of the North Anatolian Fault to the city, coupled with the absence of a major earthquake within a 250-year cycle, exacerbates the risk each day. While all these results indicate that Istanbul is under significant threat, this research, which assesses risk potential and scenarios, emphasizes that the city must always be prepared for an earthquake.

Istanbul has experienced significant earthquakes throughout its history. This city must always remain resilient to earthquakes and continuously prepare itself for the next seismic event. As it is impossible to predict when earthquakes will occur, one way to ensure preparedness is through structural inspections. Buildings that are not earthquake-resistant must be identified, and urban transformation initiatives should be initiated under the leadership of local authorities. The public should be educated on this matter to create a society that is aware of earthquake preparedness.

Before, during, and after an earthquake, local and national authorities should conduct seminars for the public to raise awareness and develop plans. It is essential to foster habits such as residing in earthquake-resistant structures and having emergency kits and earthquake bags prepared for potential seismic events.

Damage mitigation efforts should be initiated in preparation for the inevitable large earthquake, the timing of which remains uncertain. In Istanbul, priority must be given to the renovation or reinforcement of buildings constructed before 1980, as well as those built between 1980 and 2000. Efforts to enhance building resilience and implement urban transformation projects should involve collaboration between local authorities and all relevant stakeholders to safeguard Istanbul from potential hazards.

Additionally, critical infrastructure, including electricity, water, and sewage systems, must be strengthened. Infrastructure and pipeline systems should be redesigned and upgraded to withstand the maximum potential earthquake impact.

Earthquake planning should be undertaken, and gathering areas for post-disaster needs must be designated. Supplies such as tents, blankets, canned food, and water mentioned in the research should be kept in stock and readily available.

Authorities responsible for maintaining public order in the region must be prepared for the chaos that may ensue following an earthquake. Additionally, rescue teams should be deployed in identified risky areas and should concentrate their efforts in regions likely to experience greater intensity.

A potential 7.6 magnitude earthquake in Istanbul is anticipated to cause direct damage to Türkiye's economy. Given that a significant portion of the population and economic activities are managed from Istanbul, substantial economic losses are expected. This scenario could lead to the loss of economic independence for both Istanbul and Türkiye as a whole.

Finally, collaborative efforts involving different disciplines should be initiated to reduce structural damage, and all stakeholders including the public, local, and national government must work together to implement all possible measures in anticipation of the expected earthquake in Istanbul.

6. REFERENCES

Ahmed, T., Rehman, K., Shafique, M., & Ali, W. (2023). GIS-based earthquake potential analysis in Northwest Himalayan, Pakistan. *Environmental Earth Sciences*, *82*(4), 113.

AHP-OS, AHP Priority Calculator, https://bpmsg.com/ahp/ahp-calc.php (Accessed by 18.09.2024)

Atik, M. E., & Safi, O. (2024). Investigation of GIS-based Analytical Hierarchy Process for Multi-Criteria Earthquake Risk Assessment: The Case Study of Kahramanmaras Province. *International Journal of Environment and Geoinformatics*, *11*(3), 156-165.

Avcı, Y. & Gezerler, G. (2024). Konstantinapolis kelimesinin yapısı üzerine. Anadolu Dil ve Eğitim Dergisi, 2(1), 10-16. Doi: https://10.5281/zenodo.12583743

Aydın, M. C., Birincioğlu, E. S., Büyüksaraç, A., & Işık, E. (2024). Earthquake Risk Assessment Using GIS-Based Analytical Hierarchy Process (AHP): The Case of Bitlis Province (Türkiye). *International Journal of Environment and Geoinformatics*, *11*(1), 1-9.

Bayraktar, H., & Hossın, A. (2021). Sakarya ilinin depreme duyarli bölgelerinde CBS tabanlı hasar tahmini. *Resilience*, *5*(2), 173-185.

Boğaziçi Üniversitesi, & Kandilli Rasathanesi(BU-ARC) (2003). Earthquake Risk Assessment for the İstanbul Metropolitan Area. Boğaziçii University Press.

Bohnhoff, M., Bulut, F., Dresen, G., Malin, P. E., Eken, T., & Aktar, M. (2013). An earthquake gap south of Istanbul. *Nature communications*, *4*(1), 1999.

Cansız, S. (2022). Türkiye'de Kullanılan Deprem Yönetmeliklerinin Özellikleri ve Deprem Hesabının Değişimi. International Journal of Engineering Research and Development, 14(1), 58-71.

Cebeci, N. L. (2017). İstanbul Paleozoyiğinin Paleomanyetik Verilerle İncelenmesi Ve Hersiniyen Orojenezindeki Yeri.

de Klerk, G. (2024). NSSC Geography Module 1. Cambridge University Press. https://assets.cambridge.org/97805216/80592/excerpt/9780521680592_excerpt.pdf

Deligiannakis, G., Papanikolaou, I. D., & Roberts, G. (2018). Fault specific GIS based seismic hazard maps for the Attica region, Greece. Geomorphology, 306, 264-282.

Demir, M., & Altaş, N. T. (2024). Kars kentinde deprem hasar risk potansiyeli taşıyan alanların CBS tabanlı AHP analizlerine dayalı olarak belirlenmesi. *Geomatik*, *9*(1), 123-140.

Demirelli, K. (2001). *İstanbul'da Meydana Gelmiş Büyük Depremler Ve İstanbul'un Geoteknik Açıdan İncelenmesi* (Doctoral dissertation, Fen Bilimleri Enstitüsü).

Dişkaya, F., & Emir, Ş. (2021). AHP-TOPSIS Bütünleşik Yaklaşımıyla Deprem Riski Tabanlı İstanbul İli Kentsel Dönüşüm Öncelik Sıralaması. *Afet ve Risk Dergisi*, *4*(2), 203-223.

Efthymiou, E., & Makris, N. (2022). Pulse-period–moment-magnitude relations derived with wavelet analysis and their relevance to estimate structural deformations. *Earthquake Engineering & Structural Dynamics*, *51*(7), 1636-1656.

ELER, Earthquake Loss Estimation Routine (ELER) methodology and software, https://eqe.bogazici.edu.tr/en/eler-methodology-and-software (Accessed by 18.09.2024)

Emre, Ö., Elmacı, H., Özalp, S., & Kırman, E. (2020). Merzifon–Esençay splay fault within the North Anatolian Fault system: segmentation and timing of the last two surface faulting events on Esençay segment. Mediterranean Geoscience Reviews, 2(3), 359-382.

Erdem, U. (2013). Yerleşimlerin taşıdığı deniz taşkını, sel ve deprem afet tehlikelerinin CBS kullanılarak yorumlanması: Balıkesir örneği. *Balıkesir Üniversitesi Fen Bilimleri Enstitüsü Dergisi*, *15*(2), 40-57.

Erıs, M. B., Alparslan, C., Karadayı, M. A., Alkan, A., Demırel, D. F., & Gonul-sezer, E. D. (2023). Economic impacts of expected Istanbul earthquake: scenario generation. The Eurasia Proceedings of Science Technology Engineering and Mathematics, 22, 364-376.

Goepel, K. D. (2018). Implementation of an online software tool for the analytic hierarchy process (AHP-OS). *International journal of the analytic hierarchy process*, *10*(3).

Hancılar, U., Şeşetyan, K., & Çaktı, E. (2019). İstanbul'daki 2000 Yılı Sonrası Binalar İçin Tasarım Depremi Altında Karşılaştırmalı Yapısal Hasar ve Mali Kayıp Tahminleri. Teknik Dergi, 30(3), 9107-9123.

Hassanzadeh, R., Nedović-Budić, Z., Razavi, A. A., Norouzzadeh, M., & Hodhodkian, H. (2013). Interactive approach for GIS-based earthquake scenario development and resource estimation (Karmania hazard model). *Computers & geosciences*, *51*, 324-338.

Hosseinpour, V., Saeidi, A., Nollet, M. J., & Nastev, M. (2021). Seismic loss estimation software: A comprehensive review of risk assessment steps, software development and limitations. Engineering structures, 232, 111866.

IMM. (2024). https://ibb.istanbul/istanbul/tarihce (Accessed by 18.09.2024)

IMM, (2024) https://data.ibb.gov.tr/en/ (Accessed by 18.09.2024)

Işık, E., Sağır, Ç., Tozlu, Z., & Ustaoğlu, Ü. S. (2019). Farklı deprem senaryolarına göre Kırşehir ili kayıp tahmin analizleri.

Jena, R., Pradhan, B., Beydoun, G., Al-Amri, A., & Sofyan, H. (2020). Seismic hazard and risk assessment: a review of state-of-the-art traditional and GIS models. Arabian Journal of Geosciences, 13(2), 50.

Karimzadeh, S., Miyajima, M., Hassanzadeh, R., Amiraslanzadeh, R., & Kamel, B. (2014). A GIS-based seismic hazard, building vulnerability and human loss assessment for the earthquake scenario in Tabriz. Soil Dynamics and Earthquake Engineering, 66, 263-280.

Khilyuk, L.F., Chilingar, G.V., Robertson, J.O. & Endres, B. 2000, "Chapter 8 - Magnitude and Intensity of Earthquakes" in *Gas Migration* Gulf Professional Publishing, , pp. 133-143.

Kramer, S. L. (1996). Geotechnical earthquake engineering (Vol. 653). Prentice Hall.

Kusky, T. M. (2008). Earthquakes: plate tectonics and earthquake hazards. Infobase Publishing.

Lom, N., Ülgen, S. C., Sakinç, M., & Şengör, A. C. (2016). Geology and stratigraphy of Istanbul region. *Geodiversitas*, *38*(2), 175-195.

Malakar, S., & Rai, A. K. (2022). Earthquake vulnerability in the Himalaya by integrated multi-criteria decision models. *Natural Hazards*, 1-25.

Martin, P., van Hunen, J., Parman, S., & Davidson, J. (2008). Why does plate tectonics occur only on Earth? Physics Education, 43(2), 144.

Nemutlu, Ö. F., Sarı, A., & Balun, B. (2023). 06 Şubat 2023 Kahramanmaraş Depremlerinde (Mw 7.7-Mw 7.6) Meydana Gelen Gerçek Can Kayıpları Ve Yapısal Hasar Değerlerinin Tahmin Edilen Değerler İle Karşılaştırılması. Afyon Kocatepe Üniversitesi Fen Ve Mühendislik Bilimleri Dergisi, 23(5), 1222-1234.

Ozer, U., Karadogan, A., Sahinoglu, U. K., Ozyurt, M. C., Sertabipoglu, Z., Günay, M. K., ... & Zaif, C. B. (2020). An analytical and applied blasting approach to facilitate rock-socketed bored pile excavation. *Arabian Journal of Geosciences*, *13*, 1-11.

Özgül, N. (2011). İstanbul il alanının jeolojisi. İstanbul Büyükşehir Belediyesi, 308.

Özkazanç, S., Sıddıqui, S. D., & Güngör, M. (2020). Sensitivity Analysis of Earthquake Using the Analytic Hierarchy Process (AHP) Method: Sample of Adana. *İdealkent*, *11*(30), 570-591.

Rajasekaran, S. (2009). Structural Dynamics of Earthquake Engineering - Theory and Application Using MATHEMATICA and MATLAB. Woodhead Publishing. Retrieved from https://app.knovel.com/hotlink/toc/id:kpSDEETAU5/structural-dynamics-earthquake/structural-dynamics-earthquake

Rao, N. P. (2015). Earthquakes. Amaravathi Popular Science Series, AP Akademi of Sciences, 26 pp. https://www.ncess.gov.in/images/Earthquakes_Comp.pdf

Saaty, T. L. (1977). A scaling method for priorities in hierarchical structures. *Journal of mathematical psychology*, *15*(3), 234-281.

Saaty, T. L. (1980). Marketing applications of the analytic hierarchy process. *Management science*, *26*(7), 641-658.

Sabah, L., & Bayraktar, H. (2020). Düzce merkez ve ilçelerinin deprem senaryolarına göre karşılaştırmalı olarak incelenmesi. *Düzce Üniversitesi Bilim ve Teknoloji Dergisi*, *8*(2), 1695-1705.

Sarvar, H., Amini, J., & Laleh-Poor, M. (2011). Assessment of risk caused by earthquake in region 1 of Tehran using the combination of RADIUS, TOPSIS and AHP models. *Journal of Civil Engineering and Urbanism*, *1*(1), 39-48.

Shrestha, H. L., & Poudel, M. (2018). Landslide susceptibility zonation mapping in post-earthquake scenario in Gorkha District. *Forestry: Journal of Institute of Forestry, Nepal*, *15*(15), 45-56.

Şengör, A. C., & Zabcı, C. (2019). The north Anatolian fault and the north Anatolian shear zone. Landscapes and landforms of Turkey, 481-494.

Şimşek, P., & Gündüz, A. (2021). A big earthquake awaits İstanbul: Mini review. *Afet ve Risk Dergisi*, *4*(1), 53-60.

TUIK. (2024) https://data.tuik.gov.tr/Bulten/Index?p=Adrese-Dayali-Nufus-Kayit-Sistemi-Sonuclari-2023-49684 (Accesed by 18.09.2024)

Tüysüz, O., & Serim, A. (2000). Marmara deprem senaryoları için coğrafi bilgi sistemi. TÜBİTAK Bilim ve Teknik, Eylül, 86-90.

USGS, United States Geological Survey, https://earthexplorer.usgs.gov (Accessed by 18.09.2024)

Uzun, Ö., & Balyemez, S. (2020). İSTANBUL ve ANTAKYA ŞEHİRLERİNDE DEPREM RİSK AZALTMA ÇALIŞMALARI ÜZERİNE KARŞILAŞTIRMALI BİR DEĞERLENDİRME. İstanbul Aydın Üniversitesi Dergisi, 12(3), 229-250.

Ülgen, S. C., Lom, N., Sunal, G., Gerdes, A., & Şengör, A. M. C. (2018). The Strandja Massif and the İstanbul Zone were once parts of the same palaeotectonic unit: new data from Triassic detrital zircons. *Geodinamica Acta*, *30*(1), 212-224.

Wen, H., Xie, P., Xiao, P., & Hu, D. (2017). Rapid susceptibility mapping of earthquake-triggered slope geohazards in Lushan County by combining remote sensing with the AHP model developed for the Wenchuan earthquake. *Bulletin of Engineering Geology and the Environment*, *76*(3), 909-921.

Yalçın, Cihan & Sabah, Levent. (2017). Açık Kaynak Kodlu CBS ve Analitik Hiyerarşi Proses (AHP) Yöntemi Kullanılarak Edirne Sanayi İşletmelerinin Deprem Tehlike Analizi. Düzce Üniversitesi Bilim ve Teknoloji Dergisi, 5(2), 524-537.

Zülfikar, Ö., Zülfikar, C., & Alçık, H. (2012). ELER Yazılımı ile Deprem Şiddeti, Hasar ve Kayıp Tahmini Earthquake Intensity, Damage and Casualty Estimation by ELER.

Zülfikar, A. C., Tekin, S., Akcan, S. O., & Gök, M. G. (2020). 26 Eylül 2019 Silivri açıkları (Marmara Denizi) depreminin kuvvetli yer hareketi verilerinin değerlendirilmesi. Journal of the Institute of Science and Technology, 10(3), 1720-1736.

APPENDICIES

List of Appendix

A1. Pairwise comparison survey prepared with AHP- OS

	A - wrt AHP priorities - or B?		Equal	How much more?
1	◉ PGA	○ distance to fault	○1	○2 ◉3 ○4 ○5 ○6 ○7 ○8 ○9
2	◉ PGA	○ lithology	○1	○2 ○3 ○4 ◉5 ○6 ○7 ○8 ○9
3	◉ PGA	○ earthquake events	○1	○2 ○3 ○4 ○5 ○6 ◉7 ○8 ○9
4	◉ PGA	○ buildings (total)	○1	○2 ○3 ○4 ○5 ○6 ○7 ○8 ◉9
5	◉ PGA	○ buildings ages	○1	○2 ○3 ○4 ○5 ○6 ○7 ○8 ◉9
6	◉ PGA	○ population	○1	○2 ○3 ○4 ○5 ○6 ○7 ○8 ◉9
7	◉ PGA	○ landuse	○1	○2 ○3 ○4 ○5 ○6 ◉7 ○8 ○9
8	◉ PGA	○ DEM	○1	○2 ○3 ○4 ○5 ○6 ○7 ○8 ◉9
9	◉ PGA	○ Slope	○1	○2 ○3 ○4 ○5 ○6 ○7 ○8 ◉9
10	◉ PGA	○ distance to road	○1	○2 ○3 ○4 ○5 ○6 ○7 ○8 ◉9
11	◉ distance to fault	○ lithology	○1	○2 ◉3 ○4 ○5 ○6 ○7 ○8 ○9
12	◉ distance to fault	○ earthquake events	○1	○2 ○3 ○4 ◉5 ○6 ○7 ○8 ○9
13	◉ distance to fault	○ buildings (total)	○1	○2 ○3 ○4 ○5 ○6 ◉7 ○8 ○9
14	◉ distance to fault	○ buildings ages	○1	○2 ○3 ○4 ○5 ○6 ◉7 ○8 ○9
15	◉ distance to fault	○ population	○1	○2 ○3 ○4 ○5 ○6 ◉7 ○8 ○9
16	◉ distance to fault	○ landuse	○1	○2 ○3 ○4 ◉5 ○6 ○7 ○8 ○9
17	◉ distance to fault	○ DEM	○1	○2 ○3 ○4 ○5 ○6 ○7 ○8 ◉9
18	◉ distance to fault	○ Slope	○1	○2 ○3 ○4 ○5 ○6 ○7 ○8 ◉9
19	◉ distance to fault	○ distance to road	○1	○2 ○3 ○4 ○5 ○6 ○7 ○8 ◉9
20	◉ lithology	○ earthquake events	○1	○2 ◉3 ○4 ○5 ○6 ○7 ○8 ○9
21	◉ lithology	○ buildings (total)	○1	○2 ○3 ○4 ◉5 ○6 ○7 ○8 ○9
22	◉ lithology	○ buildings ages	○1	○2 ○3 ○4 ◉5 ○6 ○7 ○8 ○9
23	◉ lithology	○ population	○1	○2 ○3 ○4 ○5 ○6 ◉7 ○8 ○9
24	◉ lithology	○ landuse	○1	○2 ○3 ○4 ◉5 ○6 ○7 ○8 ○9
25	◉ lithology	○ DEM	○1	○2 ○3 ○4 ○5 ○6 ◉7 ○8 ○9
26	◉ lithology	○ Slope	○1	○2 ○3 ○4 ○5 ○6 ◉7 ○8 ○9
27	◉ lithology	○ distance to road	○1	○2 ○3 ○4 ○5 ○6 ○7 ○8 ◉9
28	◉ earthquake events	○ buildings (total)	○1	○2 ○3 ○4 ◉5 ○6 ○7 ○8 ○9
29	◉ earthquake events	○ buildings ages	○1	○2 ○3 ○4 ◉5 ○6 ○7 ○8 ○9
30	◉ earthquake events	○ population	○1	○2 ○3 ○4 ○5 ○6 ◉7 ○8 ○9
31	◉ earthquake events	○ landuse	○1	○2 ○3 ○4 ◉5 ○6 ○7 ○8 ○9
32	◉ earthquake events	○ DEM	○1	○2 ○3 ○4 ○5 ○6 ◉7 ○8 ○9
33	◉ earthquake events	○ Slope	○1	○2 ○3 ○4 ○5 ○6 ◉7 ○8 ○9
34	◉ earthquake events	○ distance to road	○1	○2 ○3 ○4 ○5 ○6 ○7 ○8 ◉9
35	○ buildings (total)	◉ buildings ages	○1	○2 ◉3 ○4 ○5 ○6 ○7 ○8 ○9
36	◉ buildings (total)	○ population	◉1	○2 ○3 ○4 ○5 ○6 ○7 ○8 ○9
37	○ buildings (total)	◉ landuse	○1	○2 ◉3 ○4 ○5 ○6 ○7 ○8 ○9
38	○ buildings (total)	◉ DEM	○1	○2 ◉3 ○4 ○5 ○6 ○7 ○8 ○9
39	○ buildings (total)	◉ Slope	○1	○2 ◉3 ○4 ○5 ○6 ○7 ○8 ○9
40	◉ buildings (total)	○ distance to road	○1	○2 ○3 ○4 ◉5 ○6 ○7 ○8 ○9
41	◉ buildings ages	○ population	◉1	○2 ○3 ○4 ○5 ○6 ○7 ○8 ○9
42	○ buildings ages	◉ landuse	○1	○2 ◉3 ○4 ○5 ○6 ○7 ○8 ○9
43	◉ buildings ages	○ DEM	◉1	○2 ○3 ○4 ○5 ○6 ○7 ○8 ○9
44	◉ buildings ages	○ Slope	◉1	○2 ○3 ○4 ○5 ○6 ○7 ○8 ○9
45	◉ buildings ages	○ distance to road	◉1	○2 ○3 ○4 ○5 ○6 ○7 ○8 ○9
46	○ population	◉ landuse	○1	○2 ◉3 ○4 ○5 ○6 ○7 ○8 ○9
47	◉ population	○ DEM	◉1	○2 ○3 ○4 ○5 ○6 ○7 ○8 ○9
48	◉ population	○ Slope	◉1	○2 ○3 ○4 ○5 ○6 ○7 ○8 ○9
49	◉ population	○ distance to road	◉1	○2 ○3 ○4 ○5 ○6 ○7 ○8 ○9
50	◉ landuse	○ DEM	○1	○2 ◉3 ○4 ○5 ○6 ○7 ○8 ○9
51	◉ landuse	○ Slope	○1	○2 ◉3 ○4 ○5 ○6 ○7 ○8 ○9
52	◉ landuse	○ distance to road	○1	○2 ○3 ○4 ◉5 ○6 ○7 ○8 ○9
53	◉ DEM	○ Slope	◉1	○2 ○3 ○4 ○5 ○6 ○7 ○8 ○9
54	◉ DEM	○ distance to road	◉1	○2 ○3 ○4 ○5 ○6 ○7 ○8 ○9
55	◉ Slope	○ distance to road	◉1	○2 ○3 ○4 ○5 ○6 ○7 ○8 ○9

Figure A- 1. Pairwise Comparison Survey

A2. Reclassified raster data and maps.

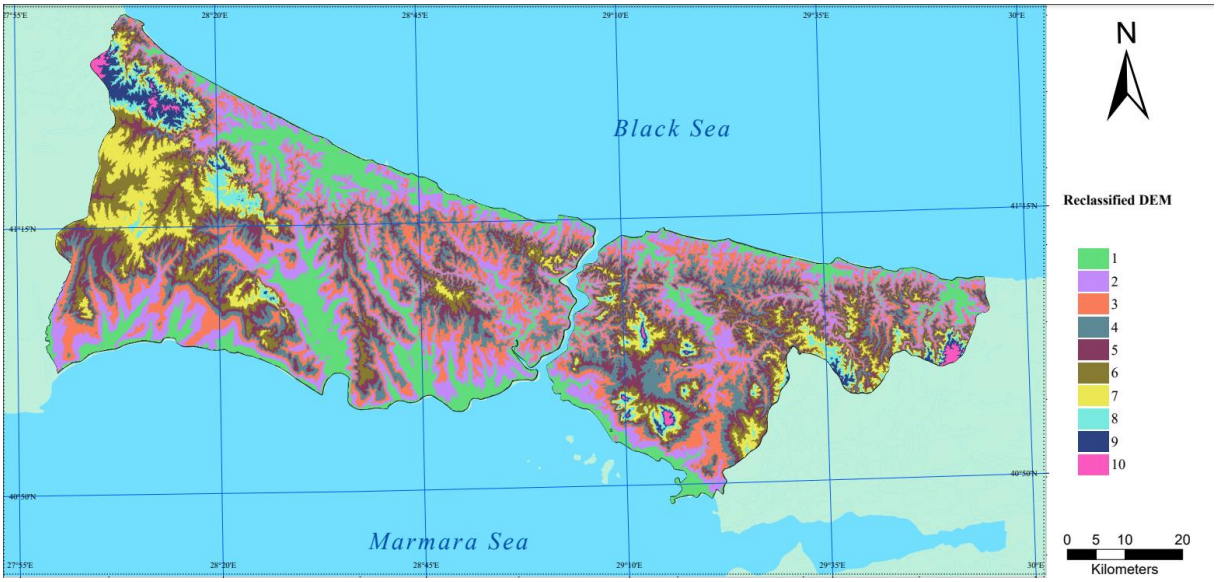

Figure A- 2. Reclassified DEM Map.

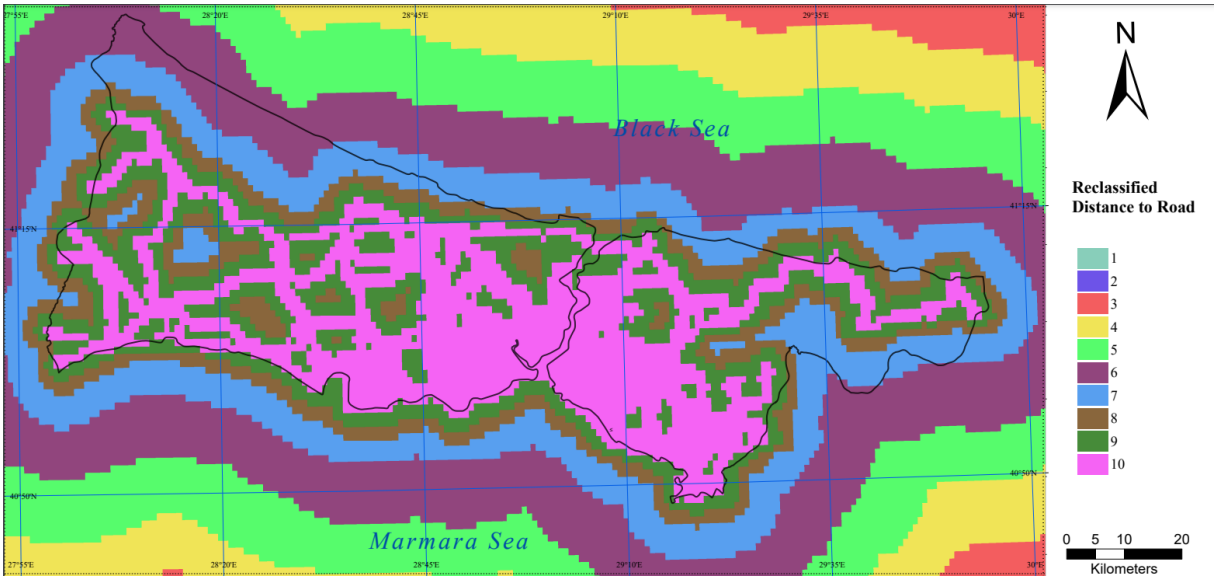

Figure A- 3. Distance Map to Reclassified Road.

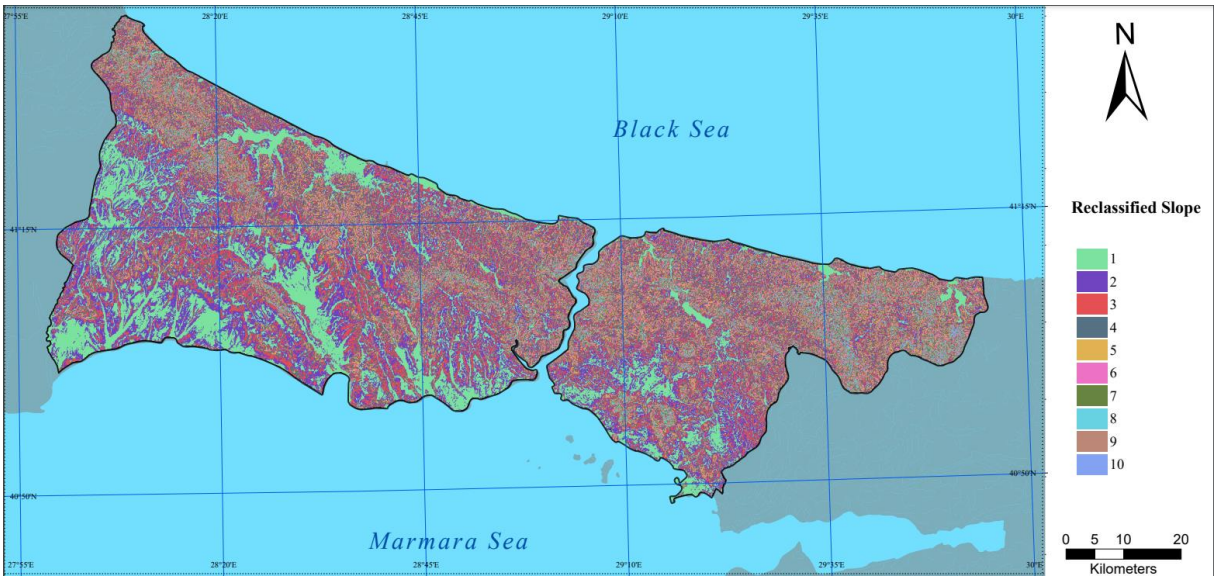

Figure A- 4. Reclassified Slope Map.

Figure A- 5. Reclassified Population Map.

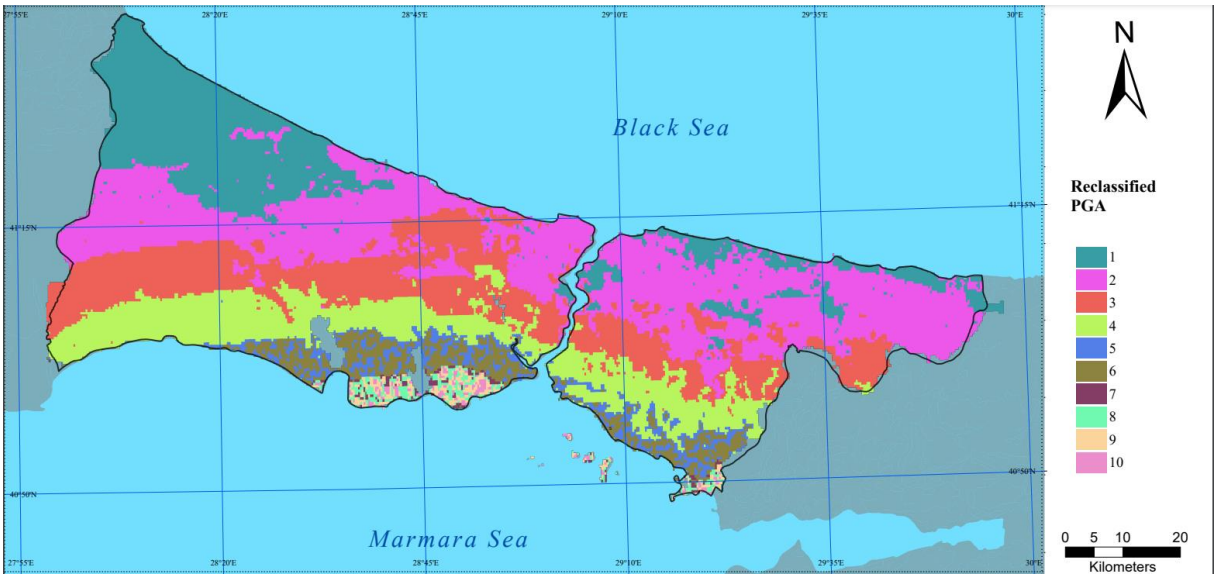

Figure A- 6. Reclassified PGA Map.

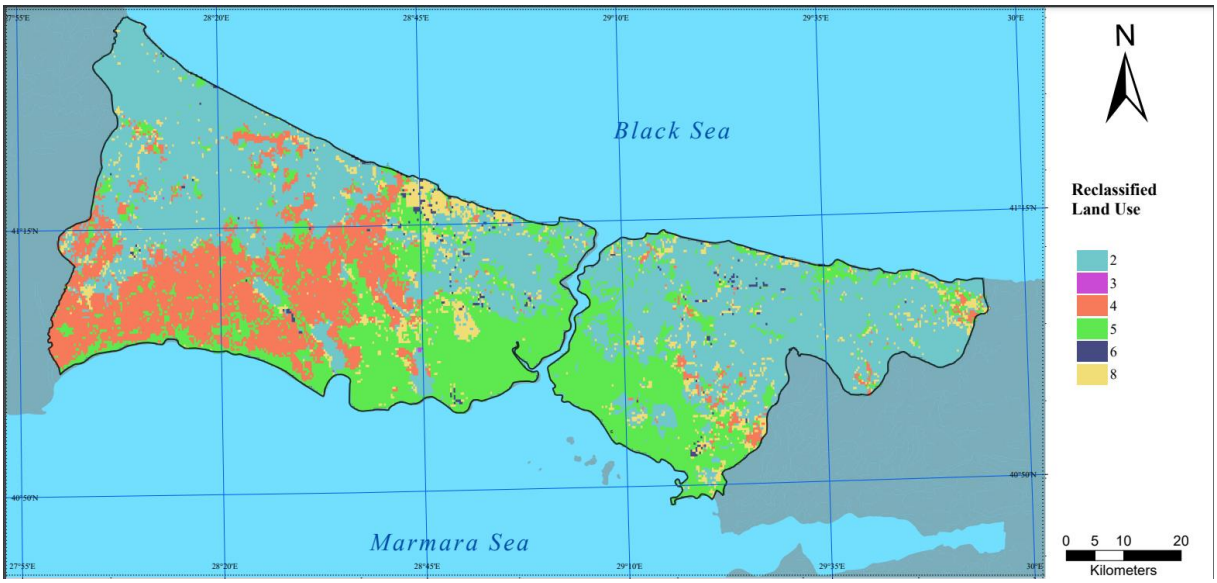

Figure A- 7. Reclassified Land Use Map

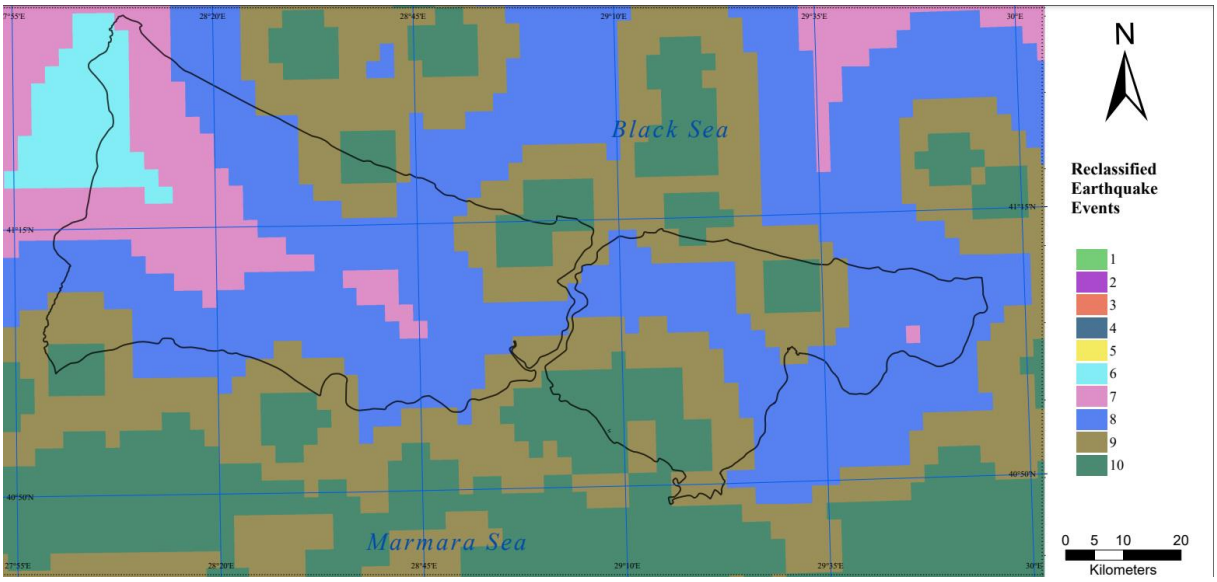

Figure A- 8. Reclassified Earthquake Events Map.

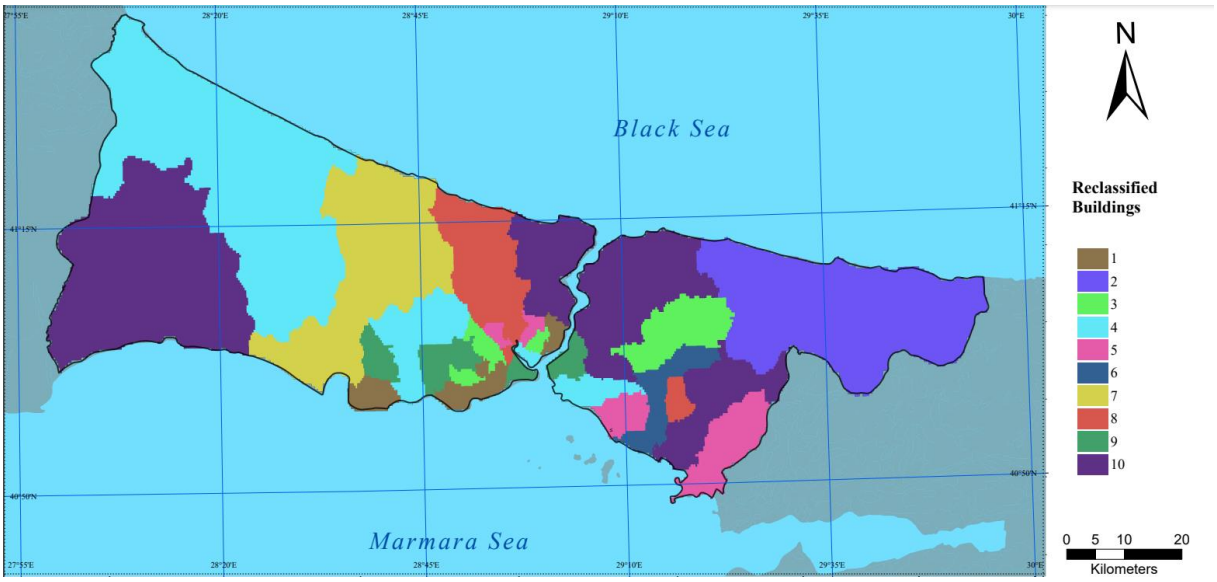

Figure A- 9. Reclassified Buildings Map.

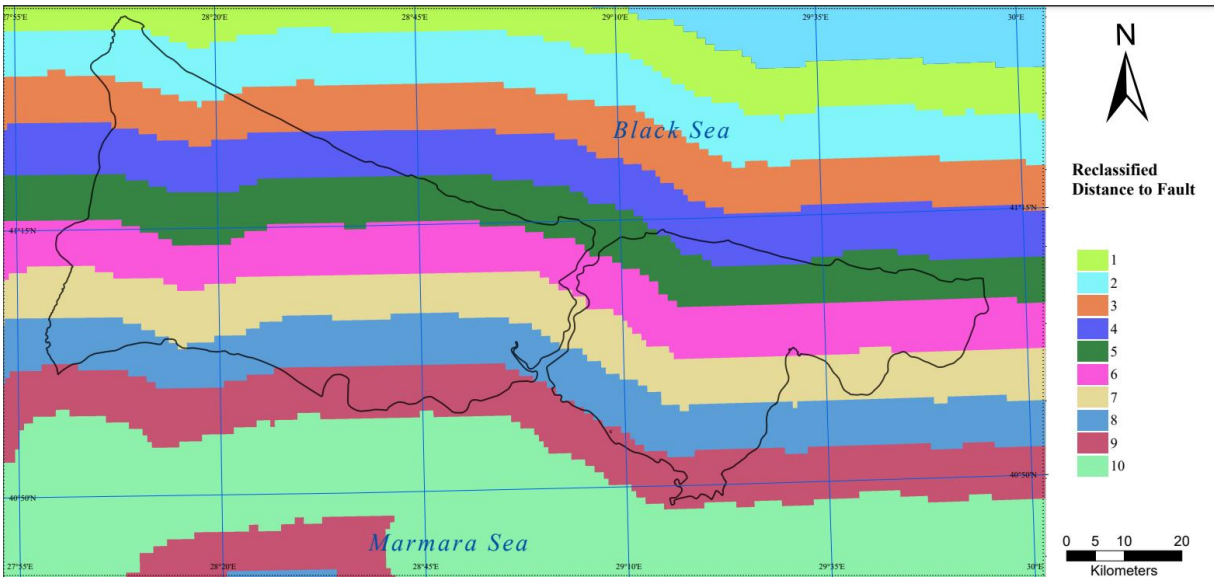

Figure A- 10. Reclassified Fault Distance Map.

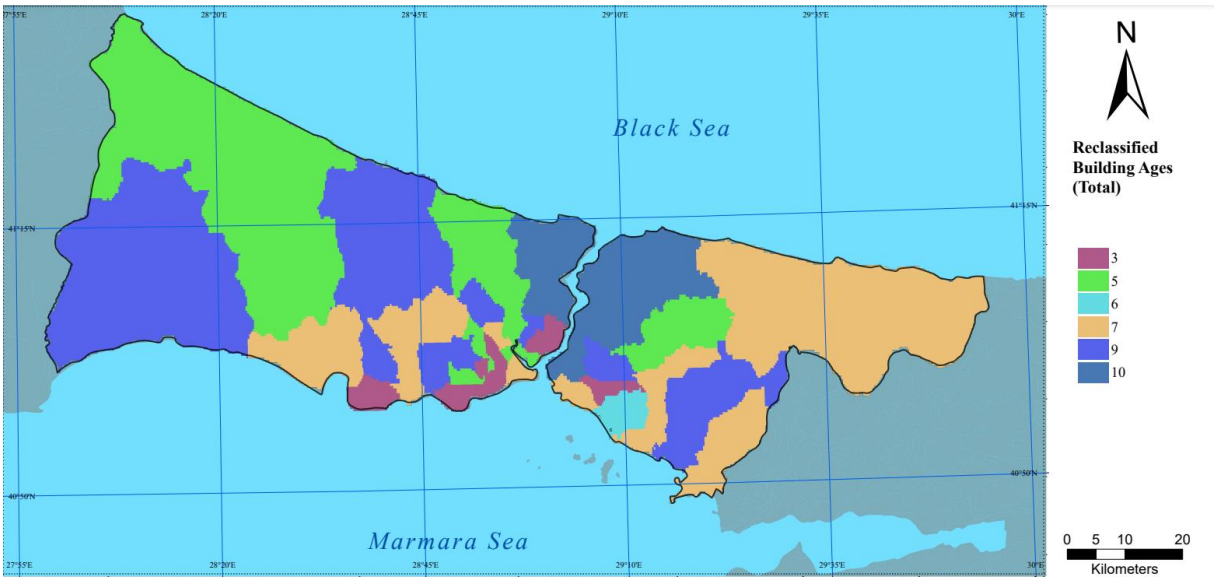

Figure A- 11. Building Age Map Reclassified by District.

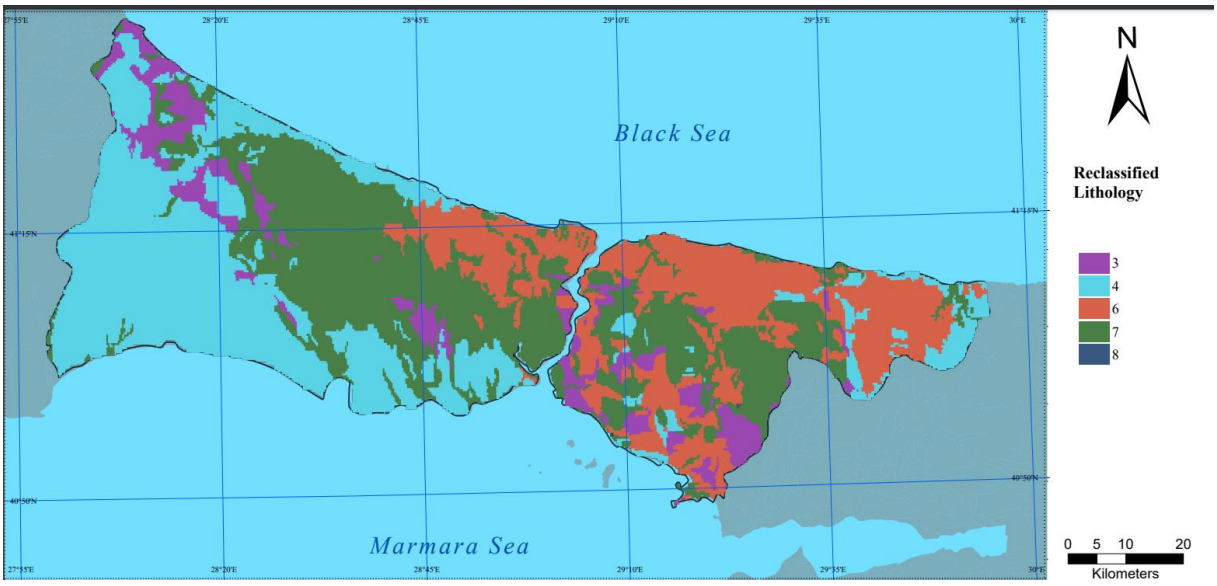

Figure A- 12. Building Age Map Reclassified by District.

A3. Household number map of Istanbul

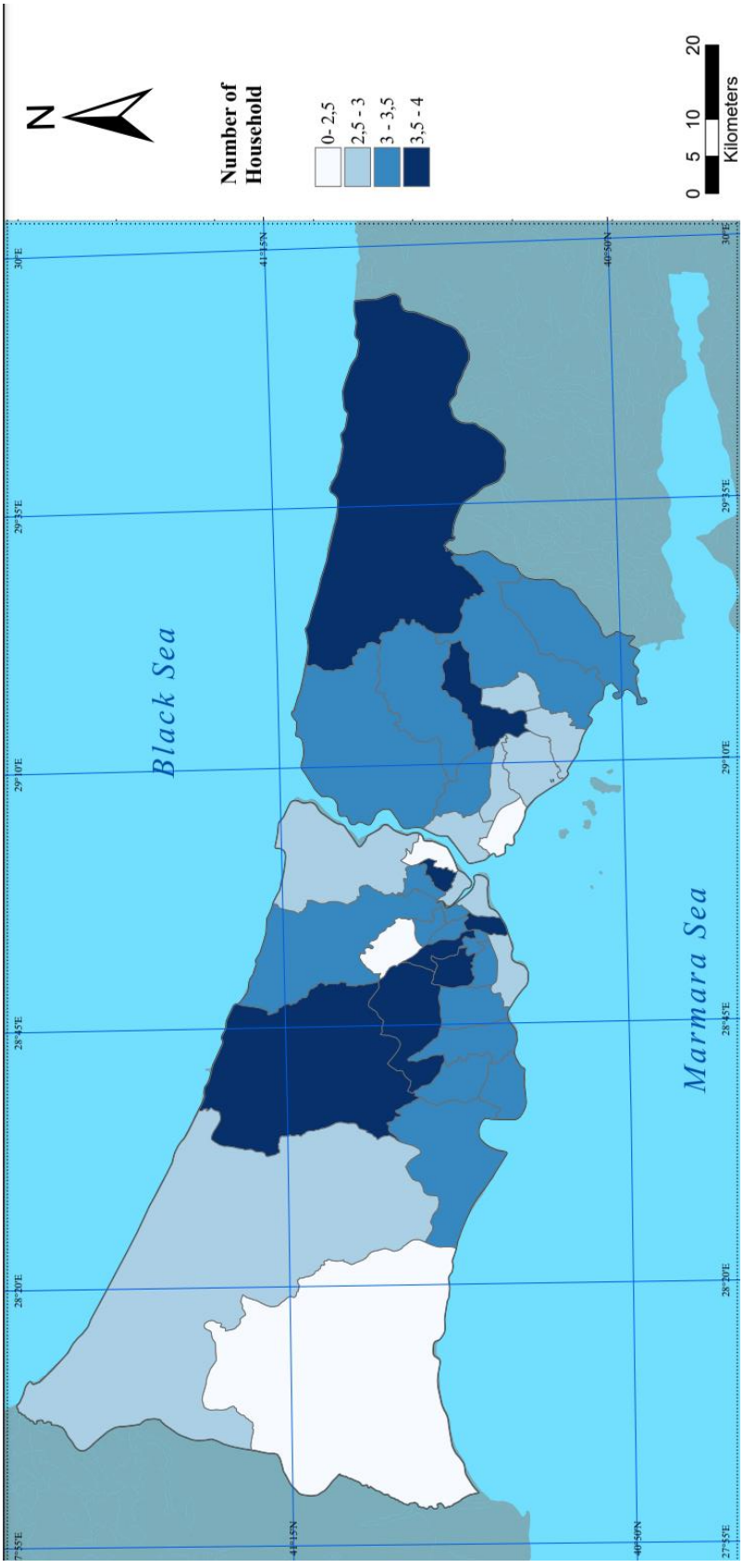

Figure A- 13. Household Number Map.

A4. Scenario-1 maps

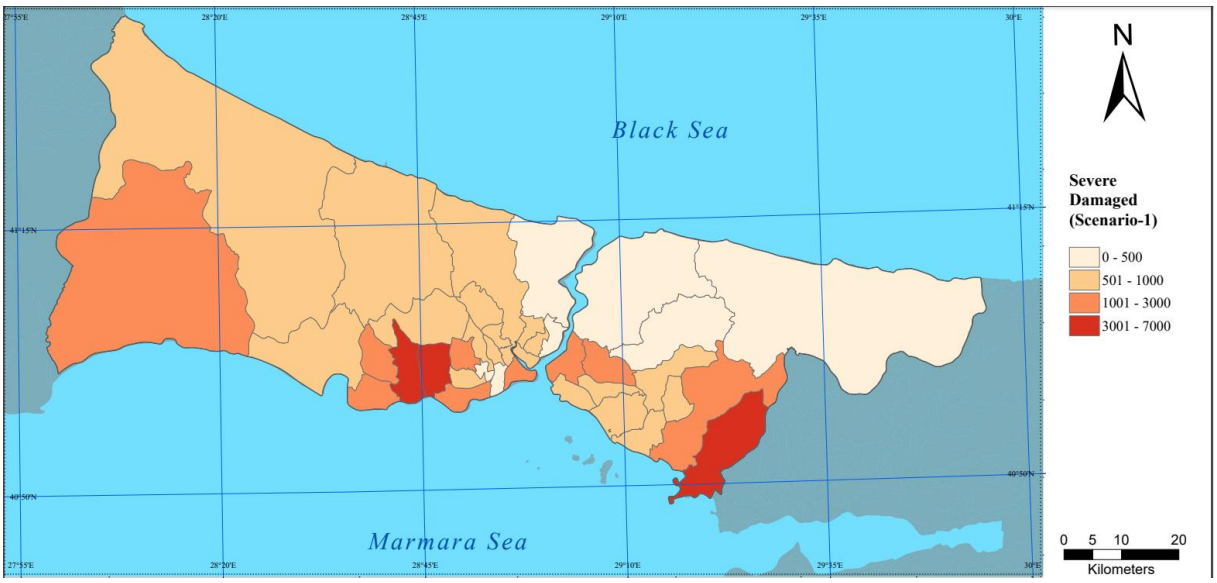

Figure A- 14. Map of Severely Damaged Buildings

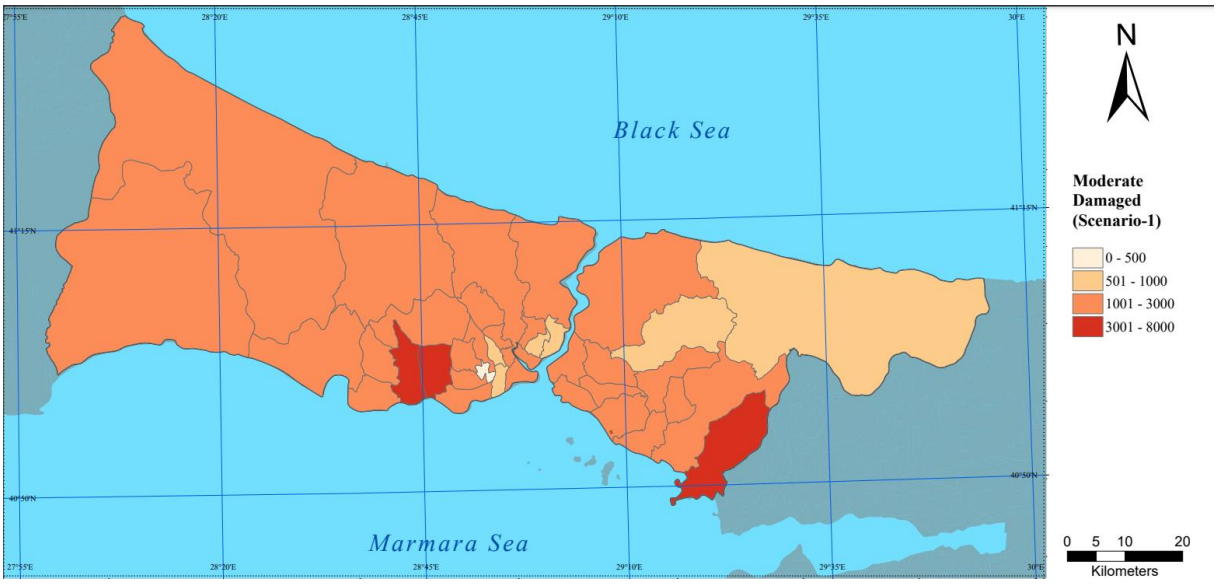

Figure A- 15. Map of Moderate Damaged Buildings

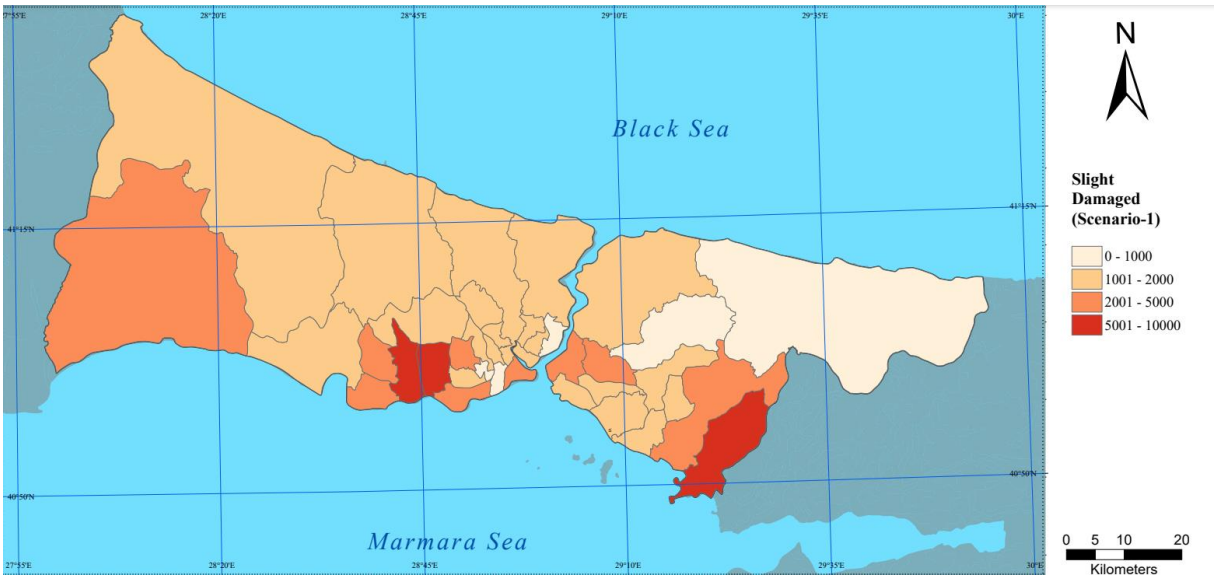

Figure A- 16. Map of Slight Damaged Buildings

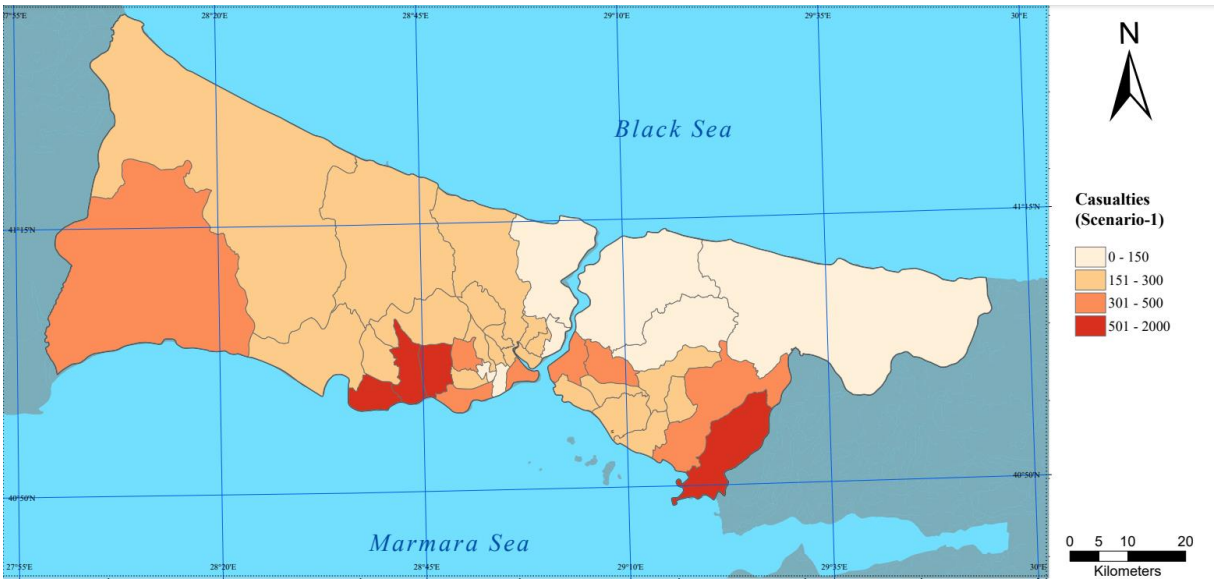

Figure A- 17. Map of Casualties by District of Istanbul

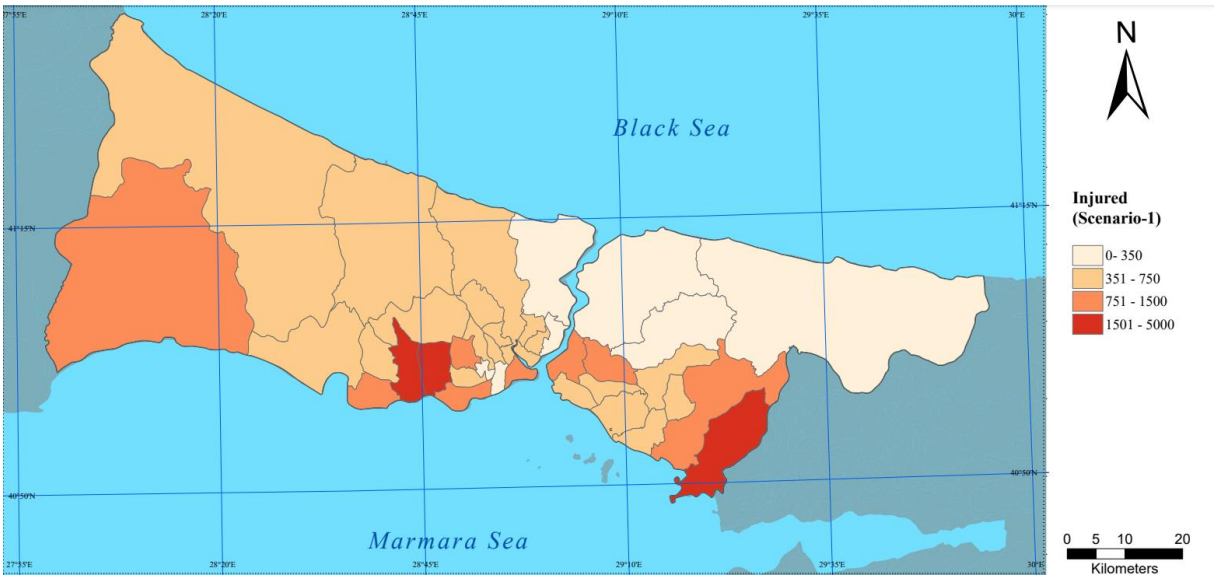

Figure A- 18. Map of Injured by District of Istanbul

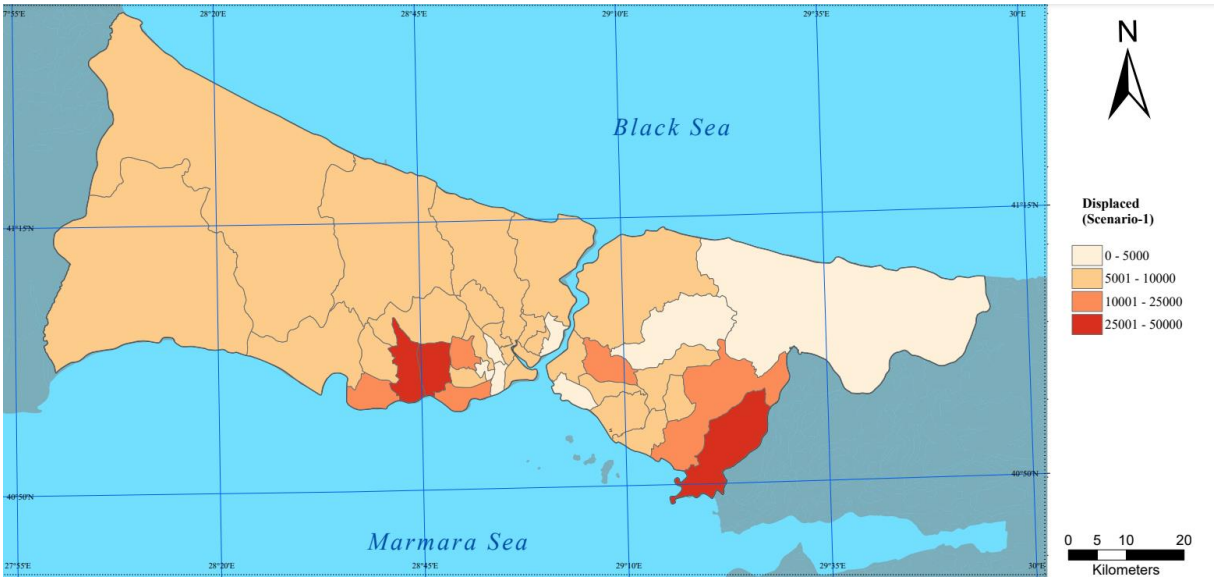

Figure A- 19. Map of People Displaced After Earthquake

A5. ELER

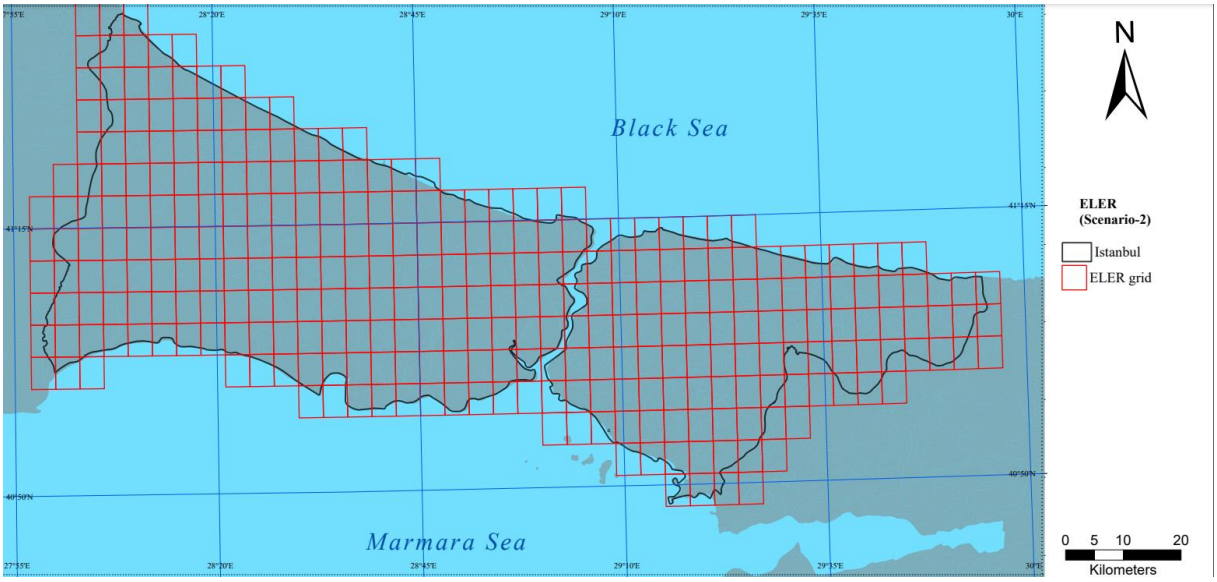

Figure A- 20. ELER Istanbul Grid

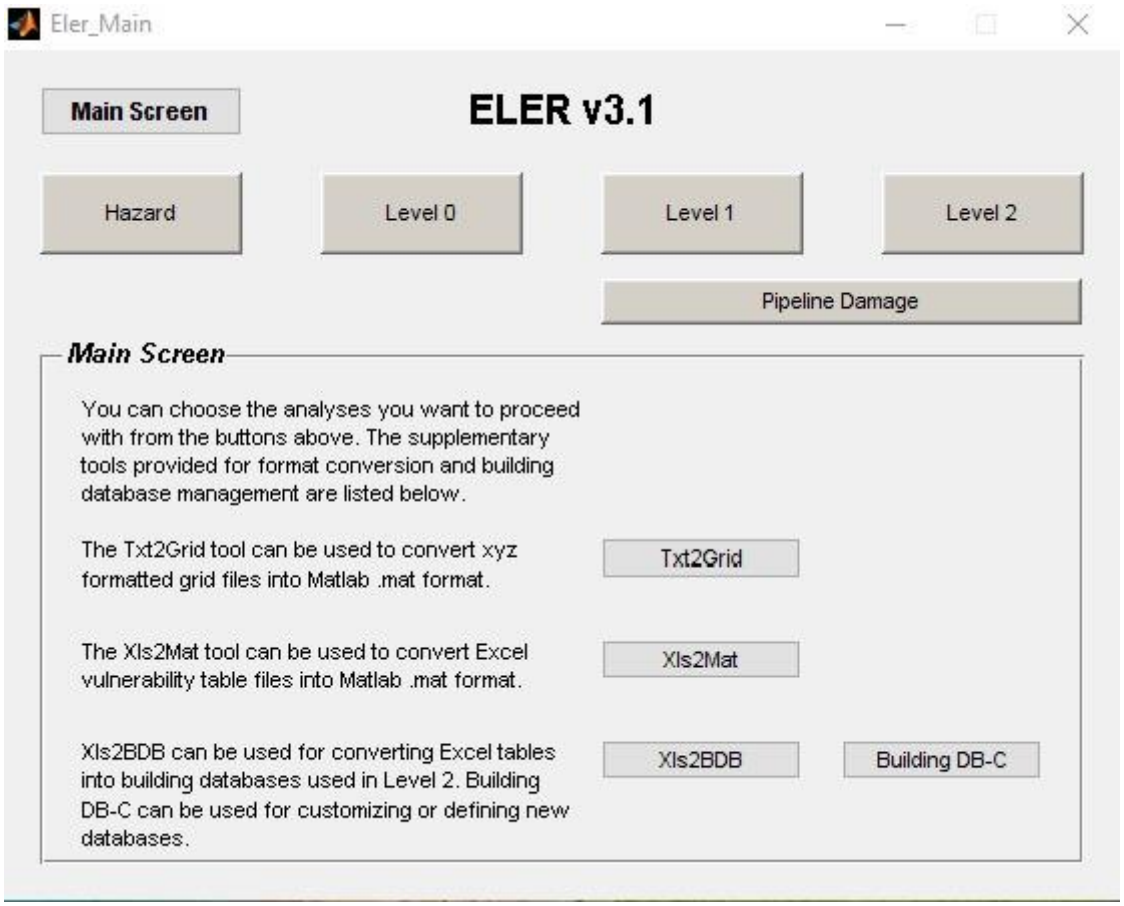

Figure A- 21. ELER Main Screen

N

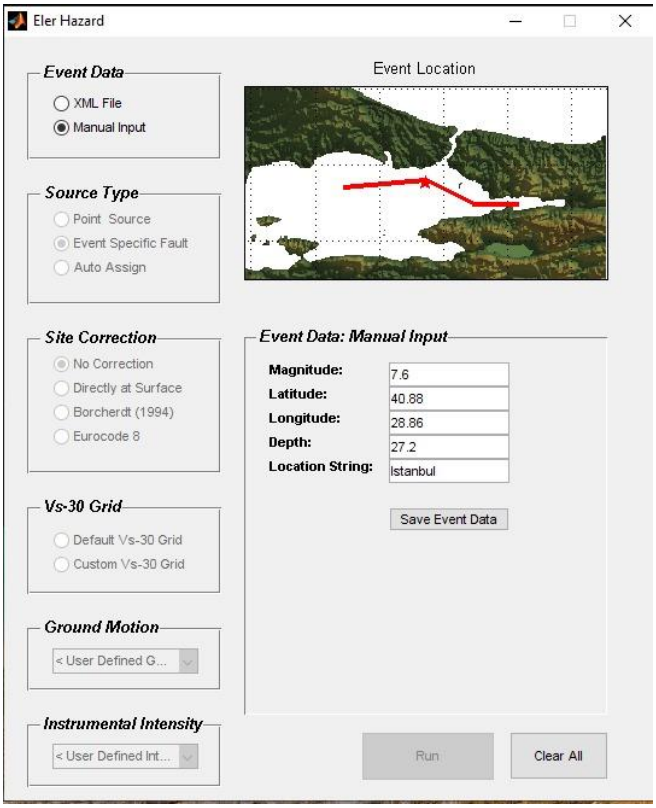

Figure A- 22. Earthquake Parameters Input (Hazard Analysis)

O

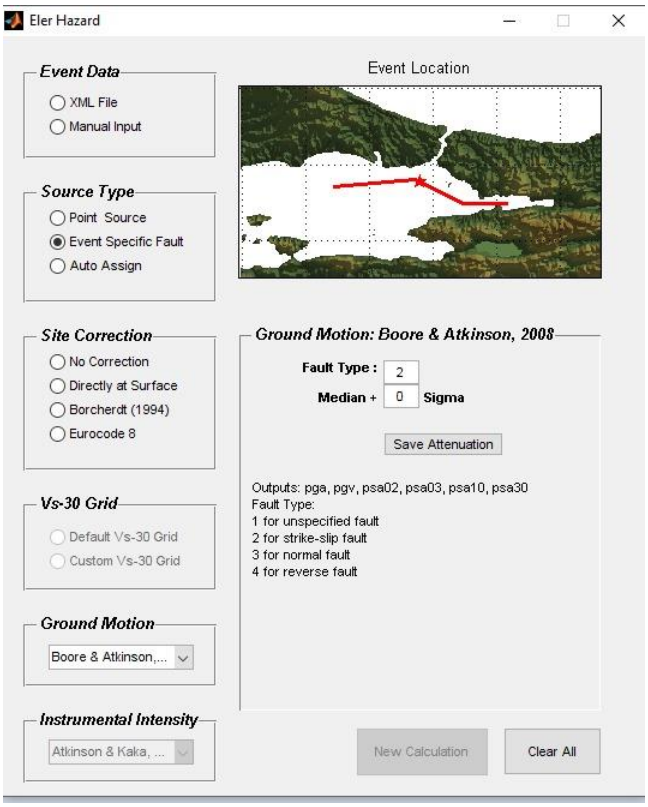

Figure A- 23. Fault Type Selection Screen (Hazard Analysis)

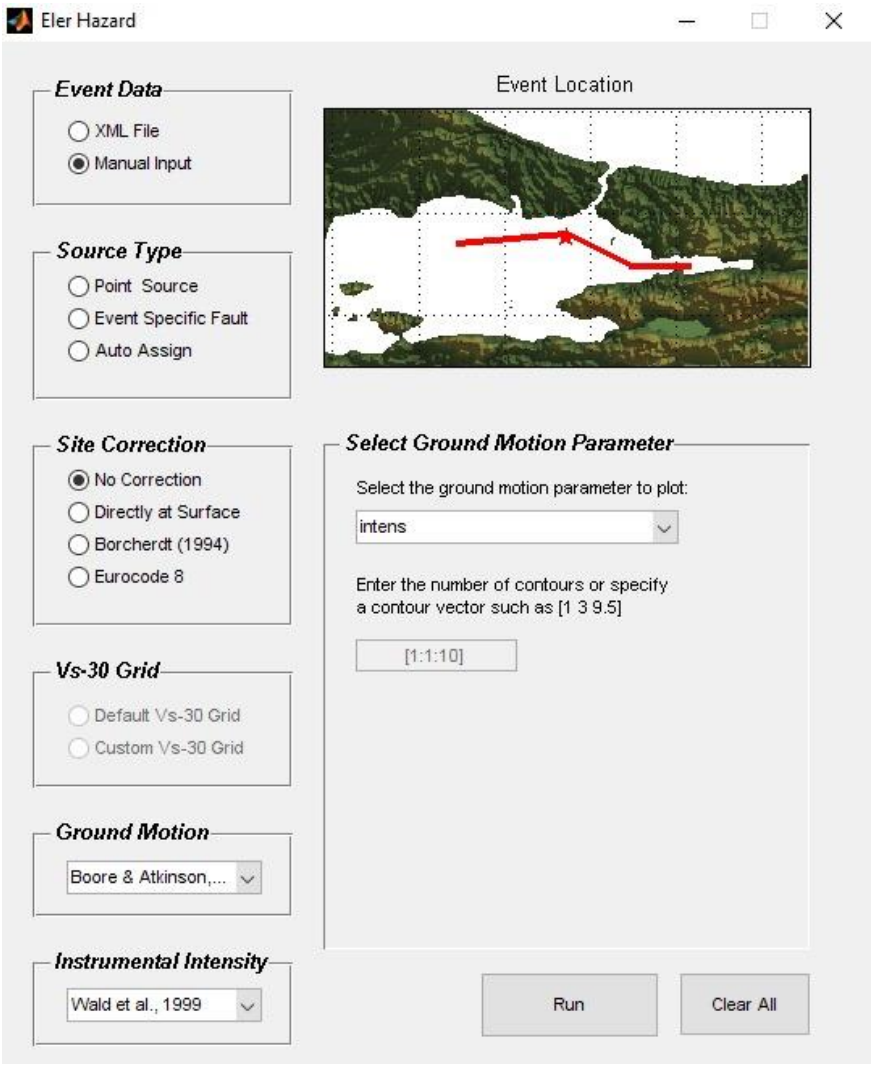

Figure A- 24. Intensity Generation Selection (Hazard Analysis)

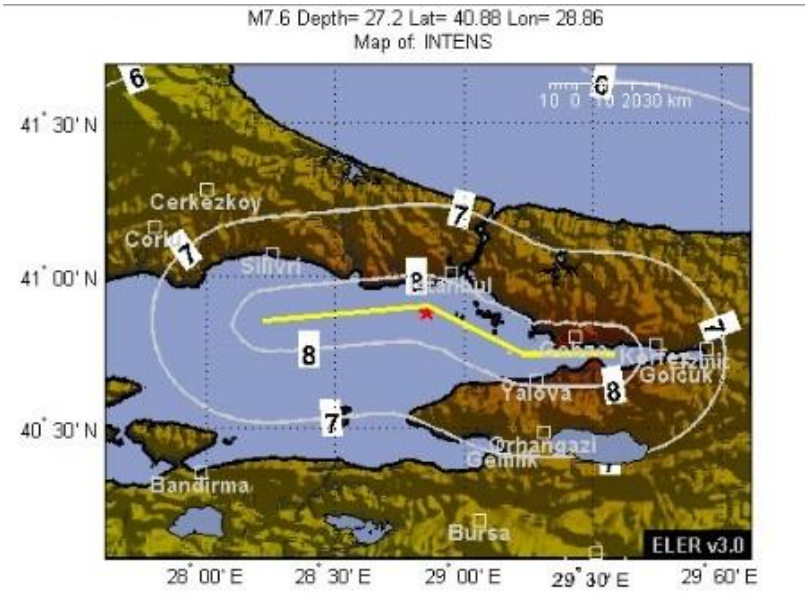

Figure A- 25. Map of Intensity (Hazard Analysis)

Q

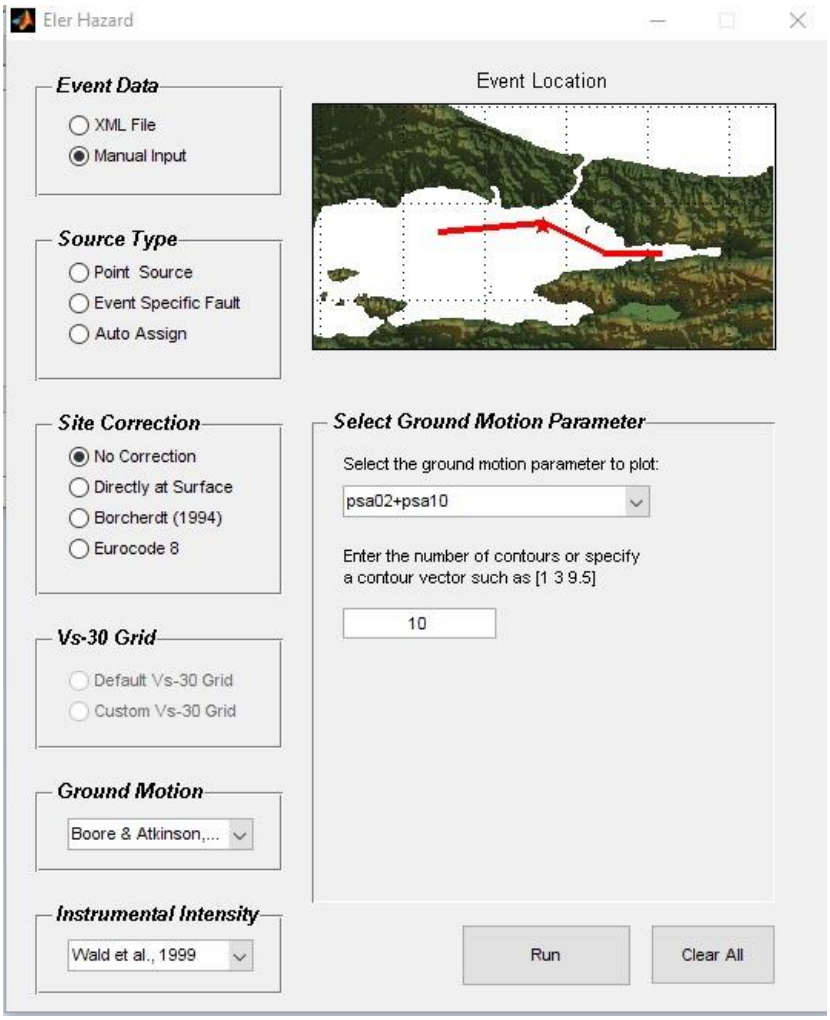

Figure A- 26. Creating Acceleration Period for 0.2s and 1s (Hazard Analysis)

R

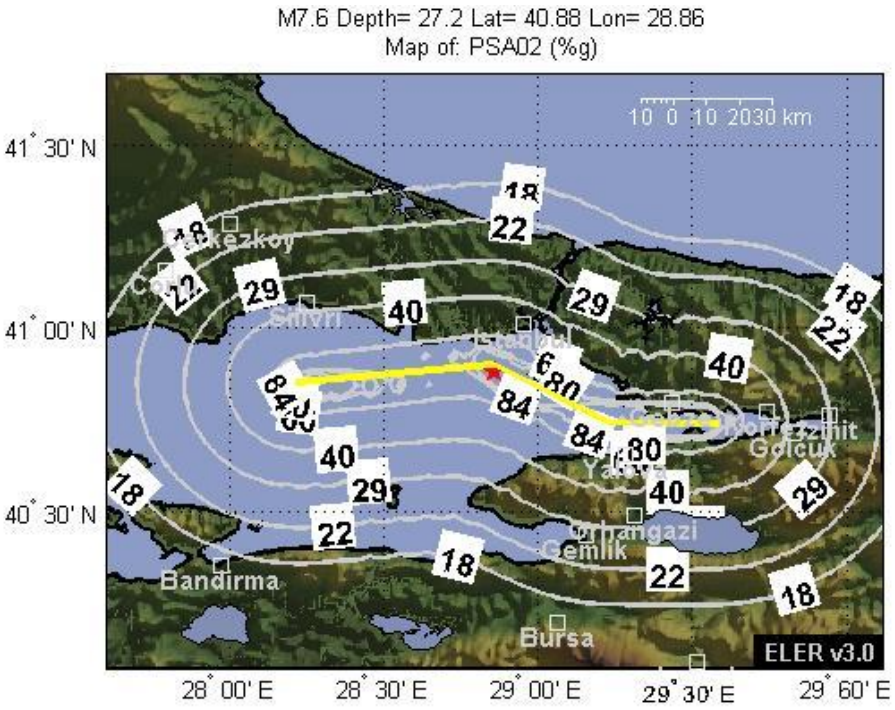

Figure A- 27. Acceleration Period Map for 0.2s (Hazard Analysis)

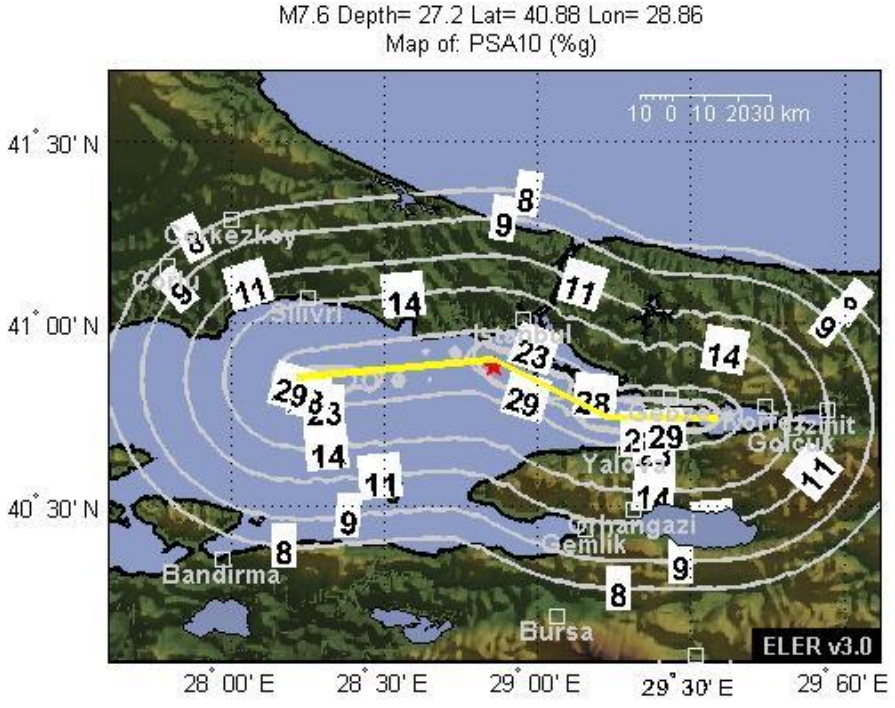

Figure A- 28. Acceleration Period Map for1s (Hazard Analysis)

S

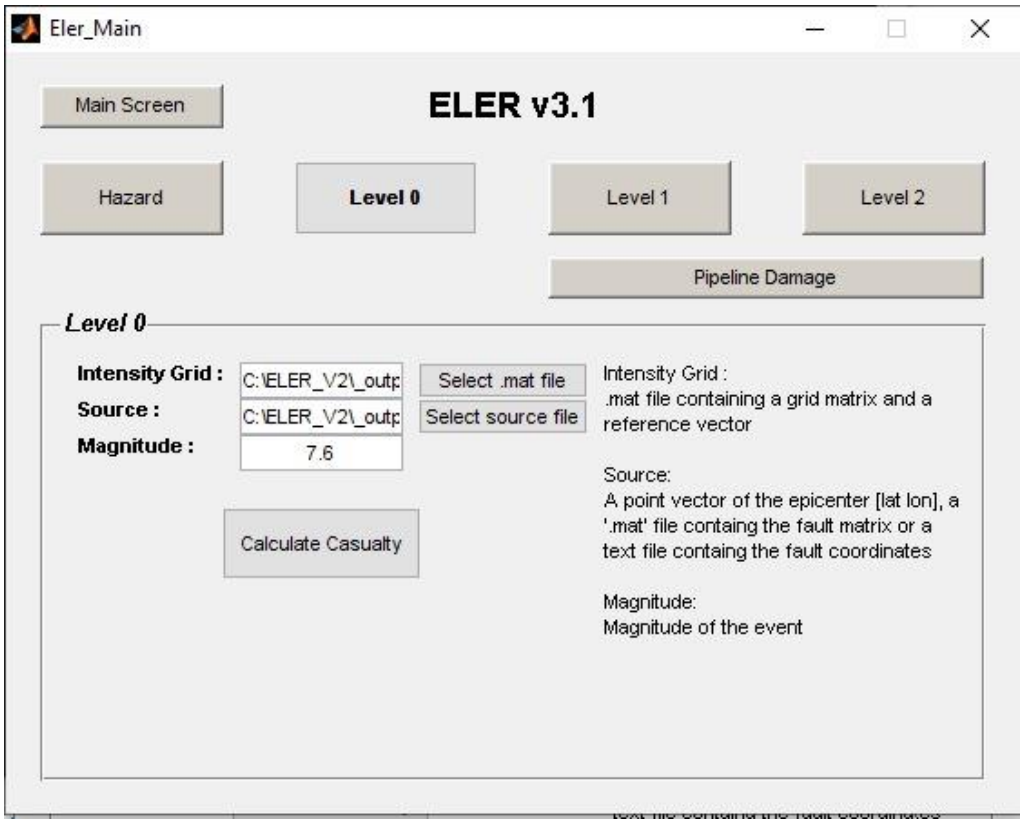

Figure A- 29. Input Screen for Level 0

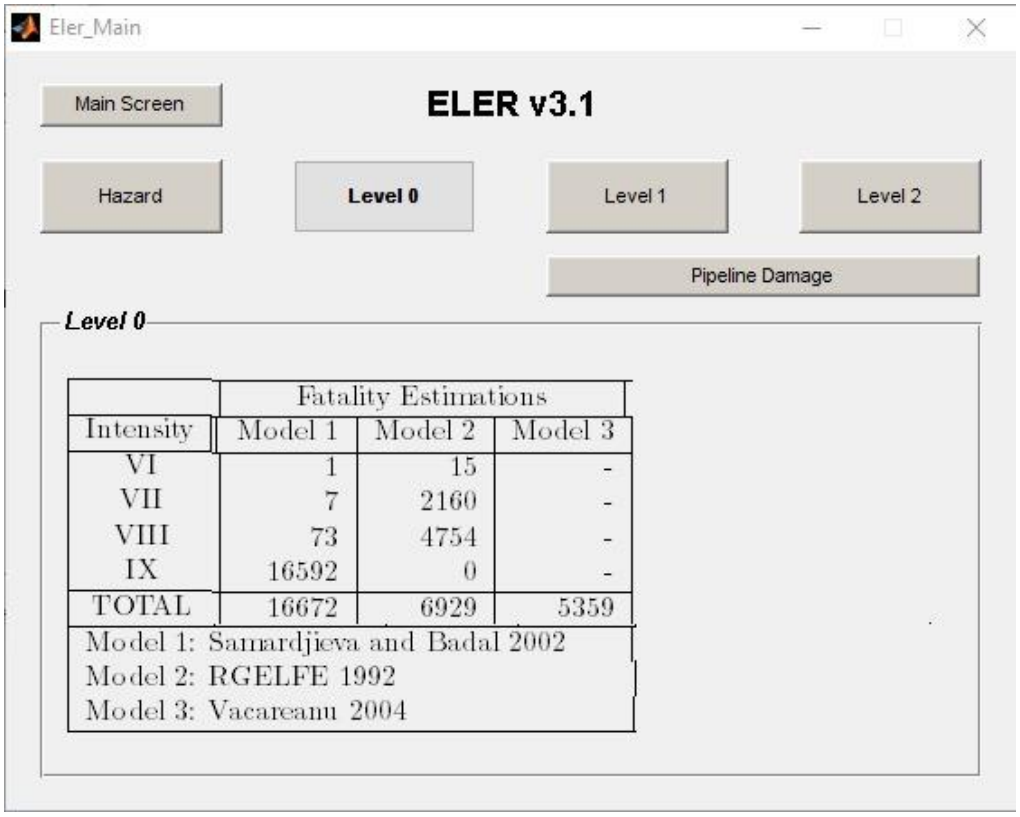

	Fatality Estimations		
Intensity	Model 1	Model 2	Model 3
VI	1	15	-
VII	7	2160	-
VIII	73	4754	-
IX	16592	0	-
TOTAL	16672	6929	5359

Model 1: Samardjieva and Badal 2002
Model 2: RGELFE 1992
Model 3: Vacareanu 2004

Figure A- 30. Casualties' Estimation (Level 0)

T

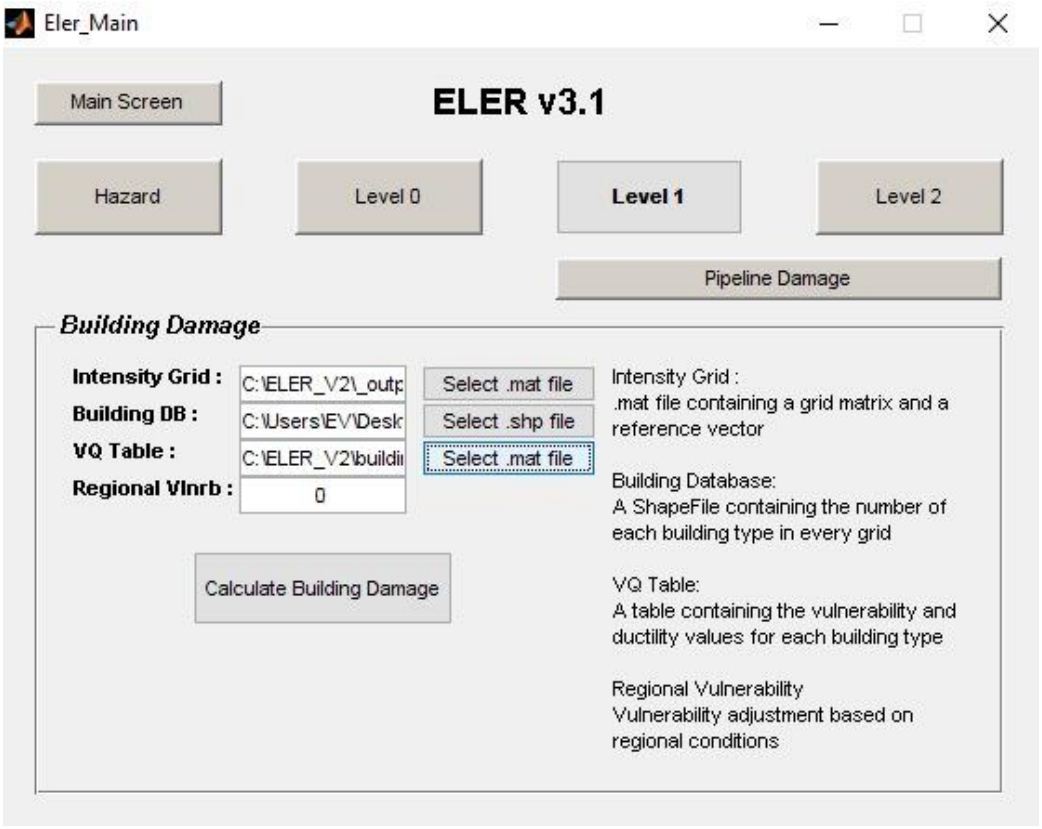

Figure A- 31. Input Screen for Level 1

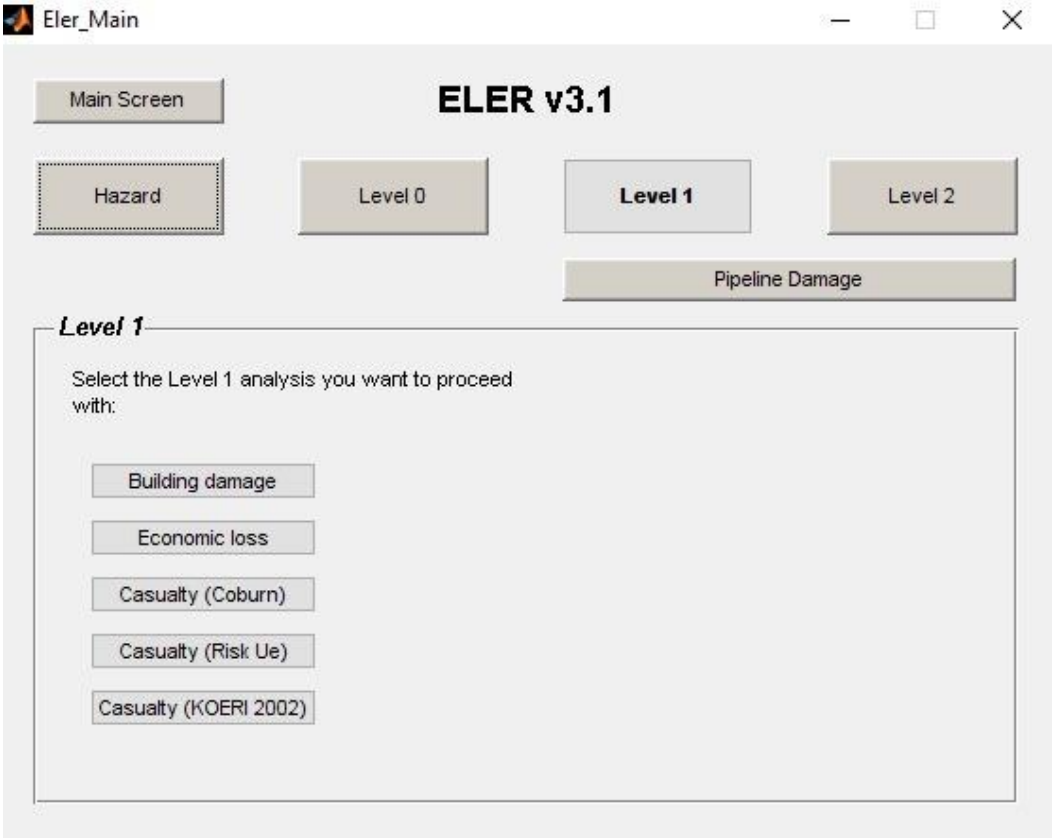

Figure A- 32. Output Options for Level 1

U

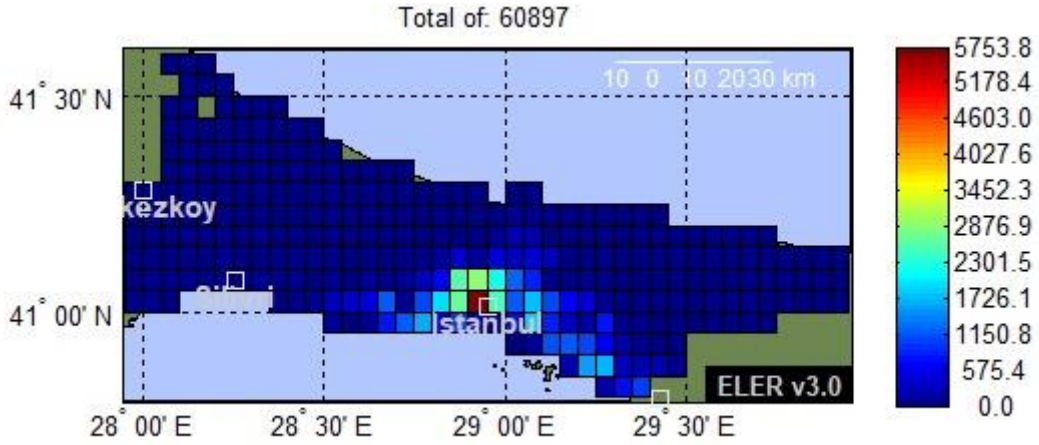

Figure A- 33. Map of Building Damaged Estimation (Level 1)

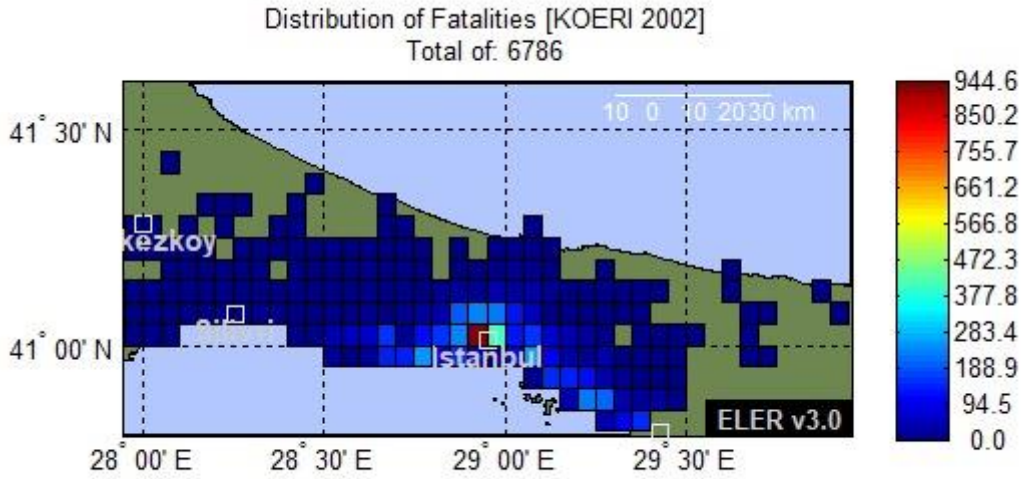

Figure A- 34. Map of Casualties by KOERI (2002), (Level 1)

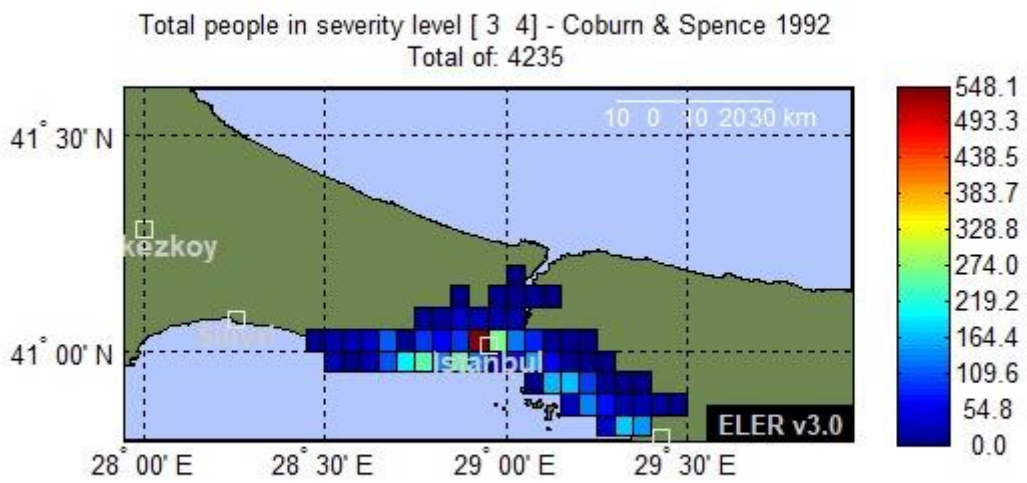

Figure A- 35. Map of Casualties by Coburn and Spence (1992), (Level 1)

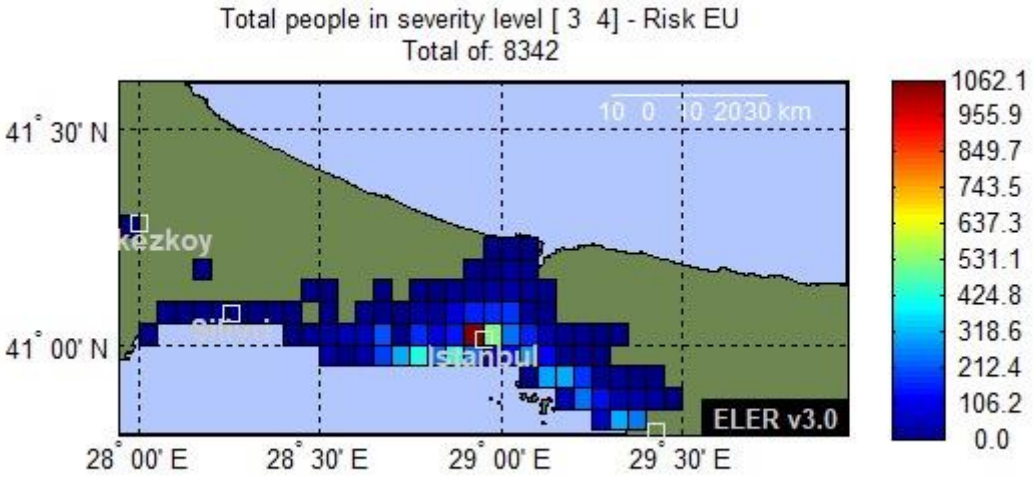

Figure A- 36. Map of Casualties by Risk EU (Level 1)

W

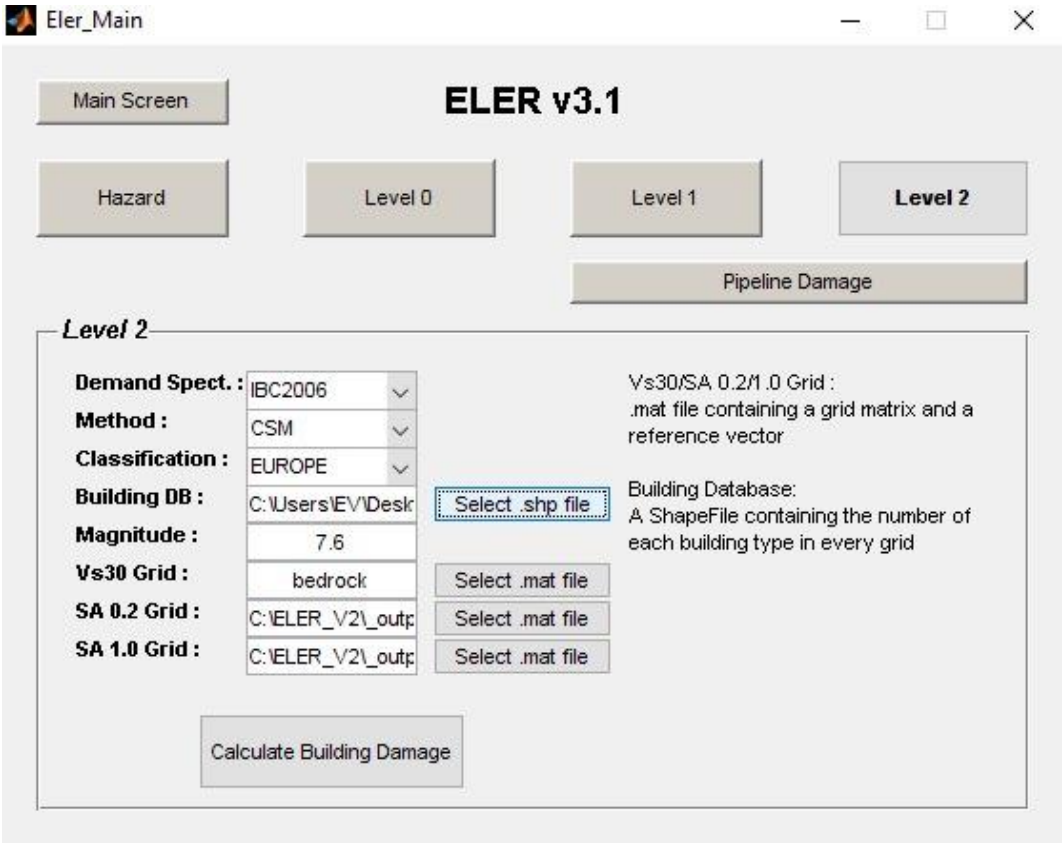

Figure A- 37. Input Screen for Level 2

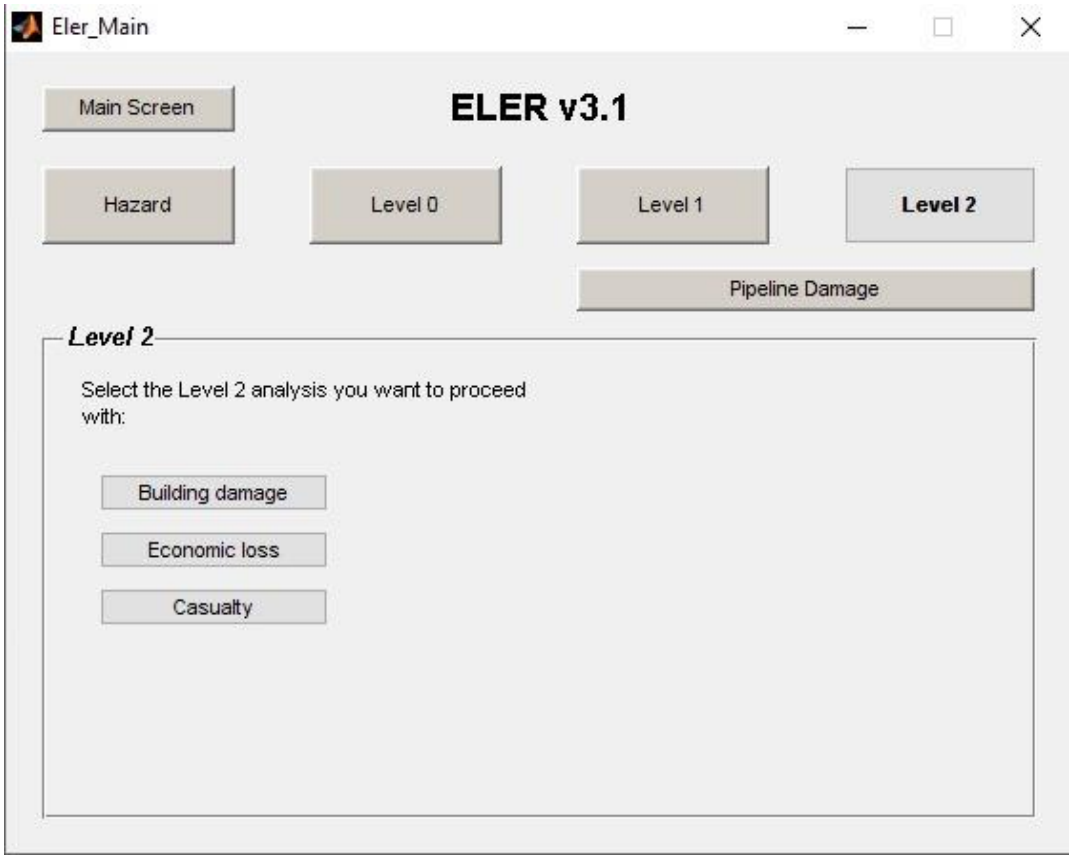

Figure A- 38. Output Options for Level 2

A6. Istanbul District Map

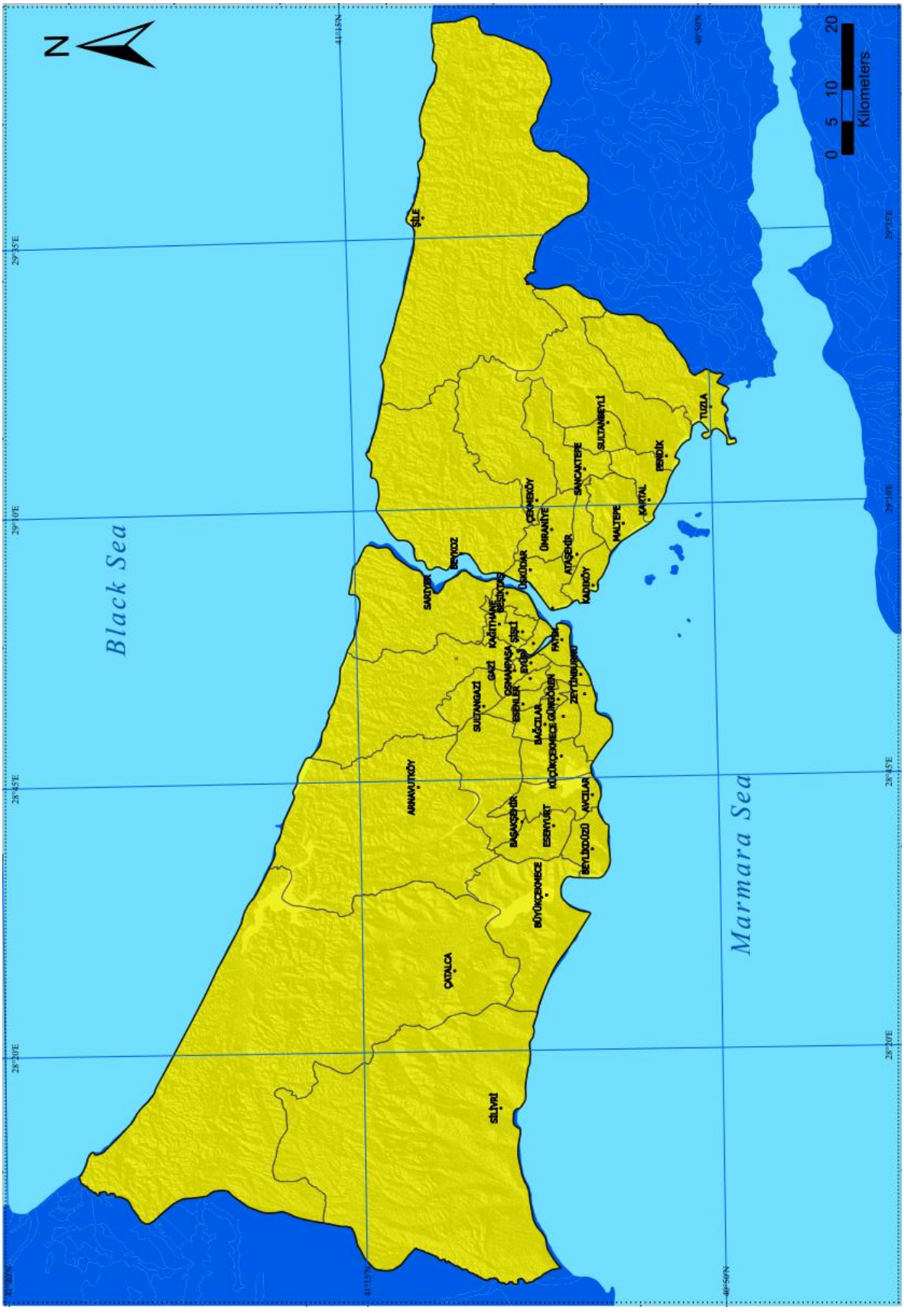

Figure A- 39. Istanbul District Map

Y

A7. Ratio of Potential Risk in the District

Table A-1. District Based Values of the Risk Map

DISTRICT NAME	MIN	MAX	RANGE	MEAN	STD	SUM	MEDIAN	PCT90
ARNAVUTKÖY	5,05	6,75	1,7	5,68662	0,365498	403,75	5,7	6,2
ATAŞEHİR	5,65	6,9	1,25	6,39	0,425911	31,95	6,5	6,8
AVCILAR	6,05	7,55	1,5	6,928572	0,533758	48,5	7,15	7,52
BAĞCILAR	7,4	7,4	0	7,4	0	22,2	7,4	7,4
BAHÇELİEVLER	8	8,2	0,2	8,066667	0,094281	24,2	8	8,16
BAKIRKÖY	7,45	7,7	0,25	7,5625	0,11388	30,25	7,55	7,685
BAŞAKŞEHİR	6,2	6,9	0,7	6,582353	0,241284	111,9	6,6	6,87
BAYRAMPAŞA	6,5	6,5	0	6,5	0	6,5	6,5	6,5
BEŞİKTAŞ	5,65	6,25	0,6	5,85	0,282843	17,55	5,65	6,13
BEYKOZ	4,2	6,3	2,1	5,332609	0,419785	245,3	5,2	5,9
BEYLİKDÜZÜ	7,6	7,85	0,25	7,771429	0,095832	54,4	7,85	7,85
BEYOĞLU	6,4	6,55	0,15	6,475	0,075	12,95	6,475	6,535
BÜYÜKÇEKMECE	4,4	7,7	3,3	6,621154	0,6113	172,15	6,725	7,175
ÇATALCA	2,75	6,3	3,55	4,312079	0,833604	767,55	4,3	5,395
ÇEKMEKÖY	4,8	6,05	1,25	5,419231	0,371089	140,9	5,45	5,925
ESENLER	6,65	6,95	0,3	6,8	0,15	27,2	6,8	6,95
ESENYURT	7,4	7,9	0,5	7,68125	0,14987	61,45	7,65	7,9
EYÜP	5,150001	7,2	2,05	5,8375	0,465232	210,15	5,85	6,375
FATİH	7,25	7,25	0	7,25	0	14,5	7,25	7,25
GAZİ OSMANPAŞA	7,1	7,1	0	7,1	0	7,1	7,1	7,1
GÜNGÖREN	6,9	6,9	0	6,9	0	6,9	6,9	6,9
KADIKÖY	6	7,25	1,25	6,5	0,540062	19,5	6,25	7,05
KAĞITHANE	6,25	6,5	0,25	6,333333	0,117851	19	6,25	6,45
KARTAL	6,6	7,55	0,95	7,033333	0,314466	42,2	6,95	7,425
KÜÇÜKÇEKMECE	6,4	8,65	2,25	7,766667	0,731247	46,6	7,875	8,525
MALTEPE	4,8	7,65	2,85	6,866667	0,815475	61,8	7,15	7,49
PENDİK	6,05	7,7	1,65	6,84	0,463393	205,2	6,85	7,465
SANCAKTEPE	5,95	6,85	0,9	6,39	0,313688	63,9	6,475	6,76
SARIYER	5,3	6,5	1,2	5,8	0,292973	139,2	5,725	6,17
SİLİVRİ	3,2	6,85	3,65	5,591729	0,606301	743,7	5,6	6,39
SULTANBEYLİ	5,9	6,8	0,9	6,35	0,325576	31,75	6,35	6,72
SULTANGAZİ	6,45	7	0,55	6,708334	0,190212	40,25	6,7	6,925
ŞİLE	3,25	5,55	2,3	4,676033	0,365738	565,8	4,65	5,15
ŞİŞLİ	6,1	6,1	0	6,1	0	6,1	6,1	6,1
TUZLA	4,6	7,75	3,150001	6,3	0,702754	138,6	6,2	7,22
ÜMRANİYE	6,6	7,35	0,75	6,925	0,241091	41,55	6,95	7,175
ÜSKÜDAR	6,25	7,25	1	6,59	0,36524	32,95	6,6	6,99
ZEYTİNBURNU	6,75	7,45	0,7	7,1	0,35	14,2	7,1	7,38

Z